REGULATION OF PROTEIN AGGREGATION BY ARFAPTIN2 IN AMYOTROPHIC LATERAL SCLEROSIS

by

Aida Mohammedeid
(BSc, MSc)

Submitted for the degree of Doctor of Philosophy (PhD)

Sheffield Institute for Translational Neuroscience

University of Sheffield

January 2015

ABSTRACT

Amyotrophic lateral sclerosis (ALS) is a devastating, adult onset motor neuron disease (MND) that has no effective treatment to date. The current study investigates the possibility of targeting protein aggregation pathway for treatment. Modulation of this pathway is approached through targeting Arfaptin2 protein. The C-terminal of Arfaptin2 (HC-ARFIP2), a dominant negative form of Arfaptin2, has been shown to have a neuroprotective property that maintains the proteasome activity and induces degradation of misfolded proteins.

We thus proposed that the HC-ARFIP2 improves neuronal survival in ALS via maintaining the proteasomal pathway, which in turn will decrease neuron toxicity and improve neuronal survival. Expression of HC-ARFIP2 in primary motor neuron cultures using LV-based vector, improved motor neuron survival significantly. The prosurvival effect was observable even in cells treated with H_2O_2 in both SOD1G93A transgenic and non-transgenic cells. A further investigation on the pathway of which HC-ARFIP2 exerts it neuroprotective effect showed that HC-ARFIP2 induces Akt phosphorylation by decreasing its dominant negative modulator, PTEN. In addition, protein degradation pathway-markers (p62, LC3II, ULK1) showed significant changes in response to HC-ARFIP2 expression. Furthermore, Arfaptin2 showed colocalisation with SOD1 and overexpression of FL-ARFIP2 caused aggregates formation in HEK293T cells compared to HC-ARFIP2 expression that maintained the cytoplasmic distribution of SOD1.

A scAAV9-based vector was produced to replicate these observations *in vivo*. The desired viral titre could not be obtained within the time course of the PhD.

In conclusion, the study presented here has provided a proof of concept that Arfaptin2 is involved in protein aggregation in ALS. In addition, HC-ARFIP2 expression can improve motor neuron survival *in vitro* through activation of Akt and proteasome activity.

ACKNOWLEDGMENTS

First of all, I would like to thank Allah, the most gracious, the most merciful, for giving me this chance to convert a dream into reality. A big thanks to my parents, who I can not thank enough, for believing in me and providing me with their unconditional support, courage and love which made me achieve a goal that I considered impossible. Many thanks to my brothers and sisters who provided me with the strength and advice especially when I needed them most.

I would like to thank my supervisor, Dr. Ke Ning for his endless support, guidance and scientific input. The knowledge I gained from him during the course of this PhD made me develop scientifically and academically. I would like to thank Prof. Mimoun Azzouz for his strong guidance and support throughout the PhD. Also, I would like to thank Dr. Andrew Grierson for his valuable input and Dr. Vera Lukashchuk for her useful feedbacks. I would like also to thank Prof.Azzouz group and the technical team in SITraN for their technical support.

I would like to thank the Saudi Ministery of Higher Education for granting me this scholarship as part of King Abdullah Scholarship Programme. Thanks to all the people working hard in the Saudi Cultural Bureau in London to support and encourage all Saudi students in the UK.

A big thanks to all my friends. I am truly blessed to have you in my life. Thanks to everybody for making this journey easier and full of joyful memories.

This thesis is dedicated to my family.

PUBLICATIONS

Review

Mohammedeid AM, Lukashchuk V, Ning K. 2014. Protein aggregation and Arfaptin2: A novel therapeutic target against neurodegenerative diseases. New Horizons in Translational Medicine 2: 12-15

Abstracts

Mohammedeid A., Kong SC., Grierson A., Azzouz M., Ning K. Regulation of protein aggregation by Arfaptin2 in amyotrophic lateral sclerosis. Human Gene Therapy. May 2014, 25(5): A1-A22.

AWARDS

The medical school 3rd year presentation 2014 (3rd place).

Table of Contents

LIST OF FIGURES

LIST OF TABLES

LIST OF ABBREVIATIONS

4E-BP1	4E binding protein 1
a.a	Amino acid
AD	Alzheimer's disease
Akt/PKB	Serine/Threonine specific protein kinase, Protein kinase B
ALS	Amyotrophic lateral sclerosis
AMPA	α-amino-3-hydroxy-5-methyl-4-isoxazolepropionic acid
APS	Ammonium persulfate
ARF	ADP-ribosylation factor
Arfaptin2/POR1/ARFIP2	ADP-ribosylation factor-interacting protein 2/ partner of Rac1
Atg13	Autophagy-related protein 13
BCA	Bicinchoninic acid
BiP	Immunoglobulin binding protein
β-ME	Beta-mercaptoethanol
BSA	Bovine serum albumin
C9ORF72	Chromosome 9 open reading frame 72
Carb	Carbenicillin
CGRP	Calcitonin gene related peptide
CK2α	Casein kinase 2 alpha
CMV	Cytomegalovirus
CNS	Central nervous system
cPPT	Central polypurine tract element
dH_2O	Distilled water
DMEM	Dulbecco's modified eagle medium
DMF	N,N-dimethyl formamide
DMSO	Dimethyl sulfate
E1	Ubiquitin-activating enzyme
E13	Embryonic day 13
E2	Ubiquitin-conjugating enzyme

E3	Ubiquitin-ligase
EAAT	Excitatory amino acid transporter
ELISA	Enzyme-linked immunosorbent assay
ERAD	Endoplasmic reticulum-associated degradation
ER	Endoplasmic reticulum
ERK1/2	Extracellular signal-kinase
FALS	Familial ALS
FBS	Foetal bovine serum
FL-ARFIP2	Full length Arfaptin2
FTLD	Frontotemporal lobar degeneration
FUS/TLS	Fused in sarcoma/translocated in liposacroma
GDNF	Glial cell-derived neurotrophic factor
GEF	Guanine nucleotide exchange factor
GFP	Green fluorescent protein
GluR2	Glutamate receptor subunit 2
GRIP1	Glutamate receptor interacting protein 1
GS	Goat’s serum
HA	Hemagglutinin
HBSS	Hank’s balanced salt solution
HC-ARFIP2	C-terminal half of Arfaptin2
HD	Huntington’s disease
HEK293T	Human embryonic kidney cells with T antigen
HIV	Human immunodeficiency virus
HRP	Horseradish peroxidase
hSOD1	Human SOD1
IL	Interleukin
KA	Kainate receptor
LBa	LB agar
LBb	LB broth
LC3	Microtubule-associated protein 1A/1B-light chain 3
LMN	Lower motor neurons
LPS	Lipopolysaccharide
LV	Lentivirus

LV-ARFIP2	Lentivirus expressing the Arfaptin2 gene
LV-HC	Lentivirus expressing the HC-ARFIP2 gene
MCP-1	Monocyte chemotactic protein 1
min	Minutes
MND	Motor neuron disease
MOI	Multiplicity of infection
mRNA	Messenger RNA
mtDNA	Mitochondrial DNA
mTOR	The mammalian target of rapamycin
mTORC1	mTOR complex 1
NB-medium	Neurobasal medium
NF-H_2O	Nuclease free water
NF-κB	Nuclear factor kappa B
NLS	Nuclear localisation signal
NMDA	N-methyl D-aspartate
NTG	Non-transgenic
Opti-MEM	Opti-minimal essential medium
OPTN	Optineurin
P-4EBP1	Phosphorylated 4E-binding protein 1
p62	Sequestosome 1
PBP	Progressive bulbar palsy
PBS	Phosphate buffered saline
PCR	Polymerase chain reaction
PD	Parkinson’s disease
PDI	Protein disulphide isomerase
Pen/Strep	Penicillin/Streptomycin
PFA	Paraformaldehyde
PGK	Phosphoglycerate kinase
Phospho-Akt	Phosphorylated Akt
PI	Propidium iodide
PIC	Protease inhibitor cocktail
PI3P	Phosphatidylinositol 3-phosphate
PI4P	Phosphatidylinositol 4-phosphate

PI5P	Phosphatidylinositol 5-phosphate
PIP2	Phosphatidylinositol 4,5 bisphosphate
PIP3	Phosphatidylinositol 3,4,5 trisphosphate
PLS	Primary lateral sclerosis
PMA	Progressive muscular atrophy
polyQ-huntingtin	Polyglutamine repeat in huntingtin gene
PORN	Poly-DL-ornithine hydrobromide
PTEN	Phosphatase and tensin homolog
PVDF	Polyvinylidene difluoride
RGG	Arginine-glycine-glycine repeat
ROS	Reactive oxygen species
RRM	RNA-recognition motif
RT	Room temperature
SALS	Sporadic ALS
scAAV	Self-complementary adeno-associated virus
sec	Seconds
Ser	Serine
Sin	Self-inactivating
SOD1	Superoxide dismutase 1
SOD1G93A	Mutation of glycine to alanine at position 93 of SOD1 gene
TAE	Tris, acetic acid and EDTA buffer
TBST	Tris-buffered saline with Tween 20
TG	Transgenic
TDP-43	Transactive response DNA-binding protein 43
TUJ1	Neuronal class III β-tubulin
UBQLN2	Ubiquilin 2
ULK1	Unc-51 Like autophagy activating kinase 1
UMN	Upper motor neuron
UPR	Unfolded protein response
UPS	Ubiquitin-proteasome system
UTD	Untransduced
UTF	Untransfected

VCP	Valosin-containing protein
WT	Wild-type
X-gal	5-bromo-4-chloro-3-indolyl-B-D-galactoside

CHAPTER 1: INTRODUCTION

1.1 Amyotrophic lateral sclerosis

Amyotrophic lateral sclerosis (ALS) is an adult onset motor neuron disease (MND), in which mainly upper motor neurons (UMN) in motor cortex and lower motor neurons (LMN) of brainstem and spinal cord degenerate. Nevertheless, it is now considered a multisystem disease as other types of neurons in addition to motor neurons can be affected. The average age of onset is 50-60 years; however, juvenile onset has been reported. The incidence is approximately 4/100,000 worldwide in which men are more commonly affected than women. It is a progressive and devastating disease in which the average survival is three years from the onset of symptoms, and death usually occurs due to respiratory failure (Shaw, 2005, Ferraiuolo et al., 2011).

MND can be subdivided into four subclasses according to the affected motor neurons; ALS, in which both UMNs and LMNs are affected; primary lateral sclerosis (PLS), in which only the UMNs are affected; progressive muscular atrophy (PMA), in which only LMNs are affected; and progressive bulbar palsy (PBP), in which only the bulbar musculature is affected. However, most of these subclasses progress into ALS. ALS has been reported to be accompanied with frontotemporal lobar degeneration (ALS/FTLD) in 20% of cases (Shaw, 2005). Definitive diagnosis of ALS is complicated and follows specific criteria. According to El Escorial criteria, ALS diagnosis can be divided into: definite, in which both UMN and LMN in three or more regions are affected; probable, in which UMN and LMN are affected in less than three regions; possible, in which either UMN or LMN are affected; and laboratory-supported probable, in which UMN and LMN are affected and supported by laboratory tests (Bradley et al., 2003).

Symptoms develop due to muscle weakness and muscle wasting; most commonly starts in the upper limbs. Depending on which muscles are affected, ALS patients may show symptoms like fasciculation, muscle cramps, dysphagia and bulbar impairment (Bradley et al., 2003).

1.1.1 Types

ALS is divided into two types according to the genetic cause:

1.1.1.1 Familial ALS (FALS)

FALS accounts for approximately 10% of ALS cases. It mostly shows autosomal dominant inheritance, however, autosomal recessive and X-linked inheritance have been reported (Hentati et al., 1994, Maruyama et al., 2010, Orlacchio et al., 2010, Deng et al., 2011b). Over 10 genes have been identified to be involved in the FALS and some of them have unknown functions. The most studied mutated gene in FALS is the copper-zinc superoxide dismutase-1 gene (*SOD1*), which was first identified by Rosen and colleagues, present in 20% of FALS cases (Rosen et al., 1994, Ferraiuolo et al., 2011). However, the most common mutation found in FALS is a hexanucleotide GGGGCC repeat expansions at chromosome 9 open reading frame 72 (*C9ORF72*) (DeJesus-Hernandez et al., 2011, Renton et al., 2011)

1.1.1.2 Sporadic ALS (SALS)

SALS accounts for the remaining 90% of ALS cases. The exact causes of SALS are still unknown but there is a hypothesis that an acquired nucleic acid change triggers the initiation of ALS that is age- and environmental-dependent. Such factors are smoking (Kamel et al., 1999), ingestion of foods containing neurotoxins such as Cycad flour (Esclaire et al., 1999, Armon, 2005), and increased cardiovascular fitness (Turner et al., 2011).

1.1.2 Pathogenesis

ALS seems to be a multi-factorial disease and the exact pathogenesis of the disease is still debated. However, several factors have been identified to be involved in the pathogenesis of ALS (Figure 1.1), which are:

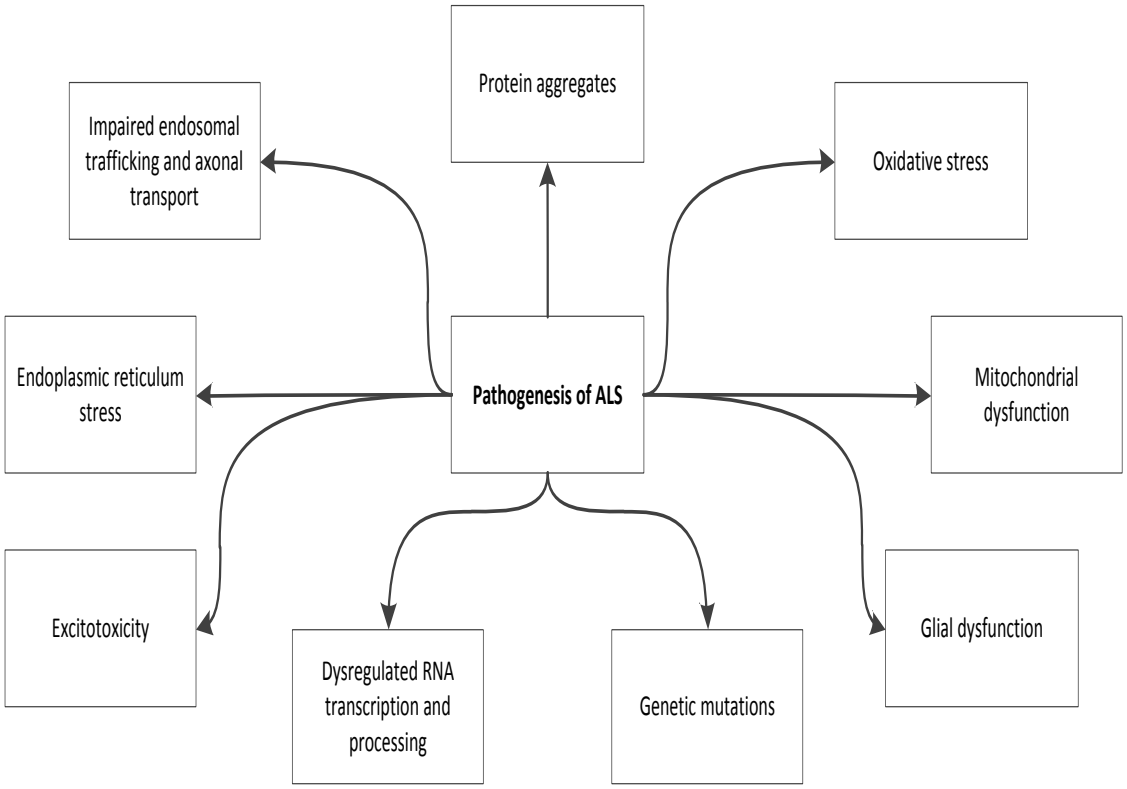

Figure 1.1: Pathogenic pathways involved in ALS.

1.1.2.1 Genetic mutations

Genetic mutations were reported in some ALS cases. Genes reported to be mutated in ALS cases are listed in Table 1.1. Some mutations might be involved in ALS pathogenesis through a toxic gain of function mechanism rather than loss of function, a hypothesis was raised after noticing that *SOD1* knockout mice did not develop MND phenotype (Reaume et al., 1996, Cho et al., 2011), while expressing mutant human SOD1 (hSOD1) did show MND symptoms (Gurney et al., 1994). Mutant SOD1 is the most studied gene defect in ALS. Over 140 mutations in *SOD1* gene have been identified (Chattopadhyay & Valentine 2009, Polymenidou & Cleveland 2011)

Some mutations might affect protein folding and involve the protein degradation pathway. For instance, mutated valosin-containing protein **(**VCP) causes disruption to the ubiquitin proteasome system (UPS) which causes accumulation of protein aggregates in motor neurons (Johnson et al., 2010b). In support of this hypothesis, many ALS-related mutated genes are involved in protein degradation pathways. Such genes are *CHMP2B, UBQLN2, P62, OPTN* and *VCP* (Chalasani et al., 2014). However, a study on Dutch cohorts showed that *VCP* mutations in ALS are very rare and that the identified mutations were shown to be benign according to protein prediction software (Koppers et al., 2011).

Other mutations cause a disease by loss of function mechanism. An example is *ALS2* mutations that cause the production of unstable proteins. These products degrade frequently and the protein level were found to be significantly decreased in lymphoblasts of ALS patients (Yamanaka et al., 2003).

The hexanucleotide repeat expansion in *C9ORF72* is the most common mutation related to ALS, and it is detected in many FALS and SALS cases (DeJesus-Hernandez

et al., 2011, Renton et al., 2011). It has been reported that these hexanucleotide repeats are expanded in about 50% of FALS and 21% of SALS (Renton et al., 2011). Although the actual function of *C9ORF72* is still unknown, it is highly conserved between species. The normal repeat size range between 0-22, while disease associated repeats are over 1000. *C9ORF72* was found to produce three transcripts that encodes for two protein isoforms. Transcript 1 and 3 encode for isoform a, while transcript 2 encodes for isoform b. The hexanucleotide repeat expansions seem to cause variant 1 transcription interruption which leads to reduced production of isoform a (DeJesus-Hernandez et al., 2011). Therefore, it was suggested that these repeat expansions are involved in the pathogenesis by disrupting gene expression or splicing or by the formation of toxic RNA that disrupt some cellular physiological pathways (DeJesus-Hernandez et al., 2011, Renton et al., 2011).

In general, the exact effect of ALS-related mutations on motor neurodegeneration is still vague.

Table 1.1: List of genes related to ALS.

Gene	Gene locus	Function/ pathogenic pathway	References
SOD1	21q22.11	Superoxide metabolism	(Rosen et al., 1993)
FUS	16q11.2	RNA processing	(Kwiatkowski et al., 2009)
TARDBP	1p36.22	RNA processing	(Sreedharan et al., 2008)
C9ORF72	9p21.2	Unknown, RNA processing, endosomal trafficking	(DeJesus-Hernandez et al., 2011, Renton et al., 2011, Farg et al., 2014)
OPTN	10p13	Vesicular trafficking, autophagy	(Maruyama et al., 2010)
VCP	9p13.3	Vesicular trafficking, autophagy	(Johnson et al., 2010a)
UBQLN2	Xp11.21	Protein degradation	(Deng et al., 2011b)
SQSTM1/p62	5q35	Protein degradaiton	(Fecto et al., 2011)
profilin 1 (PFN1)	17p13.3	Cytoskeleton arrangement	(Wu et al., 2012)

ALS2	2q33.1	Vesicle trafficking, guanine-nucleotide exchange factor (GEF).	(Yang et al., 2001)
Senataxin (SETX)	9q34.13	DNA repair	(Chen et al., 2004)
Vesicle-associated membrane protein/ synaptobrevin-associated membrane protein B (VAPB)	20q13.33	Vesicle trafficking	(Nishimura et al., 2004)
Dynactin1 (DCTN1)	2p13	Vesicle trafficking	(Munch et al., 2004)
Angiogenin (ANG)	14q11.1-q11.2	RNA processing	(Greenway et al., 2006)
charged multivesicular body protein 2B (CHMP2B)	3p11.2	Vesicle trafficking	(Parkinson et al., 2006)
Polyphosphoinositide phosphatase (FIG4)	6q21	Vesicle trafficking	(Chow et al., 2009)
D-amino-acid oxidase (DAO)	12q24	Excitotoxicity	(Mitchell et al., 2010)
Ataxin 2 (ATXN2)	12q24.1	RNA processing	(Elden et al., 2010)

Matrin 3 (MATR3)	5q31.2	RNA processing	(Johnson et al., 2014)
Sigma receptor 1 (SIGMAR1)	9p13.3	Calcium homeostasis	(Luty et al., 2010, Al-Saif et al., 2011)
Spatacsin/spastic paraplegia 11 (SPG11)	15q14	Unknown	(Orlacchio et al., 2010)

1.1.2.2 Oxidative stress

Oxidative stress is a mechanism in which cell damage is induced by excessive reactive oxygen species (ROS). ROS are produced normally as part of cellular metabolism and they maintain cellular homeostasis. However, increased production of ROS may cause damage to several cellular components such as proteins, lipids and DNA. Thus, increased ROS production might play a critical role in ALS pathogenesis. These highly reactive radicals are inactivated by antioxidants (Ramalingam and Kim, 2012). An antioxidant that is known to be involved in ALS pathogenesis is SOD1. Although SOD1 might not be critical for the development of the nervous system, it is necessary for neuronal survival under oxidative stress, and its absence makes the cells prone to cell death by oxidative stress (Reaume et al., 1996).

1.1.2.3 Mitochondrial dysfunction

Mitochondrial dysfunction is frequently associated with aging and age-related diseases. It was suggested to be involved in ALS pathogenesis through mutation or deletion of mitochondrial DNA (mtDNA) that interrupts its functions (Miquel, 1992, Wiedemann et al., 2002). These include disrupted electron transport chain, mitochondrial calcium buffering, and abnormal mitochondrial morphology. This mtDNA damage can be caused by oxidative stress which also damages the mitochondrial proteins and membrane lipids (Karbowski and Neutzner, 2011). In accordance with that hypothesis, mitochondria transfected with SALS patients' mtDNA showed similar defects to those observed in SALS patients and mouse models (Swerdlow et al., 1998). Mitochondrial dysfunction can be also caused by accumulation of protein aggregates in mitochondria that cause disruption of mitochondrial fusion (Wang et al., 2009).

1.1.2.4 Excitotoxicity

Excitotoxicity causes neurodegeneration by excessive glutamatergic neurotransmission. Glutamate is the major excitatory neurotransmitter, which is released from presynaptic neurons and activates ionotropic glutamate receptors on the postsynaptic neurons. Postsynaptic receptors are the α-amino-3-hydroxy-5-methyl-4-isoxazolepropionic acid (AMPA) receptor, N-methyl D-aspartate (NMDA) receptor and the kainate (KA) receptor; which then induce an influx of calcium and sodium ions. The ion influx causes depolarization of the neuron and production of action potential. Excitotoxicity is induced by increased glutamate release from the presynaptic neuron (Alexander et al., 2000), decreased glutamate up-take by excitatory amino acid transporters (EAAT) (Maragakis et al., 2004) or increased sensitivity of post synaptic neurons which is caused by either a defect in glutamate receptors (Kuner et al., 2005), or by increased cell vulnerability due to mitochondrial damage (Novelli et al., 1988, Van Den Bosch et al., 2006). Further evidence of the involvement of glutamate excitotoxicity in the pathogenesis of ALS is that Riluzole, which acts as a glutamate neurotransmission inhibitor, is the only partially-effective therapy for ALS (Cheah et al., 2010). However, its effect is modest, which indicates the involvement of other pathways in the pathogenesis.

1.1.2.5 Impaired endosomal trafficking and axonal transport

Endosomal trafficking and axonal transport might play a role in ALS pathogenesis as the distinct structure of neurons make them require proper intracellular trafficking for protein and organelle transport between the dendrites, cell body and axon, and the turnover of membrane proteins (Ferraiuolo et al., 2011). In accordance with that hypothesis, mutations to *ALS2* gene, which encodes for alsin, has been found in juvenile ALS cases. Alsin is involved in nuclear import and export, vesicle transport

and endosomal trafficking. ALS-related mutations in *ALS2* showed a loss of function mechanism (Yang et al., 2001). Furthermore, alsin affects the AMPA glutamate receptor subunit 2 (GluR2), a calcium-impermeable subunit as its loss of function was found to affect the localisation of glutamate receptor interacting protein1 (GRIP1), which regulates the presentation of GluR2 on the synaptic surface. This disturbance of GRIP1 localisation causes decreased presentation of GluR2 on cell surface, which in turn increases calcium permeability and leads to excitotoxicity (Lai et al., 2006). In addition, pre-symptomatic transgenic mouse models expressing mutated human SOD1 at position 93 from glycine to alanine (SOD1G93A), showed impaired axonal transport signs, which indicates the involvement of this pathway in the pathogenesis of ALS (Williamson and Cleveland, 1999, Bilsland et al., 2010)

1.1.2.6 Glial dysfunction

Glial cells are a collective name for cell types present in the central nervous system (CNS) other than neurons. It includes astocytes, oligodendrocytes and microglia. They are involved in myelination, immune response, nutrition transport and homeostatic maintainance of the CNS. Glial dysfunction has been implicated in ALS in two ways. Firstly, neuroinflammation is a mechanism in which neurodegeneration is induced by inflammatory mediators that are secreted from glial cells. Increased levels of cytokines were detected in serum and cerebro-spinal fluid of ALS patients (Kuhle et al., 2009) and secreted from a SOD1 microglia model challenged by lipopolysaccharide (LPS) (Sargsyan et al., 2009). The involvement of immune system in pathogenesis of ALS is further supported by the detection of increased messenger RNA (mRNA) levels of complement system components, which are involved in the innate immune response, in spinal cord of ALS patients. In addition, increased dendritic cells and cytotoxic T-cells were found in ALS patients (Sta et al., 2011).

Secondly, glial cell pathology has been reported as a cause of neurodegeneration (Maragakis et al., 2004, Diaz-Amarilla et al., 2011). Astrocytes extracted from symptomatic SOD1G93A rat model exhibited significant differences compared with astrocytes from non-transgenic littermates and neonatal SOD1G93A. Astrocytes from symptomatic SOD1G93A were lacking the expression of EAAT2 receptor and low Glial fibrillary acidic protein (GFAP) marker. Additionally, they have an increased proliferation capability and have been found to localize with degenerating motor neurons in spinal cord of SOD1G93A mice (Diaz-Amarilla et al., 2011). Furthermore, abnormal microglial morphology and overactivation was observed *in vivo* in SOD1G93A mice that might increase their sensitivity to CNS insults (Sargsyan et al., 2009, Dibaj et al., 2011).

Emerging evidence showed that co-culture of astrocytes from ALS animal models or from FALS and SALS patients with healthy motor neurons led to increased motor neurodegeneration compared to healthy co-cultures (Diaz-Amarilla et al., 2011, Haidet-Phillips et al., 2011, Re et al., 2014). This neurotoxic effect was found to be Bax-dependent, which is a pro-apoptotic molecule from the Bcl-2 family, and caspase-independent, which is involved in apoptosis (Re et al., 2014). These studies indicate that glial cells are involved in the pathogenesis of ALS and could correlate with the progression of the disease.

1.1.2.7 Endoplasmic reticulum (ER) stress

ER stress is caused by inbalanced calcium homeostasis, oxidative stress, increased secretory protein synthesis, protein misfolding, sugar/glucose deficiency or altered glycosylation. In order to survive ER stress, ER undergoes what is called unfolded protein response (UPR) (Swarup et al., 2011). The aim of UPR is to refold unfolded

or misfolded proteins. If this aim could not be achieved, UPR induces protein degradation, in which misfolded proteins are recognised by protein chaperones, such as protein disulphide isomerase (PDI) and immunoglobulin binding protein (BiP). These molecules residing in the ER help in correcting and avert aggregation of misfolded proteins around the ER (Kaufman, 2002). Both PDI and BiP have been found to colocalise with SOD1-positive inclusions. Increased UPR activity has been found in pre-symptomatic and symptomatic SOD1G93A which indicates the involvement of ER stress in the pathogenesis of ALS (Walker and Atkin, 2011).

1.1.2.8 Dysregulated RNA transcription and processing

Dysregulated RNA processing has been proposed to be involved in ALS pathogenesis as mutations in two genes encoding RNA-binding proteins have been identified in some SALS and FALS cases. Transactive response DNA-binding protein 43 (TDP43) and Fused in sarcoma (FUS) protein are ALS-linked proteins and they are involved in RNA processing, transcription, splicing and mRNA transport. The exact mechanism of involvement of these proteins in ALS pathogenesis is undetermined. However, several mechanisms have been suggested which include disruption of axonal mRNA transport, RNA metabolism and nuclear mRNA export (reviewed by (Ferraiuolo et al., 2011).

1.1.2.9 Protein aggregation

Protein aggregates are a hallmark of many, if not all, neurodegenerative diseases. These intracytoplasmic aggregates in ALS mostly localise in the motor neuron but are often detected in glial cells (Chattopadhyay and Valentine, 2009).

Protein inclusions, are non-membranous, stable, detergent-insoluble, and contain poly-ubiquitinated proteins with high molecular weights, which are formed due to

either overexpression of a protein which exceeds the degradation capacity or defective proteolytic pathways (Johnston et al., 1998).

Some diseases feature distinct inclusion structures that might distinguish them from other neurodegenerative diseases. Three inclusion structures have been reported in the motor neurons of ALS patients which are skein-like inclusions, Bunina bodies and hyaline bodies, in which the first structure is the most common and specific to ALS (Wood et al., 2003). ALS distinct skein-like inclusions are Sequestosome 1 (p62)-, and ubiquitin-positive and consist of other different proteins (Deng et al., 2011a). These proteins may vary according to the cause of the disease. It has been found that protein inclusions start as small dot-like or filament-like aggregates that gain size by fusing with other aggregates (Li et al., 2011).

There are three common hypotheses regarding the role of protein aggregates in neurodegenerative diseases. Firstly, protein aggregates have toxic effect on neurons and induce their death. Secondly, the aggregates are formed because of other toxic effects. Finally, aggregates are formed as a defensive response to protect the cells against toxic abnormal proteins (Baloh, 2011). The first two hypothesis are somehow connected and mounting evidences support those hypotheses. More details are discussed below.

1.1.2.9.1 Proteins involved

SOD1 is a 153 amino acid (a.a) protein that is normally expressed as a dimer in the cytoplasm of neurons. SOD1 is an antioxidant that converts superoxide into hydrogen peroxide and oxygen. Mutant *SOD1* is the most studied gene defect in ALS. SOD1-positive aggregates are observed in SOD1-related ALS cases (Chattopadhyay and Valentine, 2009, Polymenidou and Cleveland, 2011). Misfolded SOD1 is not

specific to SOD1-FALS cases, as over-oxidised and aggregated wild type (WT) SOD1 has been reported in a subset of SALS cases (Guareschi et al., 2012).

TDP43 is a DNA-binding protein that is involved in maintenance of several RNA metabolism processes in the nucleus and cytoplasm (Baloh, 2011). It is a 414 a.a protein with a molecular weight of 43 kDa; however, a 37 and 25 kDa fragment have been reported in normal cells. It is predominantly expressed as a soluble monomeric or dimeric protein localised in the nucleus (Ayala et al., 2011). However, it has been found to redistribute to the cytoplasm in ALS and TDP43-positive-FTLD cases, which might induce its aggregation (van Eersel et al., 2011). It is a component of protein aggregates in 90% of ALS (Neumann et al., 2006).

The **FUS** protein, also known as translocation in liposarcoma (TLS), is a 526 a.a RNA-binding protein expressed predominantly in the nucleus and is involved in some RNA processing pathways. Mutations in the *FUS* gene have been detected in FALS cases (Kwiatkowski et al., 2009, Vance et al., 2009). However, FUS-immunoreactive inclusions were detected in all SALS, ALS/FTLD, SOD1-negative FALS cases and even in atypical FTLD cases that are TDP43-negative, but were absent from the SOD1-FALS cases (Deng et al., 2010).

Ubiquitin and p62 are proteins involved in the UPS, which is one of the proteolytic machineries. Ubiquitin is a 76 a.a protein that tags other proteins for different cellular physiological pathways. It binds to the ubiquitin-activating enzyme (E1) that transfers the ubiquitin to an ubiquitin-conjugating enzyme (E2), which either transfers the ubiquitin to an ubiquitin-ligase (E3) or forms a complex with ubiquitin and E3. Those complexes tag the target proteins with one or more ubiquitin molecules, a process called ubiquitination. The poly-ubiquitinated protein is then recognised by

26S proteasome complex, which degrades the misfolded protein. p62 is an ubiquitin-binding protein that is encoded by *SQSTM1* gene and is involved in both the UPS and autophagy degradation pathways (Figure 1.2) (Nijholt et al., 2011, Jansen et al., 2014).

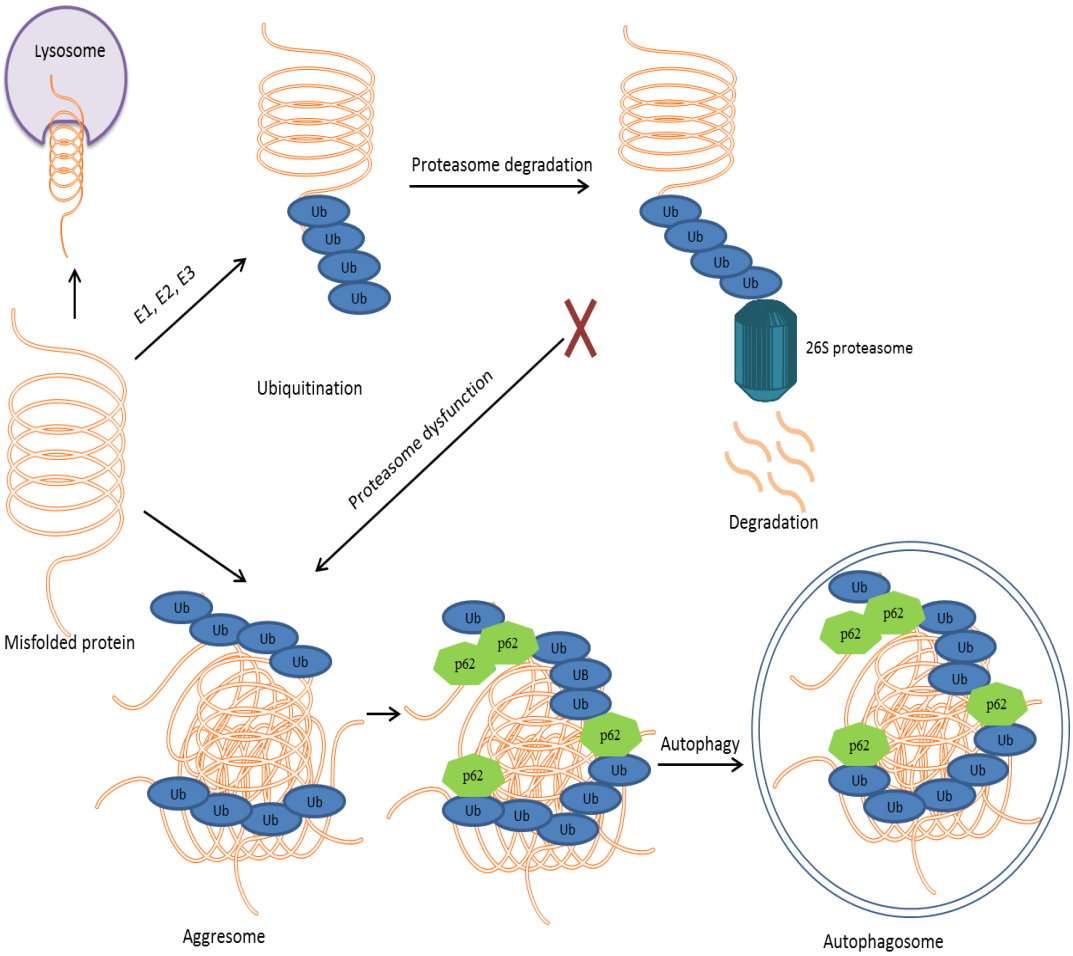

Figure 1.2: Schematic explanation of the two major protein degradation pathways. Misfolded proteins are degraded by ubiquitin-proteasome system, in which the protein is being tagged with ubiquitin Ub, facilitated by the ubiquitin-activating enzyme E1, ubiquitin-conjugating enzyme E2, and the ubiquitin-ligase E3. The ubiquitinated protein is then degraded by the 26S proteasome, or being degraded by autophagy, in which ubiquitinated protein aggregate is further tagged with p62 and engulfed in autophagosome, which is digested by the lysosome. Adapted from (Millhauser, 2007, Clague and Urbe, 2010)

Ubiquilin2 (UBQLN2) immunoreactive inclusions have been found in hippocampus and spinal cord of different ALS cases, including cases without UBQLN2, *SOD1*, *TDP43* or *FUS* mutations (Deng et al., 2011b). UBQLN2 is a member of the ubiquitin-like protein family, which are responsible for ubiquitinated protein degradation via the UPS. It is normally localised in the cytoplasm of different types of cells including neurons. However, it has been shown that under hypoxic conditions cells undergo DNA fragmentation that can be prevented by overexpression of UBQLN2. This might indicate that UBQLN2 play a crucial role in cell survival (Ko et al., 2002).

Optineurin (OPTN) immunoreactive inclusions found in motor neurons of SALS and SOD1-FALS subjects were also TDP43 and ubiquitin-positive (Maruyama et al., 2010, Ito et al., 2011). However, this has been contested by two other groups (Deng et al., 2011a, Hortobagyi et al., 2011), in which the former found that OPTN-immunoreactive inclusions present in all SALS, SOD1-negative and OPTN-negative FALS cases but not SOD1-FALS cases. While the later found that the majority of TDP43-positive aggregates in ALS patients samples were OPTN-negative and none of the FUS-positive or SOD1-positive FALS patient samples was associated with OPTN. OPTN is involved in endocytosis, signal transduction, vesicular trafficking and autophagy (Zhu et al., 2007, Nagabhushana et al., 2010, Chalasani et al., 2014).

VCP is a cytosolic protein that is involved in many cellular processes such as membrane fusion, cell proliferation, nuclear trafficking, protein degradation and endoplasmic reticulum-associated degradation (ERAD). VCP-immunoreactive aggregates were detected in ALS and Parkinson's disease (PD) affected neurons (Ishigaki et al., 2004).

Finally, **c9RAN** is the collective name for C9orf72 repeat-associated non-ATG (RAN) protein products. The protein products of these translations are polyGA, polyGR, polyPR, polyPA and polyGP. Protein aggregates containing some of the c9RAN has been detected in the cytoplasm and nucleus of neurons from C9orf72-ALS post-mortem tissue. The function of these proteins is unknown, nonetheless their expression is toxic and forms intracellular aggregates in a repeat length-dependent manner (Zhang et al., 2014).

1.1.2.9.2 Mechanisms of protein aggregation

The exact mechanism that causes protein aggregation and its involvement in the pathogenesis of ALS is still debated; however, several pathways can be suggested:

Genetic defects

Most SOD1 mutants showed increased vulnerability for hydrophobicity change under denaturation conditions. Increased hydrophobicity induces the formation of small aggregates, which grow in a time-dependent manner (Munch and Bertolotti, 2010).

Recently, ten mutations have been identified in *SQSTM1* gene in ALS patients that occurred in highly conserved regions, and were predicted to have a deleterious effect on p62 structure and function by misfolding the protein, affecting its phosphorylation, protein-protein interactions or ubiquitination (Deng et al., 2011b).

Two mechanisms were suggested for *OPTN*-dependent pathogenesis in ALS. Firstly, mutation in the DFxxER conserved motif of the *OPTN* inhibits its protein binding ability to ubiquitin and subsequently inability to inhibit the nuclear factor kappa B (NF-κB), which is known to play a critical role in cell development and survival (Pizzi and Spano, 2006). Secondly, OPTN is known to be involved in

intracellular trafficking and its mutation might cause disruption of this intracellular trafficking and subsequently cause its aggregation (Maruyama et al., 2010)

Dephosphorylation

Two separate research groups have identified phosphorylation specific sites on TDP43, which are serine residues 379, 403, 404, 409 and 410 (Li et al., 2011, van Eersel et al., 2011). They showed that the unphosphorylated models showed increased or unchanged aggregation and insolubility, while hyperphosphorylation caused significantly decreased aggregation and increased solubility in relation to the number of phosphorylation sites. Expression of Casein kinase 2 alpha (CK2α), which is known to induce phosphorylation, increased the TDP43 solubility and maintained the neuronal cell growth. Same results were observed using transgenic (TG) drosophila (Li et al., 2011). In agreement with that, oxidative stress to neuronal cells induced TDP43 phosphorylation but not aggregation. However, other stressors, including ER stress and proteasome inhibition, showed induced expression and cytosolic aggregation of both TDP43 and its phosphorylated form (Ayala et al., 2011). These results indicated that dephosphorylated TDP43 has a cytotoxic effect on cells. Therefore, it has been proposed that hyperphosphorylation is a defensive mechanism against TDP43 aggregation. However, it is noteworthy that the phosphorylation and ubiquitination occurs after aggregation (Li et al., 2011).

Cytoplasmic translocation

A study showed that stressors like oxidative stress, proteasome inhibition and ER stress induced the translocation of the 37kDa fragment of TDP43 to the cytosol. This translocation was found to be correlated with aggregates formation (Ayala et al., 2011). Cellular stress has been shown to induce phosphorylation of the extracellular

signal-regulated kinase ERK1/2, a known kinase involved in many cellular processes including cell proliferation, growth, survival and gene transcription (Ayala et al., 2011, Cargnello and Roux, 2011) and inhibits transcription factors-nuclear import (Czubryt et al., 2000). However, inactivation of ERK1/2 leads to fragmentation of nuclear TDP43 and increased localisation of TDP43 in the cytosol whether the cells are stressed or not, which means that ERK1/2 is involved in regulation of TDP43 homeostasis and TDP43 cytoplasmic aggregation occurs through some kinase pathway (Ayala et al., 2011).

Interestingly, transfection of yeast cells with human FUS showed cytoplasmic localisation of FUS and this localisation was enough to form FUS aggregates and inclusions. Furthermore, induction of nuclear localisation of FUS by fusing a heterologous nuclear localisation signal (NLS) to the human FUS restricted its expression to the nucleus and was enough to eliminate its aggregation and cytotoxicity, which means that FUS cytoplasmic localisation is enough to induce its aggregation. It is noteworthy that ALS-linked FUS mutations are mostly in the C-terminus, more specifically in the NLS region (see figure 1.3). Collectively, these indicate that FUS aggregation is cytotoxic and its import defect might be involved in the pathogenesis of ALS. Despite the importance of NLS in nuclear localisation, some FUS constructs that lack NLS domain, surprisingly, showed predominant nuclear localisation. This means that a second hit, such as a second mutation or an environmental factor, might be needed for FUS redistribution and aggregation (Sun et al., 2011).

Proteasomal dysfunction

The two main proteolytic machineries are the UPS and autophagy. UPS targets the degradation of soluble and short-lived protein, and it is the main degradation

pathway. On the other hand, autophagy is the bulk clearing mechanism, in which it targets cellular organelles, long-lived aggregated proteins. Both pathways competency declines with age. As ALS is mostly an adult-disease, it is reasonable to say that proteolytic dysfunction could be involved in the pathogenesis of ALS (Jansen et al., 2014).

It has been reported that inhibition of proteasome pathways in primary motor neurons causes redistribution of TDP43 to the cytoplasm and aggregation, while other cellular stressors had no effect on its distribution. This redistribution was accompanied by increased insolubility, molecular weight (~50kDa), ubiquitination and phosphorylation. TDP43 reduction makes the neurons vulnerable, and knocking down TDP43 increases their death. Therefore, it seems that TDP43 distribution is controlled, at least partly, by the proteasome system and that a first hit, such as TDP43 dysfunction, increases the cell vulnerability and a second hit, such as proteasome dysfunction, induces neurodegeneration and vice versa (van Eersel et al., 2011).

UBQLN2 might also take this approach for aggregation as it has been proposed to mediate ubiquitinated-protein degradation by delivering the poly-ubiquitinated proteins to the proteasomes (Ko et al., 2004). In addition, VCP has been found to immunoprecipitate with Dorfin, which is an ubiquitin-ligase (Ishigaki et al., 2004). In support of these findings, a recent study showed that UPS is the main cellular degradation tool for TDP43 that maintains its homeostasis. It has been shown that aggregates form in response to failure of UPS degradation pathway but not due to autophagy inhibition. When UPS is inhibited, the non-degraded TDP43 (both wild type and mutant) accumulate and become insoluble and targeted for autophagy degradation. However, autophagy is unable to compensate for the UPS deficiency, and

therefore aggregates form and toxic protein accumulate in the cell and induce cell death (Scotter et al., 2014).

A further support for the importance of this pathway in the pathogenesis of ALS, the toxic effect and aggregation of c9RAN (polyGA) was found to be via disruption of UPS, which induce ER stress and apoptosis (Zhang et al., 2014).

It is noteworthy that UPS and autophagy are connected pathways and share some modulators like UBQLN2, VCP, OPTN and p62, all have been reported to be mutated or involved in some ALS cases, which emphasize the importance of these pathways in ALS pathogenesis

Prion-like property

Prion diseases are neurodegenerative diseases that are characterised by formation of pathological prion protein aggregates, which are proteolysis-resistant and detergent insoluble. Prion proteins are expressed in several types of cells, including cells from the nervous system, and they are normally localised on the outer surface of the cell membrane (Linden et al., 2008). A recent study showed that upon ER stress or proteasome inhibition, prion proteins import into the cell and partially localise on Golgi compartments, where they cause the formation of detergent insoluble prion protein aggregates (Nunziante et al., 2011).

The main structural characteristic of the disease-related prion proteins is their enrichment of β-sheets, unlike the normal prion proteins that are rich in α-helices. In disease, the α-helices undergo conformational changes to β-sheets that give them a protease resistance property (Baldwin et al., 1994, Biljan et al., 2012). Twenty out of thirty eight identified prion disease-related mutations and polymorphisms occurr in the α-helices regions. In addition, deletion and insertion mutations were identified in

the octapeptide (PHGGGWGQ) repeat region, which is also a glycine-rich domain (Biljan et al., 2012)

Three ALS-related proteins showed similar properties to prion proteins (Figure 1.3). Firstly, the C-terminus of TDP43 shares similarity with prion proteins in the composition of glutamine- and asparagine-rich and can execute conformational changes that cause inactivation and aggregation of the protein (Baloh, 2011, Guo et al., 2011). Purified soluble TDP43 is inherently aggregation-prone and highly prone to conformational changes. In accordance with that, flies transfected with either wild type TDP43 (WT-TDP43) or its mutants showed developmental abnormality, movement defect, axonal swelling, disorganised motor neuron clusters and neuronal loss, which show the toxic effect of overexpression of both WT-TDP43 and its mutants (Guo et al., 2011). Transfection of human embryonic kidney cells (HEK293) with WT-TDP43 or mutant TDP43 showed that only mutant TDP43 causes the formation of detergent insoluble, heat-stable and urea denaturation-resistant high molecular weight phosphorylated aggregates that are ubiquitin-negative (Guo et al., 2011).

It is suggested that the C-terminal domain of TDP43 constituting of 45a.a, which contains the prion-like domain, can form an extended β-sheet. This conformation is enhanced by mutating the alanine residue 314 to threonine (A314T), which explains the neurotoxicity in A314T mutants (Guo et al., 2011). Accordingly, omitting the C-terminus maintained the solubility of the protein while deleting the N-terminal showed protein aggregation that is similar to the full-length protein. This indicates that the C-terminus is critical for protein aggregation (Johnson et al., 2009). Furthermore, HEK293 and neuronal cells transfected with TDP43 with N-terminal deletion showed more tendencies for aggregation (Li et al., 2011).

It is noteworthy that all TDP43 mutations that are associated with ALS/FLTD occur at the C-terminus except one that occurs in the RNA binding domain (Baloh, 2011, Sun et al., 2011).

In addition, FUS shares some similarity with TDP43 but unlike TDP43, FUS consist of two prion-like domains; one is present at the N-terminus and the other one at the first arginine-glycine-glycine (RGG) repeat region (Figure 1.3). Both prion-like domains in addition to the RNA-recognition motif (RRM) domain are necessary to induce protein aggregation and toxicity in yeast and mammalian cells (Sun et al., 2011).

It has been shown that mutated SOD1 in some FALS cases and misfolded WT SOD1 in a subset of SALS cases undergo conformational changes and hence cause neurotoxicity (Chattopadhyay and Valentine, 2009, Bosco et al., 2010). It is noteworthy that although SOD1 contain only one domain; i.e. the Copper/Zinc superoxide dismutase domain, the protein structure is β-sheet enriched (Moreira et al., 2013). In addition, ALS-related *SOD1* mutations mostly occur in the β-sheets and most of the mutations cause conformational changes in the protein (Orrell, 2000).

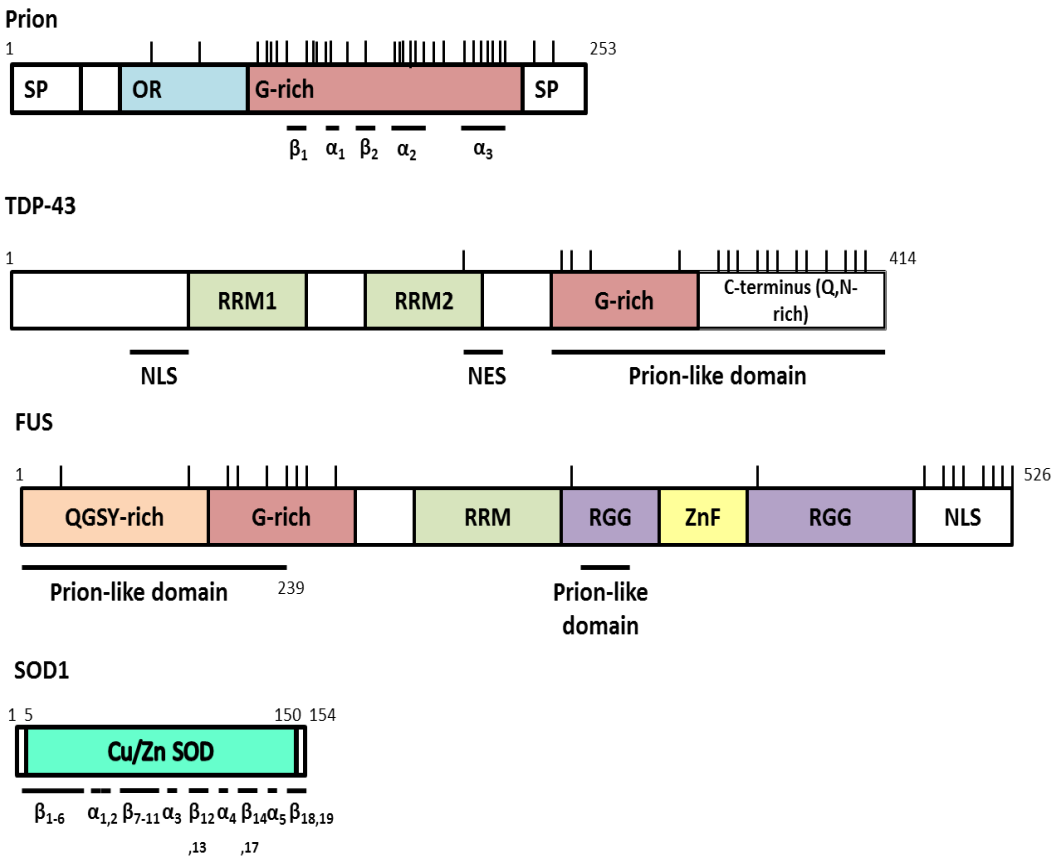

Figure 1.3: Comparison between Prion, TDP43, FUS and SOD1 proteins domains. The differences and similarities between the TDP43 and FUS domains with the prion protein domains are presented. The reported mutation sites in prion disease and ALS are presented as bars above the protein domains. SP; signal peptide. OR; octapeptide repeats region. α; α-helix structure. β; β-sheets structure. G-rich; Glycine rich. RRM; RNA-recognition motif. NLS; nuclear localisation signal. NES; nuclear export signal. Q; glutamine. G; glycine. S; serine. Y; tyrosine. N; asparagine. RGG; arginine-glycine-glycine repeat (Kozin et al., 2001, Millhauser, 2007, DeJesus-Hernandez et al., 2010, Baloh, 2011, Gitler and Shorter, 2011, Sun et al., 2011, Biljan et al., 2012)

The results of those studies show that SOD1, TDP43 and FUS share prion-like properties that may provide them with aggregation ability that is involved in ALS pathogenesis. In addition, prions reproduce by interacting with the normal endogenous prion protein and provoke conformational changes to that normal protein. This might give a clue about how ALS starts in specific cells or locations and spreads to other parts (Polymenidou and Cleveland, 2011).

Recent evidence supports the concept of prion-like propagation of misfolded protein aggregates in different proteinopathies including ALS. Results from pathological studies as well as neuroimaging studies on neurodegenerative diseases support the idea of disease spread along structural brain connections. It was shown that aggregate formation and neurodegeneration starts at specific areas of the brain and progresses through predicted anatomical connections in which misfolded aggregates spread by transsynaptic or transneuronal connection between brain areas (Guo and Lee, 2014, Verstraete et al., 2014, Agosta et al., 2015). Despite the lack of *in vivo* studies, *in vitro* evidence showed that mutant SOD1 and TDP43 can exhibit prion like properties (Chen et al., 2010, Munch et al., 2011, Nonaka et al., 2013). It was shown that inoculation of mutant SOD1 or TDP43 aggregates, which were either produced from recombinant proteins or extracted from ALS-brain lysates, into the culture media lead to their uptake by the cells. The exongenous aggregates worked as seeds that induce aggregation of endogenous, originally soluble, proteins (Chia et al., 2010, Munch et al., 2011, Nonaka et al., 2013).

These studies indicate the involvment of protein aggregates in the progression of the disease. However, the exact cause that induces formation of the first aggrgate “the seed” is still unclear. Interestingly, Munch and colleagues showed that the seeding

capability of mutant SOD1 aggregates is only effective when soluble mutant SOD1 is expressed endogenously. When aggregates are introduced to cells expressing WT SOD1, the seeding effect was not observed (Munch et al., 2011). This could support a two hit hypothesis, in which first induction of protein aggregation and second genetic mutation, serve as factors that increase the susceptibility for neurodegeneration.

In summary, the exact mechanism of ALS pathogenesis is still debated. It has been suggested that two or more hits, for example environmental factors and genetic mutation, are needed to develop the disease (Swarup et al., 2011, Field et al., 2013). Therefore, it is essential to understand the mechanisms involved in the pathogenesis of ALS more in order to find a better treatment. Otherwise, a treatment targeting different aspects of the disease needs to be developed.

1.2 ADP-ribosylation factor-interacting protein (Arfaptin2)

1.2.1 Structure

Arfaptin2, also known as partner of Rac1 (POR1), is a protein consisting of 341a.a with a molecular weight of ~38.6 kDa that is ubiquitously expressed in different types of cells. Arfaptin2 contains a leucine zipper in its N-terminus, which gives it a high positive charge that might allow it to bind to DNA. The C-terminus contains the Bin/amphiphysin/Rvs (BAR) domain, which is present in different proteins that are involved in membrane curvature (Kanoh et al., 1997, Peter et al., 2004).

1.2.2 Function

The exact function of Arfaptin2 is still unknown. However, one can speculate its function by knowing its interaction with known proteins (Table 1.2). Arfaptin2 interacts with the ADP-ribosylation factor (Arf) family proteins and Rac1 protein, which both are subfamilies of small GTPases (Ras superfamily). GTPases

continuously recycle between GTP-bound (active) state and GDP-bound (inactive) state and exert many cellular functions (Figure 1.4).

ARFs are GTP-binding proteins that are involved in intracellular vesicular transport including formation of coated vesicle and cytoskeletal reorganisation (Serafini et al., 1991, D'Souza-Schorey et al., 1997, Man et al., 2011) and transportation between the ER and Golgi (Balch et al., 1992, Kanoh et al., 1997).

Rac1 is a small GTP-binding protein from the Rho subfamily. It is involved in membrane ruffling and actin cytoskeleton rearrangement (Ridley et al., 1992), generation of superoxide, transformation of oncogenic cells and activation of transcription factors in a GTP-dependent manner. Rac has 3 isoforms, in which Rac1 is ubiquitously expressed and is the mostly studied isoform, Rac2 is hematopoietic cells specific and Rac3 is CNS specific. Rac1 is important for foetal development as Rac1 knockdown is embryonic lethal (Sugihara et al., 1998, Corbetta et al., 2005).

In Neuroblastoma cells, Rac1 is involved in growth cone dynamics. Rac1 loss of function mutations caused axonal growth defects in Drosophila (Hakeda-Suzuki et al., 2002, Ng et al., 2002). On the other hand, Rac1 activation in dorsal root ganglion decreases neurite out growth. In addition, it is involved in induction of apoptosis in neuroblastoma cells treated with metformin, a treatment that decrease cancer growth (Kumar et al., 2014). These might indicate a differential functions of Rac1 dependent on cell types and its involvement and regulation of apoptosis (Stankiewicz and Linseman, 2014).

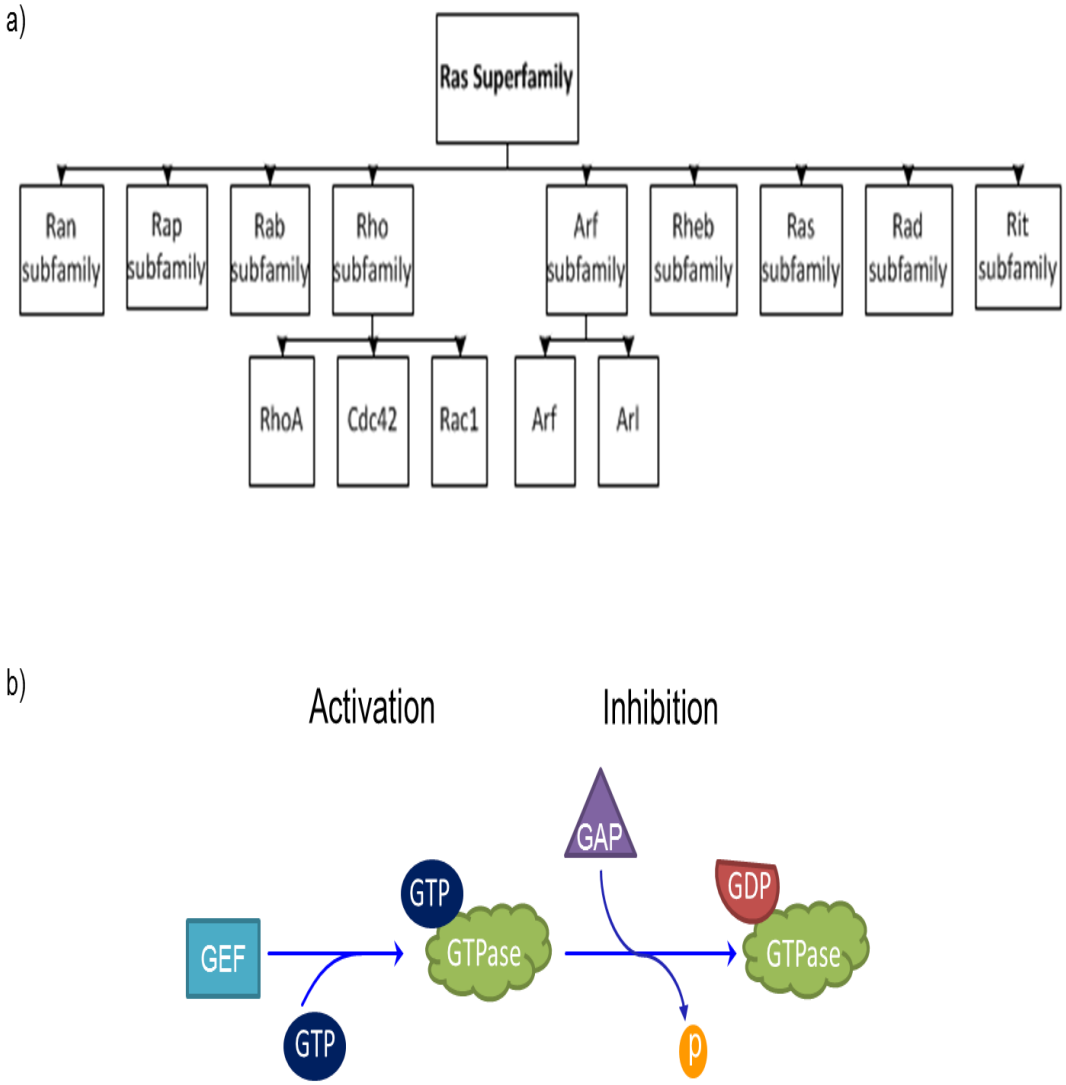

Figure 1.4: Ras superfamily GTPases classification and activation. a) Ras superfamily consist of over 100 molecules, which are subdivided based on homology into 9 subtypes. Rho consists of over 30 proteins of which 3 are most studied (RhoA, Cdc42 and Rac1). Arf family consists of two subtypes, which are Arf and Arf-like (Arl) proteins. b) GTPases are activated by guanine-nucleotide exchange factor (GEF) and deactivated by GTPase-activating protein (GAP).

Arfaptin2 binds to GTP-bound Rac1, which is the active form. Transfection of fibroblasts with the C-terminus half of Arfaptin2 (HC-ARFIP2) caused inhibition of Rac1-induced membrane ruffling (Van Aelst et al., 1996), which indicate that FL-ARFIP2 activates Rac1 while HC-ARFIP2 inhibits it. The HC-ARFIP2 in this study is formed of the last 705bp of Arfaptin2 sequence. In contrast, another study showed that Arfaptin2 binds strongly to GDP-bound Rac1 but not GTP-bound Rac1, while it binds preferentially with GTP-bound ARFs, especially Arf1, Arf5 and Arf6 in Chinese hamster ovary cell line (Shin and Exton, 2001). This controversy could be due to the use of different cell types or the fact that Arfaptin2 was lacking 114-nucleotide from the N-terminal in Van Aelst experiments compared to the full-length Arfaptin2 used in Shin and Exton study.

Arfaptin2 is normally expressed as a cytoplasmic protein that predominantly localises to the perinuclear region and is associated with the microtubule-organising centre, and colocalises with the trans-golgi marker (TGN46) (Peters et al., 2002, Peter et al., 2004, Rangone et al., 2005, Man et al., 2011). This association is facilitated by small GTPases and phosphatidylinositol-4-phosphatase (PI(4)P) (Cruz-Garcia et al., 2013).

Table 1.2: A list of molecules interacting with Arfaptin2 and their functions.

Molecule	Function	Reference
Rac1	Membrane ruffling, actin cytoskeleton rearrangement and regulate ROS production and apoptosis	(Ridley et al., 1992, Suzukawa et al., 2000, Kumar et al., 2014)
Arf1-6	Vesicle trafficking, recruit effectors to the Golgi apparatus, and cytoskeleton organisation	(Serafini et al., 1991, D'Souza-Schorey et al., 1997, Gillingham and Munro, 2007, Man et al., 2011)
Arl-1	Formation of endosomes, endosome-to-Golgi trafficking, and trans Golgi network protein sorting	(Van Valkenburgh et al., 2001, Burd et al., 2004)
PI(3)P	Endosome-derived transport vesicles, autophagy, trans Golgi network protein sorting, and cytokinesis	(Cruz-Garcia et al., 2013, Schink et al., 2013)
PI(4)P	Vesicular trafficking, ER export, autophagy, cytokinesis and actin cytoskeleton rearrangement.	(Cruz-Garcia et al., 2013, De Matteis et al., 2013)
PI(5)P	Induce apoptosis, actin cytoskeleton rearrangement, vesicular trafficking and glucose maintenance.	(Cruz-Garcia et al., 2013, Shisheva, 2013)

- Table obtained from (Mohammedeid et al., 2014) with permission.

1.2.3 Arfaptin2 in neurodegenerative diseases

Only a couple of research groups have studied the involvement of Arfaptin2 in neurodegeneration. However, similar to its function, Arfaptin2 involvement in neurodegenerative diseases can be speculated by understanding the roles of the molecules interacting with Arfaptin2 in neurodegenerative diseases.

Mounting evidence demonstrates the importance of Rac1 in neuronal development and survival (Tahirovic et al., 2010, Stankiewicz and Linseman, 2014). For instance, Fasudil is a Rho kinase (ROCK) inhibitor. Takata et al. showed that fasudil and another Rho inhibitor (Y-27632) have neuroprotective effects on NSC34 overexpressing SOD1G93A. They showed that SOD1G93A expression in NSC34 induces PTEN phosphorylation and decreases Akt phosphorylation and this effect can be reversed via inhibition of ROCK by fasudil (Takata et al., 2013). Furthermore, it has been shown that fasudil delayed the disease onset by approximately 10% in SOD1G93A mice and extended the life span by 6%. In addition, Fasudil treatment decreased motor neuron loss in SOD1G93A mice compared to WT and non-treated animals (Takata et al., 2013, Tonges et al., 2014). This protective effect was through inhibition of ROCK and hence mitigating the decreased Akt phosphorylation caused by SOD1G93A expression (Takata et al., 2013, Tonges et al., 2014).

It is noteworthy that although Rho and Rac fall in the same Rho subfamily, Rho and Rac GTPases work in a reverse manner, in which Rac has a pro-survival effect and Rho has a pro-apoptotic effect (Stankiewicz and Linseman, 2014). Similarly, Rac induced growth cone dynamics while Rho decreases it in neuronal cell line (NG108-15) and in primary neurons (Jain et al., 2004). The prosurvival effect of Rac is believed to be through two pathways, which are PI3K/Akt pathway and PAK/ERK pathway.

In support of the importance of Rac1 in neuronal survival, Alsin protein contains a GEF domain that activates Rac1 (Kanekura et al., 2005) and Rab5 (Otomo et al., 2003). ALS-related mutations to *alsin* gene produce a truncated Alsin protein that causes disruption to Rac1 activity and induce cell death. In addition, SOD1G93A-induced neurodegeneration in NSC34 was reversed by overexpression of Alsin. Furthermore, Rac1 knock down by siRNA reversed the neuroprotective activity of Alsin overexpression and induced cell death (Kanekura et al., 2005). Further support was provided by (Jacquier et al., 2006) as they showed that Alsin is crucial for motor neuron survival and axonal growth in a Rac1-dependent manner.

Another Rac1 activating factor that is involved in ALS pathogenesis is ARHGEF16, which is downregulated in post-mortem spinal cord tissues from SALS patients (Figueroa-Romero et al., 2012).

The involvement of other GTPases in neurodegeneration also has been suggested. Structural bioinformatics showed homology between C9ORF72 protein product and a known Rab GEF called differentially expressed in normal and neoplasia (DENN). Rab is involved in membrane trafficking (Levine et al., 2013). They suggested that C9orf72 is involved in ALS pathogenesis by binding to Rab and disturbing endosomal trafficking or autophagy.

Huntington's disease (HD) is a devastating neurodegenerative disease that is caused by a pathologic polyglutamine repeat expansion in *huntingtin* gene (polyQ-huntingtin). The polyQ-huntingtin pathogenic effect is through disruption of proteasomal activity (Jana et al., 2001). Arfaptin2 has been found to colocalise with huntingtin aggregates in HD cell models. Both full length and the N-terminus of Arfaptin2 induced polyQ-huntingtin aggregation in neuronal cells but expression of

the C-terminal of Arfaptin2 (HC-ARFIP2) showed extensively decreased aggregate formation. This aggregation inhibition was found to be through the proteasome pathway, as inhibition of proteasome pathway by lactacystin reversed the inhibitory effect of HC-ARFIP2 (Peters et al., 2002). In addition, Arfaptin2 expression was found to be increased in the brain of HD mouse (Peters et al., 2002) and patients (Rangone et al., 2005). Arfaptin2 has been found to retain the proteasome function in HD cell models (Peters et al., 2002, Rangone et al., 2005). Therefore, two hypotheses were raised. Firstly, Arfaptin2 is involved in the pathogenesis of HD by inhibiting the proteasome function, whereas its truncated HC-ARFIP2 form works as a negative modulator for the Arfaptin2 (Peters et al., 2002). Secondly, Arfaptin2 is a defence protein that, when phosphorylated, retains the proteasome function and inhibits protein aggregation. It was also suggested that protein aggregates act as both inhibitors and products of UPS inhibition (Rangone et al., 2005).

Another study showed that phosphorylated Arfaptin2 at serine residue 260 (Ser260) can reduce huntingtin aggregation. Insulin-like growth factor 1 decreases the PolyQ-huntingtin neurotoxic effect through phosphorylating Akt (phospho-Akt), which is a prosurvival kinase. The phosphorylated Akt in turn phosphorylates the polyQ-huntingtin. However, Akt has been shown to have another pathway for inhibiting the polyQ-huntingtin neurotoxic effect that is huntingtin phosphorylation-independent. Neuronal cells transfected with *huntingtin* that contain the pathologic polyQ expansion but lack the phosphorylation site showed significantly induced survival and decreased intracellular inclusion formation after treatment with phospho-Akt. It has been shown that phospho-Akt phosphorylates the full-length Arfaptin2 at Ser260. The de-phosphorylation of Arfaptin2 by mutating Ser260 causes its redistribution from the perinuclear region to form a network structure throughout the

cytoplasm in a microtubule-dependent manner. In addition, primary striatal neuron cultures from HD embryonic rats were double transfected with Arfaptin2 and an active form of Akt which showed that Arfaptin2 was phosphorylated by Akt leading to significant increase in survival and decreased protein inclusion formation. This survival was decreased when cells were transfected with a mutant dephosphorylated form of Arfaptin2 (Rangone et al., 2005). It is noteworthy that Ser260 is localised in the C-terminal part of Arfaptin2. The concept of Arfaptin2 involvement in protein aggregation in Huntington's disease is summarised in figure 1.5.

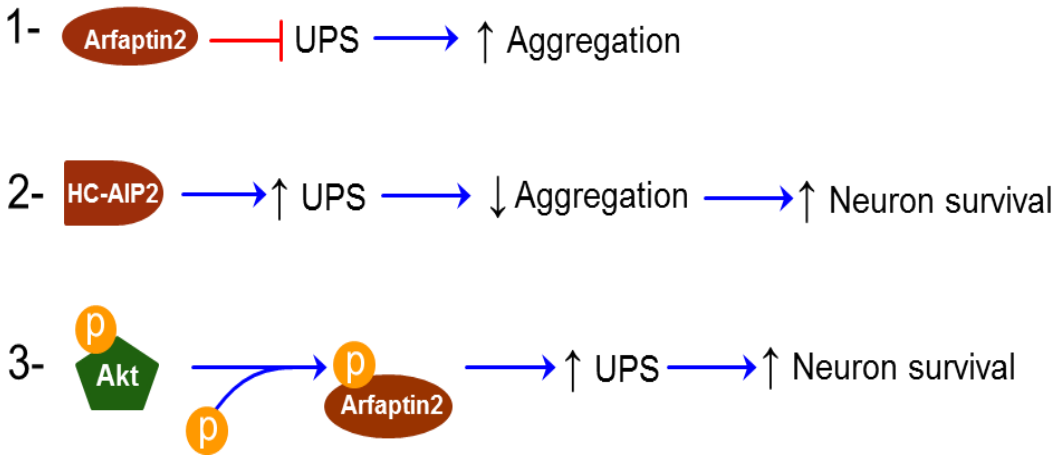

Figure 1.5: A Schematic presentation of possible involvement of Arfaptin2 in protein aggregation. Figure adapted from (Mohammedeid et al., 2014) with permission.

1.3 Hypothesis

Previous studies (Peters et al., 2002, Rangone et al., 2005) showed that Arfaptin2 regulates proteasome activity and protein aggregation in HD. A recent study showed that cytoplasmic inclusions that are immunoreactive for TDP43 coexisted with huntingtin aggregates in two HD cases that developed ALS (Tada et al., 2012). Although huntingtin-immunoreactive inclusions did not colocalise with TDP43 immunoreactive inclusions, their coexistence in some neurons in the spinal cord and motor cortex indicates that aggregation of huntingtin in HD and TDP43 in ALS might have a common pathway. In addition, the presence of TDP43-immunoreactive aggregates in those cases was associated with motor neuronal loss.

Accordingly, based on the finding that full-length Arfaptin2 inhibits proteasome activity and dominant negative form of Arfaptin2 (HC-ARFIP2) activates proteasome activity (Peters et al 2002), we hypothesise that HC-ARFIP2 expression or Arfaptin2 knockdown reduces protein aggregation in ALS via maintaining the proteasomal pathway, which in turn decreases neuron toxicity and improves neuronal survival.

1.4 Aims of the project

The aim of the project is to investigate the effect of Arfaptin2 on protein aggregation and neuronal survival in *in vitro* and *in vivo* ALS models. In addition, we aim to investigate downstream effectors of Arfaptin2/HC-ARFIP2 to identify their targeted pathway and how it correlates with neuroprotection. These would provide evidence whether Arfaptin2 is a possible target for therapeutic intervention in ALS.

Lentiviral constructs expressing FL-ARFIP2 or HC-ARFIP2 genes were generated in order to over-express the proteins efficiently *in vitro*. Subsequently, cells were transduced with the virus and the levels of protein expression were determined

by immunoblotting technique. Finally, FL-ARFIP2 and HC-ARFIP2 will be subcloned into self-complementary adeno-associated virus serotype 9 (scAAV9) to increase the transduction efficiency via systemic delivery to mouse models of ALS. This will be the tool to investigate the effect of FL-ARFIP2 or HC-ARFIP2 expression on protein aggregation in motor neurons and survival in ALS mouse model.

CHAPTER 2: MATERIALS AND METHODS

2.1 Materials

2.1.1 Molecular techniques materials

All competent cells were purchased from STRATAGENE unless otherwise specified. All plasmid preparation and gel extraction kits were purchased from QIAGEN.

All primers for PCR were purchased from Sigma. All restriction enzymes and buffers were purchased from NEB.

Western blot tools, i.e. power supplies, tanks, glass plate, protein ladder and pre-cast gels, were purchased from BIO-RAD.

2.1.2 Common solutions and buffers

Analytical grade solvents ethanol, methanol and isopropanol, and acids were purchased from Fisher Scientific. Nuclease free water (NF-H2O) was purchased from Ambion. Pipette tips were purchased from Fisher Scientific. Components for western blot solutions were purchased from Sigma except beta-mercaptoethanol (β-ME) that was purchased from Invitrogen.

Tris-acetate-EDTA (TAE) buffer

40 mM Tris base, 20mM glacial acetic acid and 1mM EDTA

Separating gel buffer

375 mM Tris base and 0.1% SDS in deionized water (dH_2O), pH 8.8

Stacking gel buffer

125 mM Tris base and 0.1% SDS in dH_2O, pH 6.8

4x Laemlli sample buffer

4 ml glycerol, 2 ml 10% SDS, 0.25 mg bromophenol blue, 2.5 ml stacking gel buffer and 0.5ml β-ME in 10 ml dH_2O

5 x Tris-glycine buffer

25 mM Tris base, 0.2 M glycine in dH_2O

Tris-buffered saline and Tween (TBST)

0.137 M NaCl, 25.92 mM Tris base, 0.1% Tween 20, pH 7.6

Phosphate buffered saline (PBS)

Provided as tablets from Sigma, one tablet dissolved in 200 ml dH_2O

4% Paraformaldehyde (PFA)

4% (w/v) PFA (Sigma) in 100 ml PBS

Western bolt running buffer

25 mM Tris base, 192 mM Glycine, 0.1% SDS and made up to volume with dH_2O

Lysis buffer (RIPA)

50 mM Tris-HCl (pH 7.4), 1% NP-40, 0.5% Na deoxycholate, 0.1% SDS, 150 mM NaCl, 2 mM EDTA and made up to volume with dH_2O

5x Transfer buffer

125 mM Tris base, 960 mM Glycine and made up to volume with dH_2O

2x Hank's buffered salt solution (HBSS)

280 mM NaCl, 100 mM HEPES, 1.5 mM Na2HPO4, pH 7.1

2.1.3 Cell lines and cell culture

Tissue culture flasks and plates were purchased from Thermo Scientific unless otherwise specified.

A stock of HEK293T cells (human embryonic kidney cell line expressing the large T antigen from SV40 virus) in 5% dimethyl sulfoxide (DMSO) was stored in a liquid nitrogen chamber. HEK293T cells were maintained in full medium that is made of Dulbecco's modified eagle medium (DMEM) (with 45 g/L glucose, L-glutamine without Na Pyruvate, Lonza BE12741F or Sigma D5796) with 10% heat inactivated foetal bovine serum (FBS) (Biosera, S1900500) and 1% penicillin/streptomycin (pen/strep) (10000 U/ml, 110000 µg/ml, Sigma, P0781). To thaw the cells, a vial of cells was thawed for 1 min at 37 º C in a water-bath, rapidly suspended in 10 ml of HEK293T full medium, and centrifuged at 500xg for 5 min. The supernatant was discarded and the cell pellet resuspended in 10 ml full medium, cultured in a T75 flask, and incubated at 37˚C with 5% CO2 in an incubator. To passage the cells, the medium was removed and cells were washed with 10 ml PBS. Cells were detached by addition of 2 ml trypsin consisting of 0.053 mM EDTA and 0.005% trypsin in HBSS (Sigma, H8264). The detached cells were resuspended in full medium and split in to four T175 flasks.

Primary motor neurons were maintained in primary motor neurons full medium that was made of Neurobasal-A medium (NB medium) (GIBCO, 10888-022) supplemented with 1% glutamax (GIBCO, 35050), 2% (v/v) horse serum donor (Linaris, SHD3250YK), 2% B-27 supplement (GIBCO, 12587-010) and 0.2µM β-ME).

2.2 Methods

2.2.1 Plasmid DNA isolation preparation

Arfaptin2 and *HC-ARFIP2* were expressed in the pcDNA3 vector with ampicillin resistance property, which were kindly provided from Dr Crislyn D'Souza-Schorey (University of Notre Dame, Notre Dame, Indiana, USA). *HC-ARFIP2* is the C-terminal part of *ARFIP2* from base 510-1026. The *WT-TDP43* was expressed in pDONR221 vector with kanamycin resistance gene (Peters et al., 2002). They were kindly provided by Dr Aaron D. Gitler (University of Pennsylvania, Philadelphia, USA). Stocks of bacterial cells expressing those vectors were kept in 15% glycerol at -80°C. Bacterial cells were inoculated in LB Broth (LBb) (Merck Millipore, 1102850500) with the suitable antibiotic (Table 2.1).

Plasmid DNA was extracted using either QIAprep Spin Miniprep Kit or QIAGEN Plasmid Plus Mega Kit, depending on the volume of the culture, following the manufacturer's protocol.

Plasmid size and purity were detected by loading the samples with DNA loading buffer blue (Bioline, bio37045) on 1% (w/v) agarose gel (MELFORD, MB1200) in 100ml TAE buffer with 0.5µg/ml ethidium bromide (Sigma-Aldrich, E1510). Samples were loaded and electrophoresed in TAE buffer at 140V for ~30minutes (min) using PowerPac 300. The gel pictures were taken using GENi system (SYNGENE, 12834038)

Nucleic acid concentrations were measured using the Nanodrop spectrophotometer (Labtech) with the ND-1000 v3.2.1 software.

Table 2.1: List of antibiotics and their concentrations used in bacterial cultures

Antibiotic	Concentration	Supplier
Carbenicillin (Carb) (substitute for Ampicillin)	50µg/ml	Sigma, C3416
Kanamycin	50µg/ml	Sigma, K4000

2.2.2 Transformation of XL1-Blue cells with Sin-LV-GDNF scAAV-CMV-GFP or plasmids for stock

XL1-blue *Escherichia coli (E.coli)* competent cells were transformed with Sin-PGK-cPPT-GDNF plasmid (Nicole Deglon, CEA Paris, France) (Lentivirus (LV) plasmid) (Figure 2.1) or scAAV-CMV-GFP (self-complementary adeno-associated virus (scAAV) plasmid) (figure 2.2) for stock preparation following the manufacturer's protocol with some amendments. Briefly, the XL1-blue cells were thawed on ice and an aliquot of 50µl of cells was placed in a pre-chilled 14-ml BD Falcon polypropylene round-bottom tube (BD Falcon, 352059). A 0.1-50ng of LV-plasmid was added to the cell aliquot and incubated on ice for 20min. Cells were heat-shocked at 42ºC for 45seconds (sec) and returned to the ice for 2min. A 0.9ml of preheated (42ºC) Super Optimal broth with Catabolite repression (S.O.C) medium (Sigma-Aldrich, S1797) was added to the transformed cells. The cell suspension was incubated at 37ºC with shaking at 225rpm for 30min. Approximately 200µl of cell suspension was spread on LB agar plate (Fisher Scientific, BP1425500) containing Carbenicillin (LBa/Carb). The culture was incubated overnight at 37ºC.

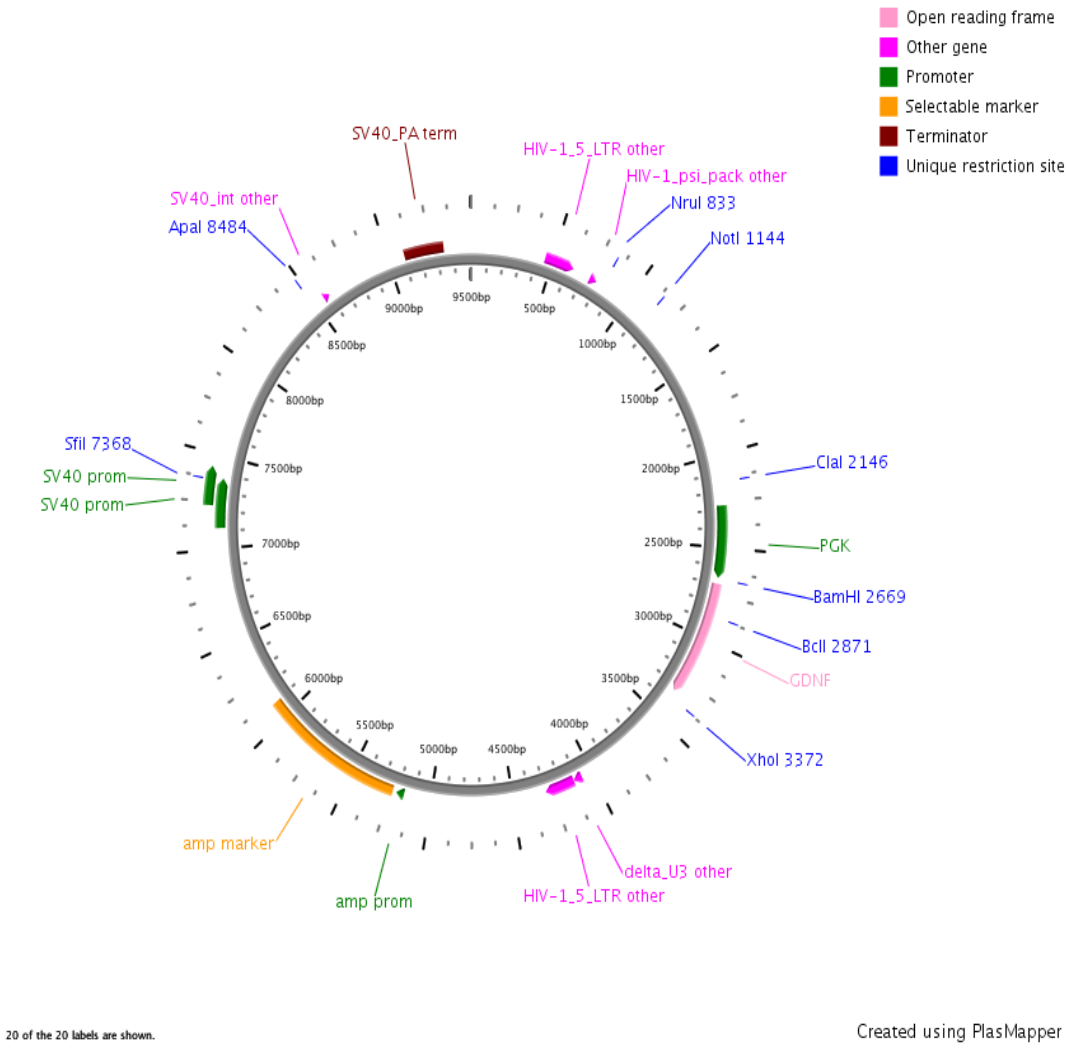

Figure 2.1: Plasmid map of SIN-PGK-cPPT-GDNF plasmid. Produced by PlasMapper version 2.0

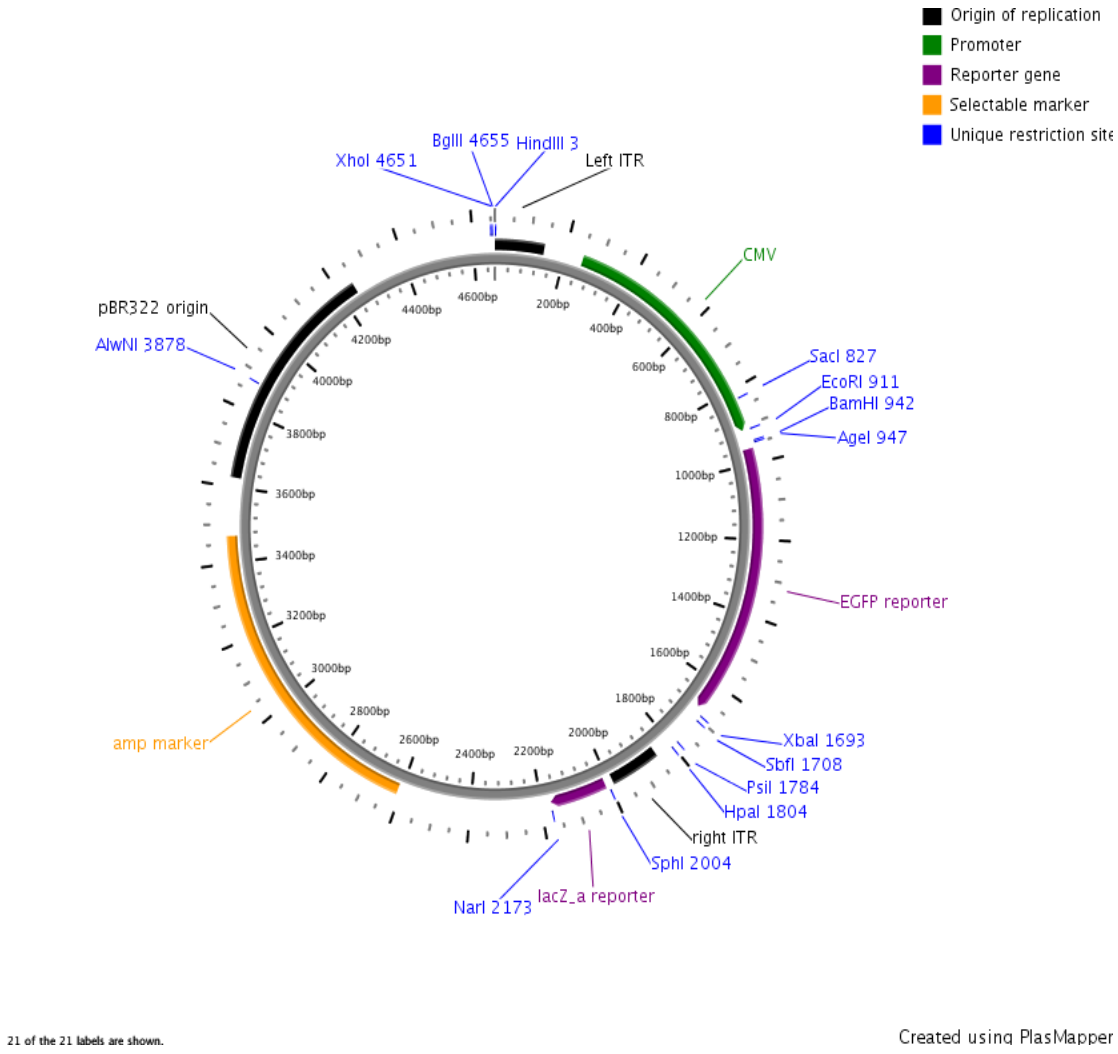

Figure 2.2: A plasmid map of scAAV-CMV-EGFP. Produced by PlasMapper version 2.0

2.2.3 Amplification of DNA fragments by polymerase chain reaction

A 50µl of PCR mix was prepared by mixing 1µl of DNA template, 1µl of 5µM of each primer; forward and reverse; 10µl of FIREPol 5x Master Mix Ready to Load with 7.5 mM MgCl2 (Solis Biodyne, 041200115) and topped up with NF-H_2O. The PCR reaction was performed using a GS2 thermal cycler (G-Storm). The temperature was set at 95ºC for 3min then each cycle was started with denaturation at 95ºC for 30sec, annealing at 60ºC for 30sec and elongation at 72ºC for 30sec, and DNA was amplified in 35 cycles. An extra elongation period for 7min at 72ºC was made and finally held at 4ºC. DNA templates and primers sequences from Sigma are listed in table 2.2.

PCR products were loaded onto 1% agarose gel and electrophoresed at 140V for ~30min. The desired DNA bands were extracted and purified using QIAquick Gel Extraction Kit following the manufacturer's protocol. PCR products were either digested and used directly in the subcloning or cloned into TOPO TA to increase the subcloning efficiency.

Table 2.2: List of DNA templates and primers used for PCR

DNA template	Desired gene	Forward primer	Reverse primer
pCDNA3-Arfaptin2	FL-ARFIP2	GTCTC**AGATCT**GCCACCA TGACGGACGGGATCCTA	ATAAT***CTCGAG***TCAAGCGT AATCTGGAACATCGTATGG GTACTGCTCCTCTAGCCAG G
pCDNA3-HC-ARFIP2	HC-ARFIP2	GTCTC**GGATCC**GCCACCA TGCTCAGCCAGAAGT	
pDONR221-TDP43	TDP43	**GGATCC**GCCACCATGTCT GAATATATTCGG	***CTCGAG***CTACATTCCCCAG CCAGA
For scAAV subcloning			
pCDNA3-Arfaptin2	Arfaptin 2	GTCTC***ACCGGT***GCCACCA TGACGGACGGGATCCTA	ATAAT*TCTAGA*TCAAGCGT AATCTGGAACATCGTATGG GTACTGCTCCTCTAGCCAG G
pCDNA3-HC-ARFIP2	HC-ARFIP2	GTCTC***ACCGGT***GCCACCA TGCTCAGCCAGAAGT	
pDONR221-TDP43	TDP43	GTCTC***ACCGGT***GCCACCA TGTCTGAATATATTCGG	ATAAT*TCTAGA*CTACATTC CCCAGCCAGA

- In bold is BglII. BamHI is bold and underlined. In Bold and italic is the XhoI. In bold italic and underlined is the AgeI. XbaI is Italic and underlined. Underlined is the Kozak sequence. HA-tag is highlighted.

2.2.4 Subcloning of viral vector plasmids

The principle of the subcloning is explained in figure 2.3

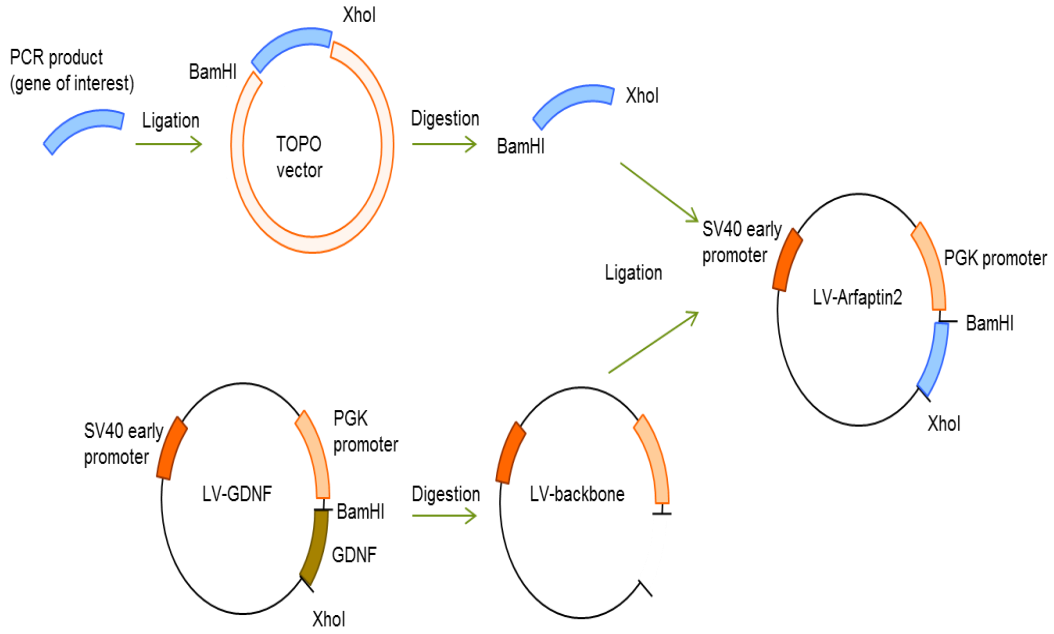

Figure 2.3: Schematic presentation of subcloning principle. Genes of interest were produced by PCR from known plasmids. The PCR products then were ligated to TOPO vector to express the restriction sites. TOPO vectors were then digested with restriction enzymes to extract the gene of interest. The target viral genome was also digested using the same restriction enzymes to linearize the plasmid to allow the gene of interest to ligate into the viral backbone using DNA ligase.

2.2.4.1 TOPO TA cloning and TOP10 cell transformation

PCR products were cloned into One Shot TOP10 chemically competent cells (Invitrogen, C4040-03), using the TOPO TA cloning kit (Invitrogen, K4500-01) following the manufacturer's protocol. Briefly, a TOPO reaction mix was prepared by mixing ~10ng of purified PCR product, 1µl of salt solution (included in the kit) and 50ng of TOPO vector (pCR 2.1-TOPO included in the kit). The mix was incubated for 1hour at room temperature (RT). A further incubation period was performed overnight at 4ºC to increase the yield number of colonies.

A LBa/Carb plate was spread with 40µl of 40mg/ml X-gal (5-Bromo-4-chloro-3-indolyl-β-D-galactoside) (MELFORD, 7240-90-6) and warmed at 37ºC. The X-gal was used for white/blue selection and the 40mg/ml stock was prepared by dissolving 200mg of X-gal in 5ml N,N-dimethylformamide (DMF) (Sigma-Aldrich, 319937) in a glass bottle covered with foil and stored at -20ºC.

TOP10 competent cells were transformed with 4µl of the TOPO reaction mix, incubated on ice for 5min then heat shocked at 42°C for 30sec, and cooled immediately on ice. A 250µl of S.O.C medium was added and incubated at 37°C with continuous shaking at 225rpm for 1hour. A 50µl of transformed cells was spread on the pre-warmed LBa/Carb-X-gal and incubated overnight at 37ºC.

2.2.4.2 Plasmid extraction and analysis by restriction enzymes

Successful transformations were analysed by extracting plasmid DNA from the cells of several colonies using the plasmid miniprep kit as mentioned above. The plasmids were analysed by restriction enzymes following the manufacturer's protocol. Briefly, up to 3µg of the extracted plasmid DNA was digested by mixing it with 2µl of 10xBSA (bovine serum albumin), 2µl NEBuffer (depends on the restriction enzymes compatibility), 0.5µl of each restriction enzyme and topped up with NF-H_2O

to get a total of 20µl mix. The digestion mix was incubated at 37ºC for 2 hours. The digestion mix was mixed with DNA loading buffer blue and loaded on 1% agarose gel. The samples were electrophoresed as mentioned above. Successful insertion of the fragment was further confirmed by sequencing.

2.2.4.3 Extraction of the desired DNA and ligation to virus-backbone

Once the subcloning of the desired DNA in the TOPO plasmid was confirmed, plasmids (LV-plasmid, TOPO, scAAV-plasmid and PCR products) were digested with corresponding restriction enzymes and electrophoresed on 1% agarose gel. The desired bands corresponding to the LV-backbone, scAAV-backbone and the target DNA inserts were extracted and purified using the QIAquick Gel Extraction Kit. The purified viruses' backbones and the inserts were ligated using T4 DNA ligase (NEB, M02025) following the manufacturer's protocol with minor modifications.

Briefly, the required concentration of the insert was calculated using the equation:

$$\text{Weight of insert (ng)} = \text{weight of vector (ng)} \times \frac{\text{size of insert (Kbp)}}{\text{size of vector (Kbp)}} \times \text{molar ratio}\,\frac{\text{insert}}{\text{vector}}.$$

30ng of vector was used and the vector: insert ratios were 1:3 and 1:5. The size of LV-backbone is 8.8kbp and the scAAV-backbone is 3.9kbp. A ligation mix of 2µl T4 DNA ligase, 30ng of LV vector, the required weight of insert, 1µl of T4 DNA ligase and the volume was topped up to 25µl with NF-H_2O. The ligation mix was incubated overnight at 4ºC.

2.2.4.4 Transformation of XL10-Gold competent cells with the ligated DNA

The ligated construct was transformed into XL10-Gold cells following the manufacturer's protocol. Briefly, cells were thawed on ice and 50µl was aliquoted into pre-chilled 14ml BD falcon polypropylene round-bottom tubes. 2µl of β-ME provided

in the kit was added to the cells and incubated on ice for 10min with periodic swirling. 2µl of the ligation mix was added and incubated on ice for 30min. The cells were heat shocked at 42ºC for 30sec then cooled on ice for 2min. Preheated SOC medium (0.9ml) was added and the cells were incubated at 37ºC for 1 hour with vigorous shaking. 200µl of cells was placed on LBa/Carb plate and incubated overnight at 37ºC. Successful transformations were checked by plasmid extraction and digestion as mentioned above and confirmed by sequencing. Plasmid megapreps of the ligated construct from the transformed XL10-gold cells were prepared and stored at -20ºC.

2.2.5 Validation of LV- and scAAV-based plasmid vectors by transfection and western blot

2.2.5.1 HEK293T cells culture

The cells were plated on 6-well plate at a density of 200,000 cells/well on the day prior to transfection. The medium was changed 2 hours prior to transfection. A stock of 1mg/ml Polyethylenimine (PEI) (Polysciences, 24765) was prepared in sterile PBS. Transfection mix was prepared by diluting 2µg of DNA/well in water containing PEI in which the PEI:DNA ratio is 3:1w/w. The mixture was left at RT for 15min then was added to the wells. The cells were incubated for 3 days.

2.2.5.2 Protein extraction

The medium was removed, and the cells were washed once with 1ml PBS. Cells were scraped with sterile cell scraper and resuspended in 1ml PBS. Cells were centrifuged at 500xg for 5min. The cell pellet was lysed with nuclear and cytoplasmic lysis buffer (0.1% SDS, 1% Igepal CA630, 2mM EDTA, 150mM NaCl, 50mM Tris-HCl pH 7.4) supplemented with 7.5% protease inhibitor cocktail (PIC) (Roche

diagnostics, 11836170001) and incubated on ice for 40min. Cells were centrifuged at 13,000xg for 5min and the supernatant was collected and stored at -20ºC.

2.2.5.3 Bicinchoninic acid protein assay

Pierce BCA protein assay kit (Thermo scientific, 23225) was used to determine the protein concentration following the manufacturer's protocol. A serial dilution of standards of bovine serum albumin (BSA) was prepared from a 2mg/ml BSA stock. In a 96-well flat bottom plate, the first well of standard was containing 1mg/ml of BSA diluted in NF-H_2O. Standards were then serially diluted to 1:2 in NF-H_2O.

Samples were diluted to 1:50 in NF-H_2O and 200µl was placed in the first well of each sample. Then the samples were serial diluted to 1:2 in the subsequent wells. Two wells were used as blanks containing NF-H_2O. Samples and standards were done in duplicates. 100µl of BCA working solution was placed in each well. The plate was incubated at 37°C for 30min. The optical density was measured at a wavelength of 562nm using the FLUOstar Omega plate reader (BMG labtech). The standard curve was plotted using Microsoft Excel and the concentration of protein was calculated accordingly.

2.2.5.4 SDS-PAGE gel

A 10% separating gel for sodium dodecyl sulphate polyacrylamide gel electrophoresis (SDS-PAGE) was prepared by mixing 12.4ml distilled water (dH_2O), 9.6ml of 30% acrylamide (National Diagnostic, EC-890), 7.6ml separating gel buffer, 448µl 10% ammonium persulfate (APS) and 20µl TEMED (Sigma-Aldrich, T9281) and loaded into 1.5mm thick SDS-PAGE plate. Once the gel was polymerised, a stacking gel was prepared by mixing 4ml dH_2O, 1.2ml 30% acrylamide, 1.8ml stacking gel buffer, 112µl of 10% APS and 20µl TEMED. The stacking gel was

poured on the separating gel and a comb was placed to form the wells. Precast gels were used when available.

Samples were diluted in NF-H_2O in order to contain 10µg or 20µg of total protein. A 4x loading buffer was added and incubated at 95ºC for 5min. 20µl of samples were loaded onto the gel. The marker used was Precision Plus dual colour standards. The gel was electrophoresed in running buffer (prepared from 10x stock; 25mM Tris-base, 250mM glycine, and 0.1% SDS in dH_2O) at constant voltage 50V until the protein pass through the stacking gel then the voltage was increased to 120V.

2.2.5.5 Immunoblotting

The protein gel was blotted to a polyvinylidene difluoride (PVDF) transfer membrane (Millipore, IPVH00010), which was soaked in methanol before being placed on the gel. A transfer sandwich was electrophoresed in transfer buffer that was prepared from 1x transfer buffer with 15% methanol. The transfer was run at 250mA for one and half hours.

The membrane was blocked with 5% milk in TBST (5% milk-TBST) buffer by incubating at RT for at least 1 hour. The membrane was probed with primary antibody (list of primary antibodies used in table 2.5) in 5% milk-TBST. The blocker solution was removed and the primary antibody was added and incubated overnight at 4°C. The primary antibody was removed and the membrane was washed 3 times with TBST for 10min each wash. The secondary antibody (HRP-goat anti-rabbit or HRP-goat anti-mouse) was diluted to 1:3000 in 5% milk-TBST and placed on the membrane, which was then incubated for 1 hour at RT. The secondary antibody was removed and the membrane was washed three times with TBST for 10min each wash.

The stain was developed by EZ-ECL Chemiluminescence detection kit for HRP (Biological industries, 20-500-120). The membrane was visualised by G.Box system (Syngen).

The densities of the bands were determined using gene tools from Syngen or ImageJ1.45s software. The protein bands were selected using the selection tool in which a rectangle was drawn around each band. All rectangles were equal in size, narrowly bordering the sides of the widest band to avoid mixing between adjacent lanes but taller than the bands to allow the software to compare the dark bands against the white background. Appropriate exposures of blots were used and overexposure was avoided. The band densities are represented as arbitrary units. The density of proteins in the samples were normalised according to the density of α-tubulin or GAPDH. The expression level was calculated by comparing the normalised levels in the samples with that of the untransfected (UTF) sample.

2.2.6 Virus Production

2.2.6.1 LV production

All steps were performed under sterile conditions in a class II safety cabinet. Protocol has been described previously in (Deglon et al., 2000)

2.2.6.1.1 HEK293T cell culture for LV production

Cells were used at an early passage number (<30). Cells were counted on hemocytometer. Twenty 10cm tissue culture dishes were plated with $3x10^6$ cells/dish and incubated overnight in the incubator.

2.2.6.1.2 Transfection of HEK293T cells with LV-insert plasmid and packaging plasmids

For each petri dish, 1ml of DNA transfection mix containing 13µg pCMVΔR8.92, a packaging plasmid, 3µg pRSV-Rev, a plasmid encoding HIV-1 Rev protein which is essential for viral replication, 3.75µg pMD.G, plasmid encoding the vesicular stomatitis virus G envelope, 13µg of the LV-insert plasmid, 500µl 2x HBSS and topped up to 500µl with water and 0.25M $CaCl_2$ prepared in water. The mix was incubated for 15min at RT and became translucent, then 1ml of the mixture was distributed to each dish and incubated for 6 hours in the incubator. Half of the medium was replaced with fresh full medium and incubated for 72hours in the incubator.

2.2.6.1.3 LV purification and concentration

All tools and centrifuge tubes and buckets were disinfected with 70% ethanol prior to use. All the media from the twenty dishes were pooled into one T75 flask and filtered with 0.45µm filters into a new flask to remove any cell debris. The virus-containing supernatant was placed into 6 Ultra-clear centrifuge tubes (Beckman, 344058) and then placed into the Beckman 115.6 buckets and balanced for centrifugation. They were centrifuged in the Beckman optima L-100K ultra centrifuge (Beckman, 393253) at 19,000rpm for 90min at 4ºC. The supernatant was decanted, and the viral pellet was suspended in 200µl of 1% BSA in PBS. All suspensions were pooled and mixed thoroughly. 50µl aliquots were stored at -80ºC.

2.2.6.1.4 Determining the viral titre using HIV-1 p24 antigen ELISA kit

The HIV-1 p24 antigen concentration was determined using the HIV-1 p24 antigen ELISA kit (Zeptometrix, 0801111) following the manufacturer's protocol.

Viral sample was lysed to 1:10 in lysis buffer provided in the kit. Six serial dilutions of each sample, including dilution factors of 100, 500, 2500, 12500, 62500 and 312500, were prepared in 1% BSA in PBS. Five 1:2 serial dilutions of p24 antigen standards were prepared in the assay diluent starting with 125pg/ml. A wash buffer was prepared by diluting the provided 10Xwash buffer in autoclaved distilled water (dH_2O). The provided HIV-1 p24 antibody coated microplate strips were washed with 300µl washing buffer six times. 200µl of duplicate standards and samples were loaded into the wells, keeping 2 wells as blanks. The plate was sealed and incubated at 37°C overnight. Samples were removed and the wells were washed as above. 100µl of detector antibody was placed and the plate was sealed and incubated for 1hour at 37°C. The antibody was removed and excess antibody was washed as above. 100µl of Streptavidin-peroxidase was placed in each well and incubated at 37°C for 30min sealed. The plate was washed again as above. 100µl of substrate was placed in all wells and incubated at RT for 30min. 100µl of stop solution was added and the optical density was detected using the plate reader at a wavelength of 450nm. The standard curve was plotted using Excel (Microsoft office 2010).

After calculating the concentrations of p24 antigen in the samples from the standard curve, the virus titre was calculated by multiplying the concentration of p24 antigen by the dilution factor to determine its concentration in the stock sample:

$$\text{p24 antigen concentration in the viral stock (ng/ml)} = \frac{\text{Optical density (OD)x dilution factor}}{1000}$$

Since 1ng/ml of p24 equals to $1.2x10^4$ transducible unit (TU)/ml, so the viral titre (TU/ml) = p24 antigen concentration x 1.2 x 10^4.

2.2.6.2 scAAV9 production

A protocol has been mentioned previously in (Zolotukhin et al., 1999, Lock et al., 2010) with slight modifications

2.2.6.2.1 HEK293T cell culture for scAAV9 production

For small scale production, a very confluent T175 flask was split as mentioned above into two 150mm dishes (VWR, 734-2322) the day prior to transfection. Cells would be 60-70% confluent on transfection day.

For large scale production, fifteen very confluent 15cm dishes were split into thirty 15cm dishes the day prior to transfection. The cell confluence would be around 80-90% on the transfection day. Cells were grown in HEK293T full medium as mentioned above. For both productions the medium was replaced with serum free DMEM (SF-DMEM) 2 hours prior transfection.

2.2.6.2.2 Transfection of HEK293T cells with scAAV-insert plasmid

Cells were transfected using Polyethylenimine (PEI) protocol in which the PEI:DNA ratio is 3:1 w/w. A stock of 1mg/ml PEI was prepared in sterile PBS. For every 15cm dish a mix of 156µl PEI, 26µg of pHelper, 13µg of pAAV2/9 and 13µg of the AAV-insert plasmids was prepared in 3ml SF-DMEM. The mix was allowed to stand at RT for 15min before being added to the cells. Cells were incubated for about 5days at 37°C before harvesting.

2.2.6.2.3 scAAV harvesting

In small scale production some of the medium was collected in a falcon tube to detect virus content. In addition, cells were scraped and collected in a separate tube for virus content detection. The virus content in the cells was extracted by

homogenizing the cells in 500µl PBS and freeze-thawing the cells 3 times in a dry ice and water bath respectively. Cells were centrifuged at 10,000rpm for 5min to discard cell debris. The supernatant containing the virus was collected in fresh tube and kept at -80°C until validation.

In large scale production the virus was collected from the medium, in which the medium was collected and Benzonase (Sigma, E1014-5KU) was added to the final concentration of 25units/ml. The medium was incubated at 37°C with occasional mixing for 2 hours. Cell debris was removed by centrifugation for 5min at 500xg and the supernatant was further filtered with Nalgene filter unit with 0.22µm pore membrane (Thermo scientific, 595-3320).

2.2.6.2.4 scAAV concentration

The virus was concentrated by centrifugation in Amicon Ultra-15 centrifugal filter Unit with Ultracel-100 membrane (Millipore, UFC910024) at 3800xg at 4°C until the required volume was achieved.

2.2.6.2.5 scAAV purification by iodixanol density gradient

Different concentrations of iodixanol solutions (stock is 60% w/v) (Sigma Aldrich, D1556-250ML) were prepared in PBS with 1mM $MgCl_2$ and 2.5mM KCl (PBS-MK). The PBS-MK stock is prepared as 5x concentration. The solutions were prepared in 50ml falcon tube as follows:

- 15% Iodixanol: 12.5ml iodixanol was diluted with 10ml 5xPBS-MK 10ml of 5M NaCl and topped up to 50ml with sterile water.
- 25% Iodixanol: 20.8ml of iodixanol was diluted with 10ml 5xPBS-MK with phenol red and topped up to 50ml with sterile water

- 40% Iodixanol: 33.3ml iodixanol was diluted with 10ml 5xPBS-MK and topped up to 50ml with sterile water.
- 54% Iodixanol: 45ml iodixanol was topped up with sterile water and phenol red.

In Quick-Seal centrifuge tube (Beckman Coulter, 344326) gradient solutions were added using 10mm 18G blunt-end needle (Hamilton, 7750-09) in the following order: first the concentrated virus solution was placed in the bottom of the tube. Then the 15% iodixanol solution was added to the bottom of the tube. Next the 25% iodixanol solution was placed in the bottom. After that the 40% iodixanol was placed in the bottom of the tube. Finally, the 54% iodixanol solution was placed at the bottom of the tube and any space left was filled with PBS and bubbles were removed. The tube was sealed using a sealing device (Beckman Coulter, 358312). The tube was ultra-centrifuged using 70Ti rotor (Beckman coulter) at 69,000rpm at 18°C for 1.5 hours without brake. The 40% fraction (clear solution) was collected in 500µl aliquots in 1.5ml eppendorf tubes using a 19G syringe.

2.2.6.2.6 Fraction analysis and SYPRO Ruby staining

6µl of each fraction was diluted with water and Laemmli loading buffer (4x) and run on SDS-PAGE. SYPRO Ruby staining (molecular probes, S12000) was done following the manufacturers basic protocol, in which a fixative solution was prepared containing 50% methanol and 7% acetic acid diluted in dH_2O, and a wash solution was prepared by mixing 10% methanol and 7% acetic acid in dH_2O. The SDS-PAGE was placed in a 15cm dish and fixed twice in 60ml of fixative solution for 30min each with continuous agitation at RT. The gel was then stained with 60ml of SYPRO Ruby staining overnight with continuous agitation at RT protected from light. The gel was washed with 60ml of wash solution for 30min with continuous agitation. The gel was

transferred into a clean plate and rinsed with dH_2O twice for five minutes each. The gel was viewed under UV light using GENi. Fractions showing the three AAV capsids purely without other bands were pooled and considered as a high quality virus prep, while the rest are considered as a low quality virus prep.

2.2.6.2.7 scAAV desalting

The pooled fractions were concentrated and desalted by centrifugation in Amicon Ultra-15 filters with PBS with 35mM NaCl at 3000xg at 4°C. Centrifugation was repeated and PBS-NaCl was added each time until the solution becomes clear. Viral solution was collected and aliquoted into eppendorf tubes and kept at -80°C.

2.2.6.2.8 scAAV Titration by qPCR

10µM stocks of each primer were prepared. Standards of linearized scAAV-HC plasmid were prepared by serial dilution in NF-H_2O at 10^{-1}, 10^{-2}, 10^{-3}, 10^{-4}, 10^{-5} and 10^{-6}. Serial dilution of scAAV-HC sample was done the same way. Two master mixes were made using two different sets of primers (table 2.3).

For each sample a master mix was as follows:

- 1µl of 10µM forward primer
- 1µl of 10µM reverse primer
- 5µl of SYBR green (x2) master mix (Agilent Technologies, 600828)
- 1µl NF-H_2O

Master Mix was added to 2µl of samples or standards on PCR plate. Water was used as blank. Samples and standards were done in duplicates. The plate was sealed and qPCR was run for 35 cycles of 95°C for 5min, 95°C for 10sec and 60°C for 30 sec. Data was analyzed on Biorad CFX manager software version 3.1 and titer was

calculated by multiplying the readings by the dilution factor and by 1000 to get copies/ml.

Table 2.3: Primer sets used for scAAV titration

Primer set	Forward primer	Reverse primer
Set 1 (CMV)	GGTAAATGGCCCGCCTGGCA	GCGTCAATGGGGCGGAGTTGT
Set 2 (HC-ARFIP2)	ATGCTCAGCCAGAAGTCC	GCAGCCTCATACTGTTTCAC

2.2.7 Validation of viral products

2.2.7.1 Transduction of HEK293T cells

HEK239T cells were cultured on a 6-well plate at a density of 100,000cells/well in 2ml full medium and incubated overnight at 37ºC.

For LV transduction, the required volume of virus was calculated using the following equation:

$$\text{volume from virus stock (ml)} = \frac{\text{multiplicity of infection (MOI)x no. of cells}}{\text{viral titre}}$$

The viral vectors were thawed on ice. One ml of the medium was removed from the well and the calculated volume of viral suspension was added to each well. The cells were incubated in the incubator for 6 hours, then fed with 1ml of full medium and incubated for another 72 hours.

2.2.8 In vitro experiments

2.2.8.1 Primary motor neuron culture

Primary motor neurons of mouse embryos were extracted using the immunopanning technique (Ramon-Cueto and Nieto-Sampedro, 1992, Wiese et al., 2010, Graber and Harris, 2013). Technical support was provided by Dr.Ke Ning.

10mm coverslips were placed in 35mm dishes with 4x10mm rings (Greiner bio-one, 627170) and were coated overnight with 5% poly-DL-ornithine hydrobromide (PORN) (Sigma, p-8638) in 0.15M Borate buffered saline pH 8.2 (Fluka analytical, 08059) at 4ºC. The PORN was removed and coverslips were washed with HBSS then the coverslips were coated with 1.5µg/ml Laminin (Invitrogen, 23017-015) that was prepared by diluting 0.75mg/ml Laminin stock in 50mM Tris pH 7.4, in HBSS.

Pregnant mice were sacrificed by cervical dislocation and the embryos were collected at E13. The embryo tails were used for genotyping and the spinal cords were extracted and placed in the dissection buffer (1:1000 β-ME (Invitrogen, 313500) in HBSS). The cells were dissociated with 0.1% trypsin (Worthington, TLR3-3707) by incubating at 37ºC for 15min. Trypsin was deactivated by the trypsin inhibitor (Sigma, T-6522). Motor neurons were then selected by placing the cell suspension in a 12-well plate pre-coated with 1:5000 anti-p75 NGF receptor antibodies (Abcam, ab8877) in 10mM Tris buffer at pH 9.5. Unattached cells were washed off with washing media (NB medium with 0.2µM β-ME), and the motor neurons were detached by depolarising buffer (30mM KCl (Sigma, P9333) and 0.8% NaCl (Sigma-Aldrich, S7653) and plated on the pre-coated coverslips at concentration of 2000-5000cells/coverslip in low volume of primary motor neuron full medium. Cells were

incubated in the incubator for at least 1 hour to allow the adhesion of cells prior to addition of more medium.

2.2.8.1.1 SOD1G93A transgenic mice breeding and genotyping

SOD1G93A mice are common models used for ALS research, expressing the mutation of glycine to alanine at position 93 of human SOD1 (Gurney, 1997). The mice used in this study were generated by backcrossing C57BL/6J TG (SOD1G93A)1Gur congenic mice (Jackson Laboratories) with C57BL/6 mice (Charles River Laboratories) for more than 10 generations. To obtain SOD1G93A-TG and NTG littermates embryos, SOD1G93A male mice were mated with C57BL/6 female mice. The phenotypic characteristics of these mice have been described elsewhere (Mead et al., 2011). Mice were bred and maintained by Dr. Ellen Bennett and Ian Coldicott.

To genotype the mice, DNA extraction was done using QuickExtract DNA Extraction Solution (Epicentre Biotechnologies, QE09050) following the manufacturer's protocol in which DNA extracts from ear clip or tail clip were extracted in 50µl or 15µl of the QuickEXtract solution, respectively, and incubated at 65°C for 1hour then at 98°C for 5 min.

A PCR mix was prepared by mixing 10µl of FIREPol 5x Master Mix, 0.1µl of 50µM stock of each primer (human SOD1 (hSOD1) forward and reverse primers) and mouse IL-2 (mIL-2) primers as controls (Table 2.4), 1µl of the DNA extract and the volume was topped up to 25µl with NF-H_2O. A known positive transgenic (TG) SOD1G93A DNA was used as a positive control and a known non-transgenic (NTG) DNA and NF-H_2O were used as negative controls. The PCR was run as mentioned above. PCR products were analysed using a 2% agarose gel.

Table 2.4: List of primers used in SOD1G93A genotyping

hSOD1 forward primer	CATCAGCCCTAATCCATCTGA
hSOD1 reverse primer	CGCGACTAACAATCAAAGTGA
mIL-2 forward primer	CTAGGCCACAGAATTGAAAGATCT
mIL-2 reverse primer	GTAGGTGGAAATTCTAGCATCATCC

2.2.8.1.2 Primary motor neurons transfection with plasmid DNA

Cell transfection was performed under sterile conditions in a class II cabinet. A transfection mix was made of ~2ng/µl of DNA in serum free Opti-Minimal Essential Medium (Opti-MEM) (GIBCO, 31985-070) and Fugene transfection reagent (Promega, 31812701). Briefly, for each 35mm dish containing 2ml full medium a transfection reagent mix was prepared by mixing 3µl Fugene and 100µl Opti-MEM and left standing at RT for 10-15min, then 1µl of the 0.2µg/µl DNA was added. Each 35mm dish was treated with 100µl transfection medium, leading to a final concentration of 0.1ng DNA/µl.

Cells were incubated at 37ºC with 5% CO_2 overnight and 90% of the media was replaced with fresh full media on the following day, then cells were incubated at 37ºC for a further 3 days. Cells were checked under microscope every day. Then the cells were either treated with 10mM hydrogen peroxide (H_2O_2) or washed with 1ml Dulbecco`s Phosphate Buffered Saline (DPBS) without Ca, Mg (Lonza, 17-512F) and fixed, as detailed below.

2.2.8.1.3 Primary motor neurons transduction with LV

Cell transduction was performed under sterile conditions in class II cabinet specified for LV usage. Cells were transduced with MOI100 at low medium for 2 hours at 37°C. Primary motor neurons full medium was topped up and the cells were incubated for 5days at 37°C. Cells were checked daily and medium was added when necessary.

2.2.8.1.4 Propidium Iodide (PI) Exclusion Assay

A stock of 2M H_2O_2 was prepared by diluting 2.3ml of 30% (w/w) H_2O_2 (MW= 340.1g/mol) (PERDROGEN, 31642) in 7.7ml distilled water (dH_2O). Each 35mm dish was treated with 10µl of 2M H_2O_2 leading to a final concentration of 0.01M. The cells were incubated at 37ºC for 50min. Then 1ml of the medium was removed, and the cells were treated with 5µl PI and incubated at 37ºC for 10min. The medium was removed, and the cells were washed once with 1ml DPBS and fixed.

2.2.8.1.5 Cell fixation

The cells were fixed with 4% paraformaldehyde (PFA) (Sigma-Aldrich, P6148) by placing 1ml PFA in each 35mm dish and incubated at RT for 15min. The PFA was removed and 1.5-2ml autoclaved phosphate buffered saline (PBS) (0.01 M phosphate buffer, 0.0027 M potassium chloride and 0.137 M sodium chloride, pH 7.4)(Sigma, P4417) was placed and the plate was sealed with parafilm and kept at 4ºC until staining.

2.2.8.1.6 Statistical analysis

PI positive and PI negative cells were counted and the sum of them was considered as 100% cell number. The statistical analysis was done using GraphPad Prism 6 version 6.04 software using One-way ANOVA.

2.2.9 Immunofluorescence (IF)

2.2.9.1 Immunocytochemistry

A stock of 5% Triton X-100-PBS was prepared by diluting 5 ml of Triton X-100 (Sigma-Aldrich, X-100) in 95 ml of PBS and stored at 4ºC. A working permeabilization buffer of 0.25% Triton-PBS was prepared by diluting 2.5ml of the 5% Triton-PBS stock in 47.5ml PBS.

The PBS was removed from the plates and 50µl of 0.25% Triton-PBS was placed on each ring of the 35mm dish and incubated for 20min at RT to allow penetration of antibodies. Then nonspecific antigen recognition was blocked with 50µl of blocker, which is made of 10% Goat serum (GS) (Sigma, G-9023) in 0.25% Triton-PBS, for each ring and incubated for 30min at RT.

The primary antibody was diluted in 0.25% Triton-PBS following the concentrations specified in Table 2.5. 30µl of the primary antibody mix was placed on each ring and incubated overnight at 4ºC.

The primary antibody was removed and the cells were washed 3 times for 5min each with 1ml PBS. A secondary antibody mix diluted in 0.25% Triton-PBS with 10% GS (Table 2.6). The nucleus was stained with Hoechst stain (Sigma, 861405), diluted to 1:1000 in the same secondary antibody mix. 30µl of the secondary antibody mix was placed on each ring. The plate was covered with foil and incubated at RT for 2 hours.

The antibody was removed and the cells were washed 3 times for 5min each with 1ml PBS. The coverslips were mounted on glass slides using fluorescent mounting medium (Dako, S3023).

Table 2.5: List of primary antibodies used in immunostaining and western blot

Antibody	**Specificity**	**Dilution factor IF/WB**	**Supplier**
Mouse anti-α-tubulin	Detect the ~60kDa tubulin .Reacts with chicken, gerbil, human, mouse, rat	-/1:5000	Calbiochem, CP06
Mouse anti-Arfaptin2	Reacts with full length human Arfaptin2	1:100/1:1000	Sigma, WH0023647M1
Rabbit anti-SOD1	Reacts with mouse, rat and human full length SOD1	1:100/1:1000	Santa Cruz, sc-11407
Rabbit anti-TDP43	Detects mouse, rat and human TDP43	1:100/1:1000	Cell Signaling technology, 3448S
Rabbit anti-Arfaptin2	Reacts with 15 amino acid peptides from the C-terminal residues of mouse, rat and human Arfaptin2.	1:100/1:1000	Abcam, ab85106
Mouse anti-TDP43	Reacts with full length protein human TDP43	1:200/1:1000	Abcam, ab57105
Mouse anti-hemagglutinin (HA)	Detects YPYDVPDYA (98-106) of HA	1:200/1:1000	Sigma Aldrich, H9658
Mouse anti-SQSTM1/p62	Reacts with mouse, human and rat p62	1:100/1:1000	Millipore, MABC32

Rabbit anti-Calcitonin Gene Related Peptide (CGRP)	Detects rat and human CGRP	1:100/1:1000	Sigma, C8198
Mouse anti-beta III Tubulin (TUJ1)	Reacts with human beta III tubulin	1:200	Neuromics, MO15013
Rabbit anti-LC3	Reacts with human, mouse, rat, bacteria, bovine, porcine, hamster and zebrafish	-/1:1000	Novus biotechnology, NB100-2220
Rabbit anti-Atg13	Reacts with human, mouse, rabbit and monkey.	-/1:1000	Cell Signaling technology, 6940
Rabbit anti-ULK1	Reacts with human, mouse, rabbit and monkey.	-/1:1000	Cell Signaling technology, 8054
Rabbit anti-phospho-Akt (Ser473)	Reacts with human, mouse, rabbit and monkey	1:200/1:1000	Cell Signaling technology, 4060
Rabbit anti-Phospho-4E-BP1 (Thr37/46)	Reacts with human, mouse, rabbit and monkey.	-/1:1000	Cell Signaling technology, 9459

Rabbit anti-hSOD1	Reacts specifically with human SOD1 protein	1:200	Millipore, AB5480
Rabbit anti-PTEN	Recognizes human PTEN when phosphorylated at Ser385	1:200/ 1:1000	Life Sciences, P9182-02R
Rabbit anti-Akt	Detects Akt1 and Akt3 from human, mouse and rabbit	-/1:1000	Cell signaling, 2966

Table 2.6: List of secondary antibodies used in immunostaining and western blot

Antibody	Properties	Dilution factor	Supplier
HRP- goat anti-mouse IgG (H + L)	Reacts with whole molecule mouse IgG	1:3000	Bio-rad, 170-6516
HRP-goat anti-rabbit IgG (H + L)	Reacts with whole molecule rabbit IgG	1:3000	Millipore, 12-348
Fluorescein (FITC)-AffiniPure goat anti-rabbit IgG (H+L)	Reacts with whole molecule rabbit IgG	1:200	Jackson, 111-095-003
Alexa Fluor 350 goat anti-mouse IgG (H+L)	Goat IgG labeled with blue-fluorescent Alexa Fluor 350 dye and reacts with IgG heavy chains and all classes of immunoglobulin light chains from mouse	1:200	Invitrogen, A-11045

FITC-AffiniPure Donkey anti-mouse IgG (H+L)	Reacts with whole molecule mouse IgG	1:200	Jackson, 715-095-151
Alexa Fluor 488 goat anti-mouse IgG (H+L)	Goat IgG labeled with blue-fluorescent Alexa Fluor 488 dye and reacts with IgG heavy chains and all classes of immunoglobulin light chains from mouse	1:200	Invitrogen, A11017

CHAPTER 3: Using Lentivirus-based vectors to investigate the effect of Arfaptin2, HC-ARFIP2 and TDP43 over-expression on primary motor neuron survival

3.1 Introduction

Nucleic acid gene transfer (transfection) to neuronal cells *in vitro* presents a great challenge in research. This is due to the high sensitivity of the neurons to physical challenges and inability to proliferate. Different transfection methods have been developed and improved in order to tackle those issues. These methods include chemical (such as lipofection and calcium phosphate/DNA coprecipitation), physical (such as electroporation and microinjection) transfection methods or viral-based (such as retrovirus, adeno-associated virus and lentivirus) transduction. Each method has its strengths and limitations. However, none of them seems to be effective to be used as a standard in all experiments. Different neuronal models and expected outcomes of experiments might require different transfection method. Different transfection methods for neuronal cells have been reviewed previously (Karra and Dahm, 2010).

The transfection method that was tested in this project was the liposomal transfection method in which FuGene reagent was used. We wanted to overexpress FL-ARFIP2 or HC-ARFIP2 in primary motor neurons and study their effects on primary motor neuron survival. This transfection method led to widespread cell death. Several attempts were tried to reduce cell death caused by stress while handling. Although approximately 2000 cells/coverslip were plated, by the end of transfection incubation period only very few, if any, cells survived. This was observed in mock transfected as well as FL-ARFIP2, HC-ARFIP2 and TDP43 transfected samples. Therefore, survival analysis was not conducted. It was observed that this transfection method was unsuitable for primary motor neurons and therefore, we sought to move onto a different gene transfer method using a viral vector (transduction).

One of the major advantages of using viral based vectors as gene delivery agents is their low toxicity as they are naturally capable of entering the cells without causing

physical stress, which overcomes the problem of transfection. One of the most efficient viral vectors is the LV.

LV is a genus of the *Retroviridae* family. It consists of a double stranded RNA. LV showed the ability to integrate into the genome of non-dividing cells making it perfect for transducing primary motor neurons (Naldini et al., 1996, Gerolami et al., 2000). In addition, it provides sustained long-term gene transfer with high efficiency and low toxicity in cells of the CNS (Blomer et al., 1997). In the recombinant LV, the genes required for their replication have been removed; though handling them still requires biosafety level 2.

LV has been used in gene therapy studies in neuronal diseases, including PD, in which some LV therapeutics went into clinical trials and were proved to be safe (Palfi et al., 2014). LV vectors were used in an *in vitro* ALS model to overexpress antioxidant response element genes (*ARE*) in motor neuron-like cell line (NSC34). The overexpression of those genes was able to decrease the damage caused by oxidative stress and increase survival in NSC34 cells (Nanou et al., 2013). Furthermore, transduction of primary motor neurons using LV-based vectors have been shown to be more efficient and less toxic compared to conventional transfection methods (Bender et al., 2007).

In this project a human immunodeficiency virus (HIV)-based third generation LV vector that is replication-deficient and self-inactivating (Sin) has been used. The gene of interest was under the control of the phosphoglycerate kinase (PGK) promoter, which promotes sustained long-term expression (Zufferey et al., 1998, Gerolami et al., 2000). In addition, the LV vector expresses the central polypurine tract element (cPPT) which enhances the import of the provirus into the nucleus and subsequently induces

genetic integration of the desired gene with the cell's genome, especially in non-dividing cells (Van Maele et al., 2003).

The human influenza hemagglutinin (HA) tag was used as an epitope tag to facilitate the detection of the overexpressed proteins and identify them from the endogenous protein. It is a well-characterised-immunoreactive tag that does not affect the function and expression of the desired gene (Lo et al., 2003). It is short, so it does not affect the packaging capacity of the virus and it is not toxic as GFP (Baens et al., 2006). This tag has been used to facilitate the detection of the desired proteins on western blot and immunofluorescence staining.

3.2 Aim

The aim of this chapter is to evaluate the pro-survival potential of HC-ARFIP2 in primary motor neurons to support what has been found previously by our research group in NSC34 model (Kong, 2011). In order to achieve this aim we needed to produce LV-based vectors to overcome the low transfection efficiency and high cell toxicity in primary motor neurons, which have been observed when using liposomal transfection method, and subsequently investigate the effect of FL-ARFIP2, HC-ARFIP2 or TDP43 overexpression on primary motor neuron survival.

3.3 Results

3.3.1 Construction of LV-ARFIP2, LV-HC-ARFIP2 and LV-TDP43 plasmid vectors

In order to produce a viral vector expressing a gene of interest, the desired gene had to be subcloned into the viral genome backbone that will carry the gene inside the virus particle and mediate its expression in the cells.

3.3.1.1 FL-ARFIP2, HC-ARFIP2 and WT-TDP43 amplified by PCR

Subcloning is the procedure of transferring one gene of interest from one vector into another vector. In this case, the FL-ARFIP2 and HC-ARFIP2 were transferred from a pcDNA3 plasmid containing Arfaptin2 into the Sin-PGK-cPPT vector (hereafter called LV-backbone). All genes that were introduced into the viral vector genome were amplified by PCR. The FL-ARFIP2 and HC-ARFIP2 DNAs were amplified from pcDNA3 plasmid encoding Arfaptin2. FL-ARFIP2 was designed to contain BglII restriction site at the 5'end. The HC-ARFIP2 primer was designed to contain BamHI restriction site at the 5'end. Both primers were designed to contain an HA-tag and XhoI site at the 3'end. The PCR products were run on a 1% agarose gel and the desired bands were purified by DNA-gel extraction kit. The expected size for FL-ARFIP2 is 1kbp and the size of HC-ARFIP2 is ~0.5kbp (Figure 3.1 a).

The WT-TDP43 was amplified from pDONR221 plasmid that expresses the WT-TDP43. The amplified product was visualised on 1% agarose gel and corresponded to the predicted size at 1.25kbp (Figure 3.1 b). It was extracted and purified as above.

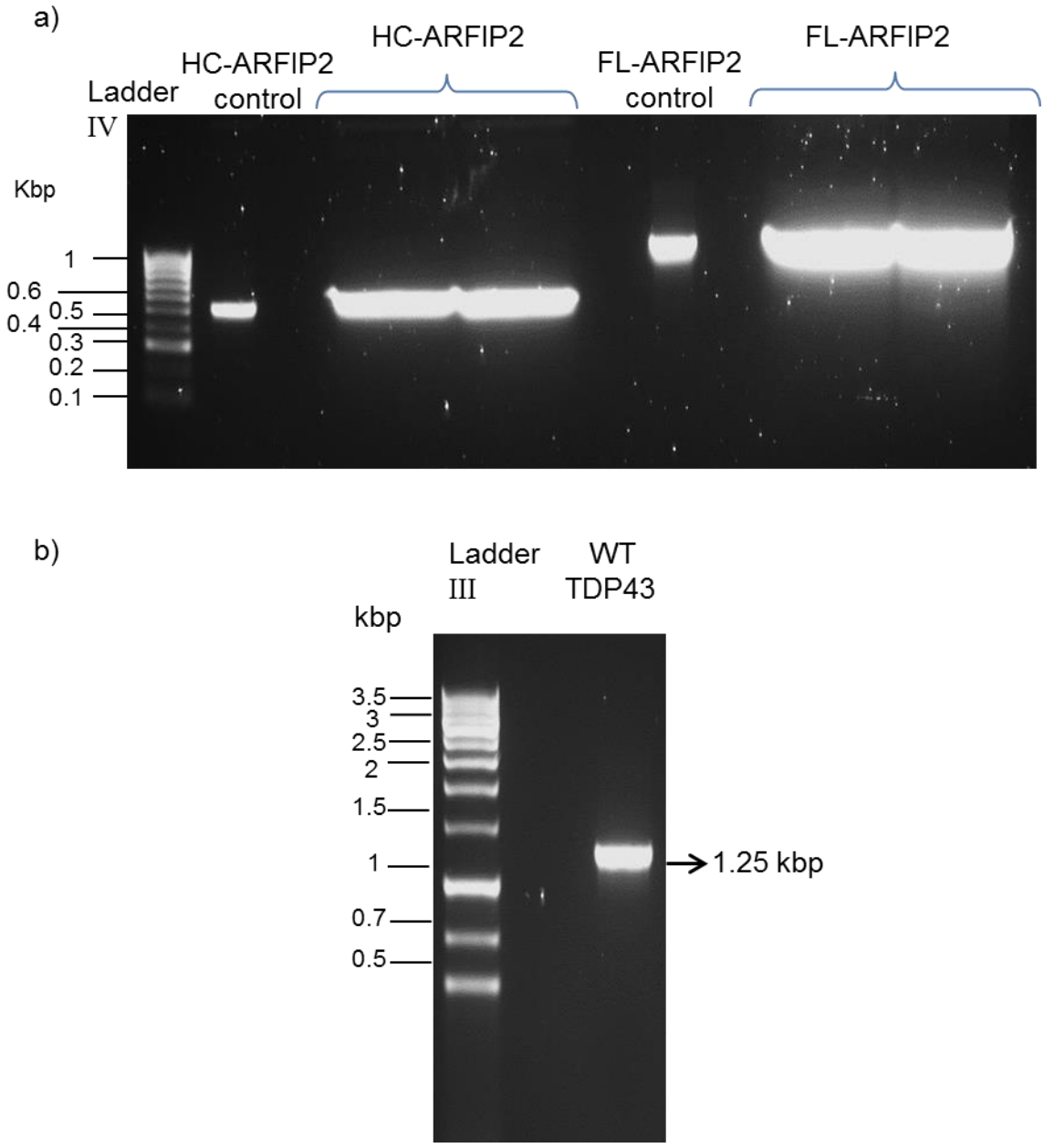

Figure 3.1: PCR products for LV subcloning. a) PCR products for HC-ARFIP2 and FL-ARFIP2 were run on 1% agarose gel. Known HC-ARFIP2 and FL-ARFIP2 samples were used as controls. The purified HC-ARFIP2 DNA is at ~0.5kbp and the FL-ARFIP2 DNA is at 1kbp. b) Amplified PCR product of TDP43 at expected size of 1.25kbp

3.3.1.2 PCR products and LV-backbone digestion

The PCR products of FL-ARFIP2 and HC-ARFIP2 were digested with BglII or BamHI, respectively, and XhoI then purified by QIAquick gel extraction kit (Figure 3.1 a). Accordingly, the Sin-PGK-cPPT-GDNF plasmid was digested with the same restriction enzymes (BamHI and XhoI) to remove the GDNF cassette and to be replaced with the desired inserts (Figure 3.2). LV-backbone at 10kbp was gel extracted and purified by gel extraction kit.

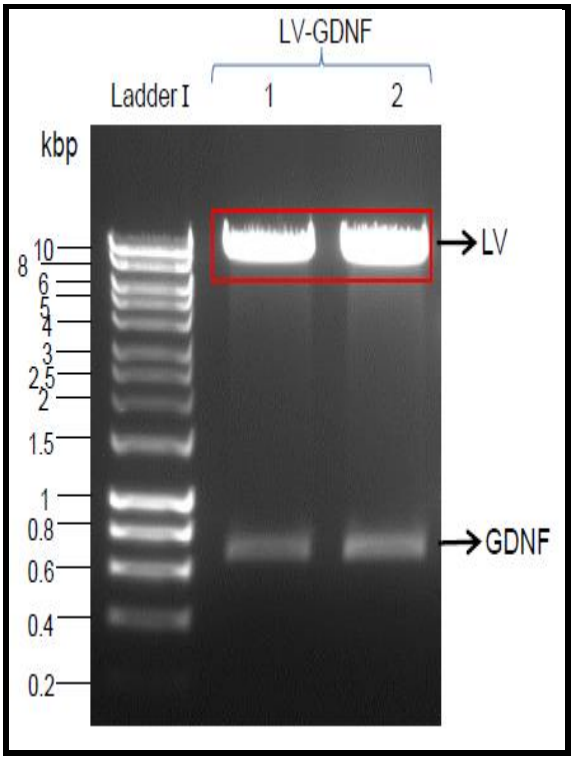

Figure 3.2: LV-GDNF digestion. The LV-GDNF plasmid was digested by BamHI and XhoI. The LV-backbone size is ~10kbp. It was extracted from the gel, purified and measured with Nanodrop.

3.3.1.3 Restriction sites added to the TDP43 construct for subcloning

TDP43 PCR product containing BamHI restriction site on the 5'end and XhoI restriction site on the 3'end was subcloned into TOPO vector using the TOPO TA cloning kit and then transformed into TOP10 *E.coli*. Transformed bacteria were cultured and plated. A Few colonies were picked and cultured to be tested for successful addition of restriction sites to the cDNA. Plasmid minipreps were extracted from the bacterial cultures and were analysed by restriction digest analysis. Plasmid DNAs were digested by BamHI and XhoI. The digested products were run on 1% agarose gels. The upper band at ~4kbp (Figure 3.3) represents the TOPO vector, while the lower band ~1.25kbp represents the TDP43. Figure 3.3 shows the successful insertion of TDP43 into TOPO vector that was successfully digested at the desired sites. Further confirmation was done by sequencing.

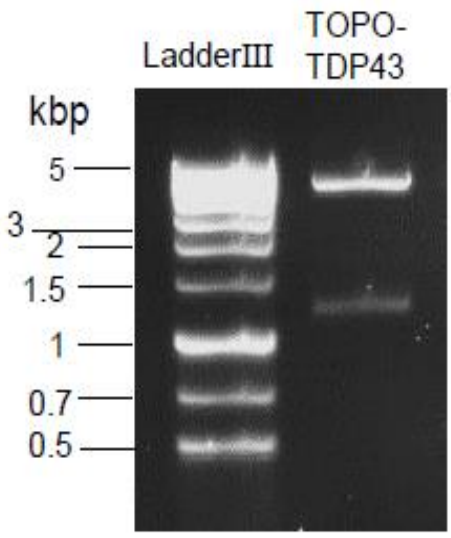

Figure 3.3: TDP43 successful ligation with TOPO vector. Successful expression and digestion of TDP43 with BamHI and XhoI in TOPO vector. TOPO vector backbone ~4kbp while the TDP43 cDNA runs at ~1.25kbp

3.3.1.4 Genes of interest subcloned into the LV plasmid

The target inserts (FL-ARFIP2 or HC-ARFIP2 from figure 3.1a and TDP43 from Figure 3.3) were ligated into the LV-backbone between BamHI and XhoI restriction sites. The ligation mixtures were transformed into XL10-gold *E.coli*. Several colonies from the transformed bacterial cultures were picked and plasmids were extracted using a plasmid miniprep kit. Plasmid-preps expressing successful ligations were analysed using BamHI and XhoI restriction enzymes and visualised on an agarose gel. Figures 3.4, 3.5 and 4.6 show representative plasmid-maps of LV vectors with the inserted FL-ARFIP2, HC-ARFIP2 or TDP43 transgene, respectively. They also show the successful insertion of the genes into the LV as validated by digestion showing LV-backbone at 10kbp, FL-ARFIP2 at 1kbp, HC-ARFIP2 at 0.5kbp and TDP43 at 1.25kbp. Figure 3.6 shows successful insertion of TDP43 into the LV-vector in four colonies (2-5) while colony one was excluded as it was not digested as desired. Correct DNA insertion was further validated by DNA sequencing to confirm that no spontaneous mutations had occurred during the cloning process (see appendices).

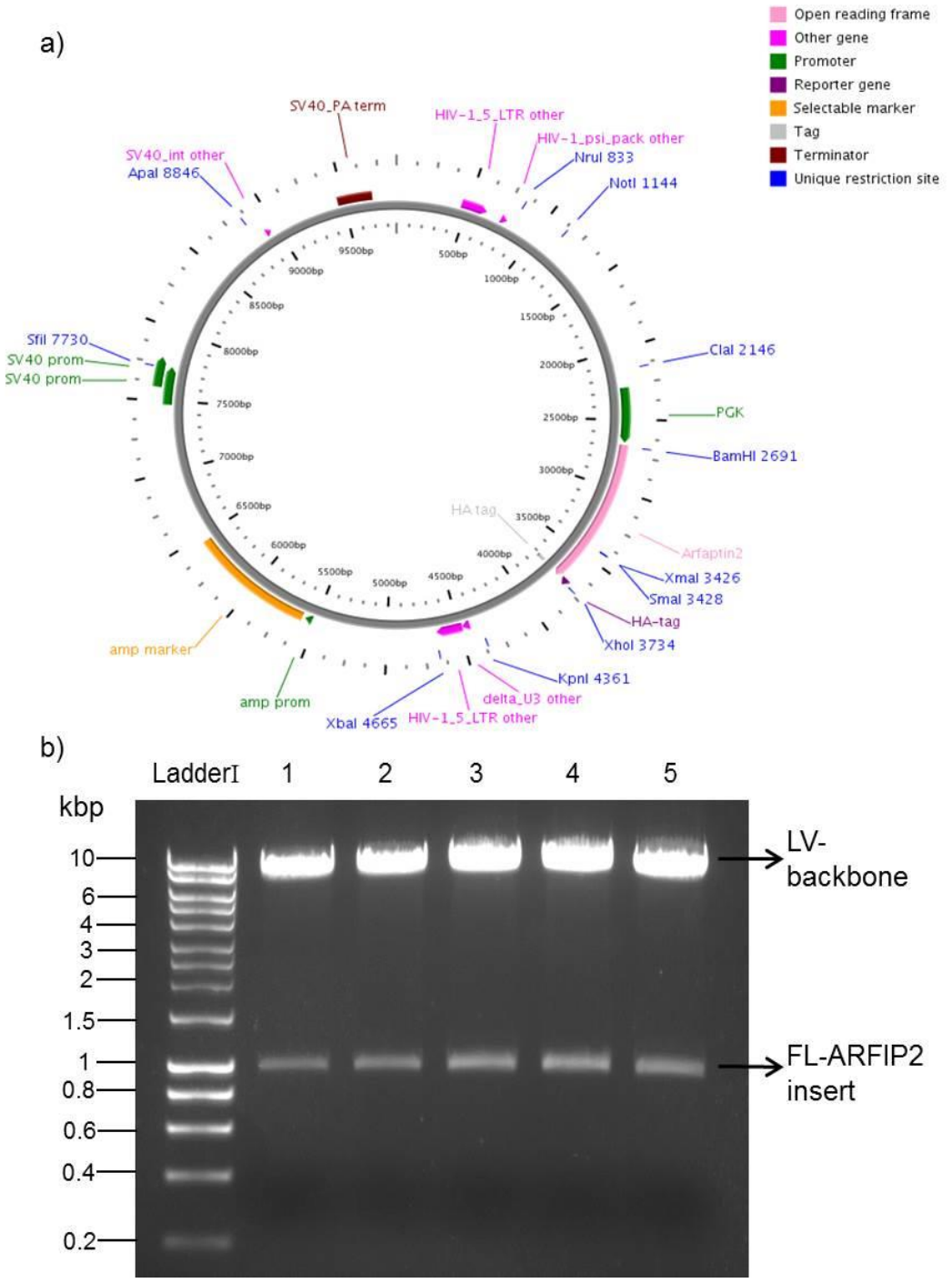

Figure 3.4: Insertion of FL-ARFIP2 into the Lentiviral vector. a) Plasmid map represents the LV-ARFIP2 sequence with unique restriction sites. b) FL-ARFIP2 was ligated into the LV-backbone then plasmid extracts were digested with BamHI and XhoI. The gel image shows successful ligation and digestion at the right sizes in all picked colonies (LV-backbone at ~10kbp and FL-ARFIP2 at 1kbp)

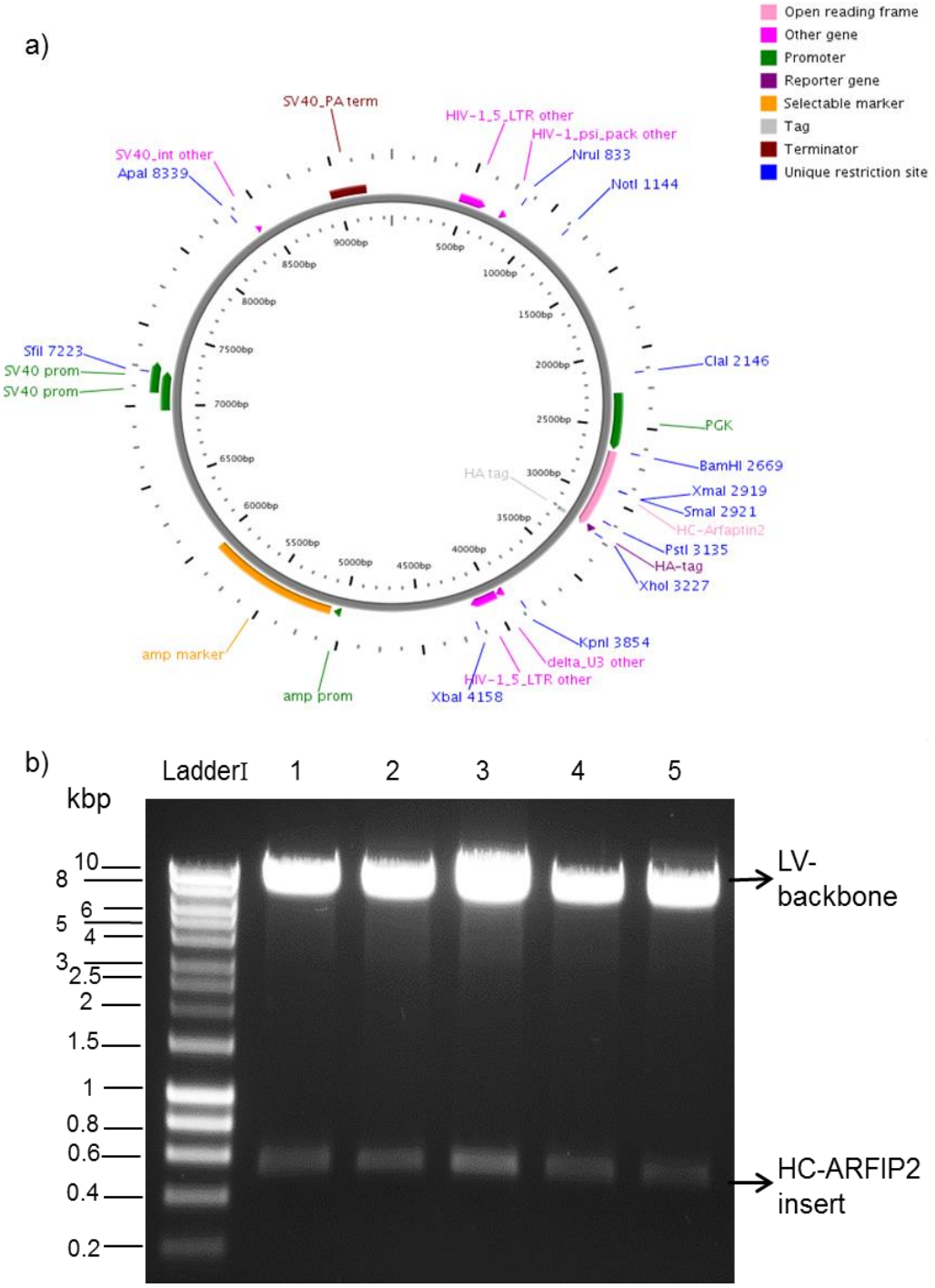

Figure 3.5: Insertion of HC-ARFIP2 into the Lentiviral vector. a) Plasmid map represents the LV-HC sequence with unique restriction sites. b) HC-ARFIP2 was ligated to the LV-backbone and transformed into XL10-gold cells. Plasmid extracts from 5 colonies were digested with BamHI and XhoI. The picture shows successful ligation and digestion at the expected sizes in all picked colonies (LV-backbone at ~10kbp and HC-ARFIP2 at 0.5kbp)

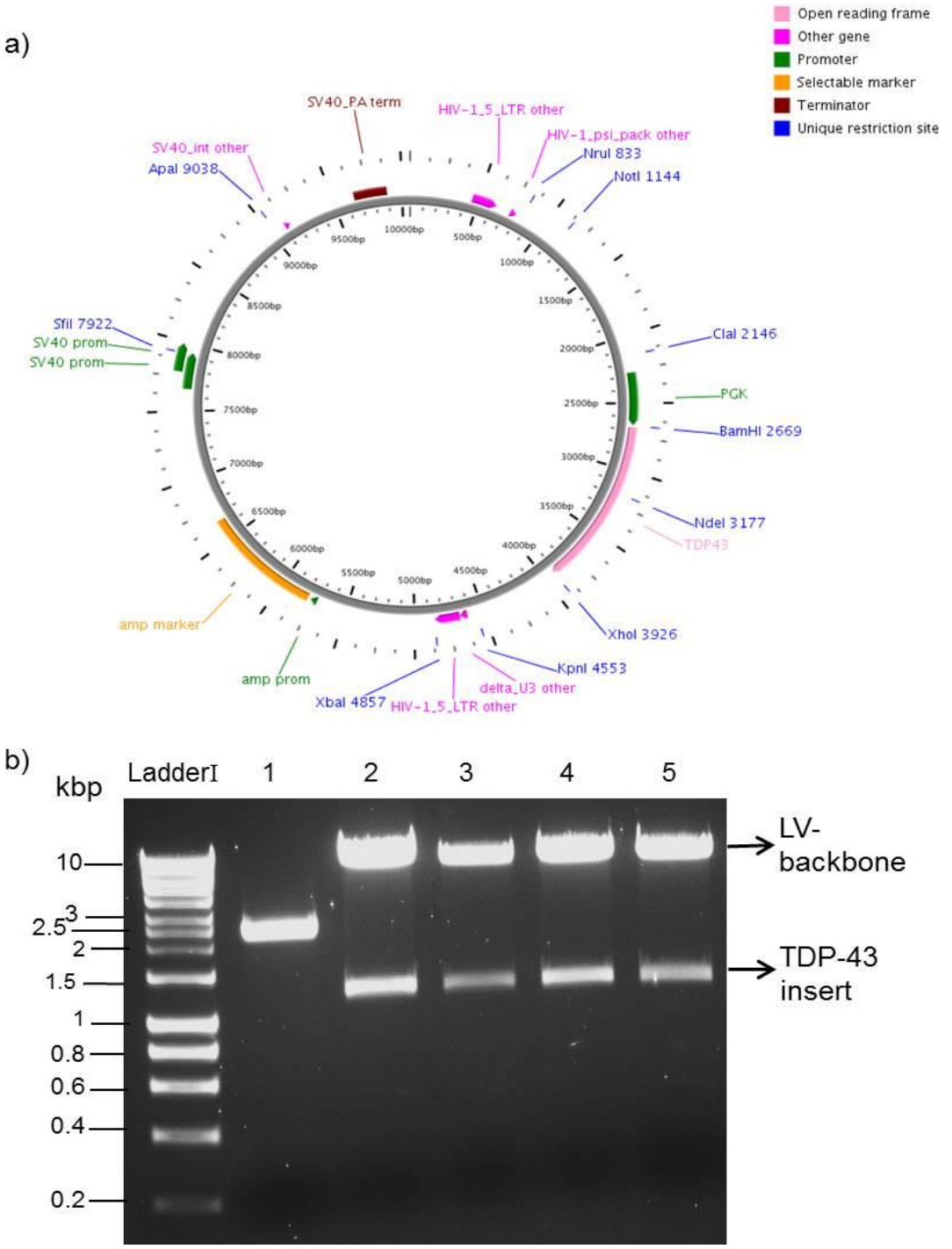

Figure 3.6: Insertion of TDP43 into the Lentiviral vector. a) Plasmid map represents the LV-TDP43 sequence with unique restriction sites. b) TDP43 was ligated to the LV-backbone and transformed into XL10-gold cells. Plasmid extracts from 5 colonies were digested with BamHI and XhoI. The sample number 1 shows incorrect digestion of the plasmid, the rest of the samples showing successful ligation and digestion at the expected sizes (LV-backbone at ~10kbp and TDP43 at ~1.25kbp)

3.3.2 LV-based vectors efficiency testing

3.3.2.1 LV-based plasmids efficiently overexpress the proteins of interest

HEK293T cells were transfected with LV-ARFIP2, LV-HC or LV-TDP43 plasmids in order to confirm the efficiency of the plasmids prior to the viral production. Calcium phosphate or PEI transfection methods were used. The proteins were extracted 3 days post transfection, and the concentrations were determined by BCA protein assay. Expression levels of FL-ARFIP2, HC-ARFIP2 and TDP43 were determined by Western blot assay, using α–tubulin as a loading control. The successful expression of FL-ARFIP2 or HC-ARFIP2 was evaluated by the presence of bands at 38kDa and 19kDa, respectively (Figure 3.7), in the transfected samples compared to the untransfected controls. Figure 3.7 shows successful expression of FL-ARFIP2 and HC-ARFIP2 as they were detected by anti-HAtag antibody.

The TDP43 was detected using rabbit anti-TDP43 antibody as a primary antibody and then stained with HRP-conjugated goat anti-rabbit antibody as a secondary antibody. The successful overexpression of TDP43 was evaluated by comparison of band densities between the transfected and untransfected cells. Comparing the band densities of the LV-TDP43 transfected samples with the untransfected control, the result shows successful overexpression of TDP43 to over 13 fold (Figure 3.8).

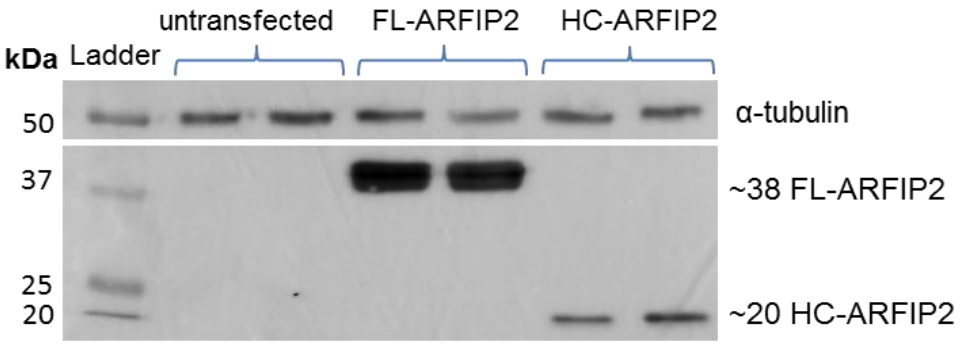

Figure 3.7: Validation of the LV-based plasmids expressing FL-ARFIP2 or HC-ARFIP2. HEK293T cells were transfected with the LV-based plasmids expressing FL-ARFIP2 or HC-ARFIP2. FL-ARFIP2 and HC-ARFIP2 expression was detected on a western blot by mouse anti-HA antibody. FL-ARFIP2 is detected at ~38kDa while the HC-ARFIP2 is detected around 20kDa. α-tubulin was used as a loading control

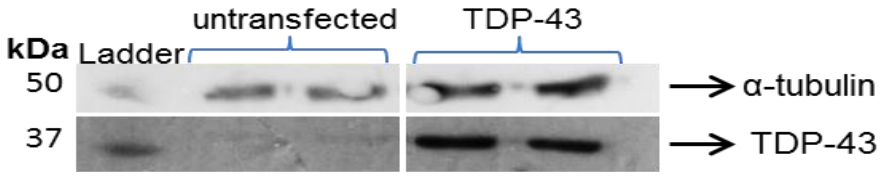

Figure 3.8: Validation of the LV-based plasmids expressing TDP43. HEK293T cells were transfected with the LV-based plasmids expressing TDP43. The TDP43 was detected by rabbit anti-TDP43 antibody at 43kDa. α-tubulin was used as a loading control

4.3.2.2 LV-based viral vectors efficiently overexpress the proteins of interest

Once plasmids were validated, LV-ARFIP2, LV-HC and LV-TDP43 viruses were produced using the 4 plasmid transfection method, in which cells were transfected with two packaging plasmids, one envelope plasmid and a lentivirus vector plasmid expressing our gene of interest (see Section 2.2.6.1 for full details about the plasmids). Viruses were collected from the culture medium, filtered from cellular debris then concentrated using ultracentrifugation. The viral titres were determined using the p24 antigen ELISA kit. Viral titres ranged between 10^5-10^8 transducable units (TU/ml) from which only viruses with high titres (10^7-10^8 TU/ml) were used in transduction assays. To validate the efficiency of the produced viruses, HEK293T cells were transduced with different multiplicity of infection (MOI) of LV-ARFIP2, LV-HC or LV-TDP43. Cells were harvested 5 days post transduction and the protein was extracted and measured as above. Transgene expression was detected by western blotting and measured by densitometry when possible.

Every validation was repeated three times before proceeding with the *in vitro* experiments. Figures 3.9 and 3.10 show that the viruses produced were efficiently overexpressing the desired proteins with both low and high MOIs. They also show that there is a correlation between the MOIs used and the level of overexpression. Figure 3.10 shows that even with low MOI there was approximately 5 fold overexpression of TDP43; while analysis of MOI10 revealed a significant increase of an average of 15 fold of TDP43 (n=3, $p<0.05$) (Figure 3.10b). This step was necessary to confirm the efficiency of the viruses prior to motor neuron transduction. It is noticeable that HC-ARFIP2 expression is relatively much lower than FL-ARFIP2 and TDP43 overexpression. Therefore, higher MOIs of LV-HC were used in subsequent experiments.

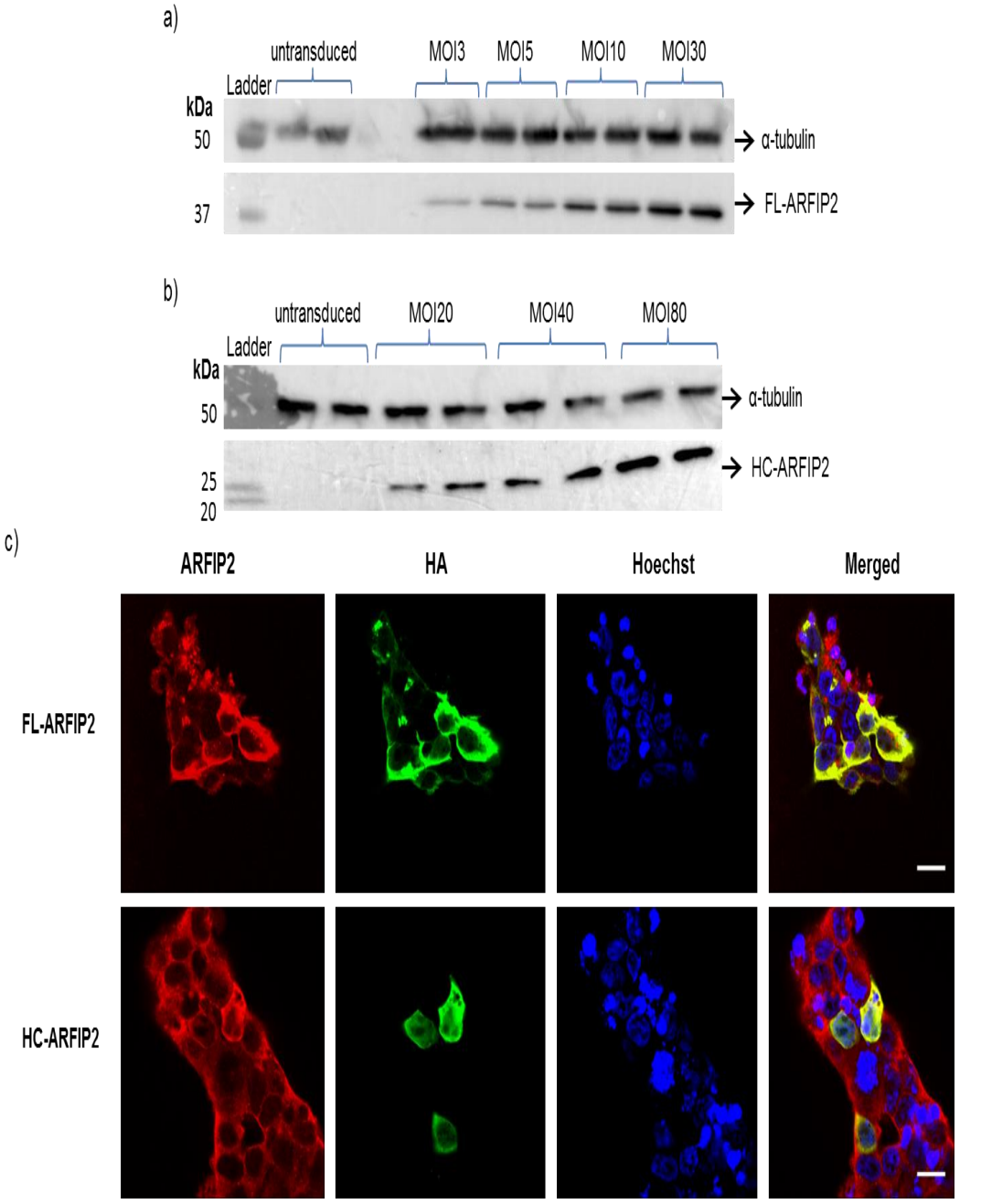

Figure 3.9: LV-ARFIP2 and LV-HC efficiently express FL-ARFIP2 and HC-ARFIP2 in HEK293T cells, respectively. HEK293T cells were transduced with LV-ARFIP2 or LV-HC virus. Protein was extracted 5 days post transduction. Western blot shows the FL-ARFIP2 (a) and HC-ARFIP2 (b) expression detected by anti-HA antibody. There is a correlation between the MOI level and the expression level of FL- and HC-ARFIP2. **c)** Cells were fixed 5 days post transduction, Immunofluorescence shows FL- and HC-ARFIP2 expression detected using anti-HA antibody (green) while endogenous ARFIP2 was detected by anti-ARFIP2 antibody (red). Scale bar = 20µm

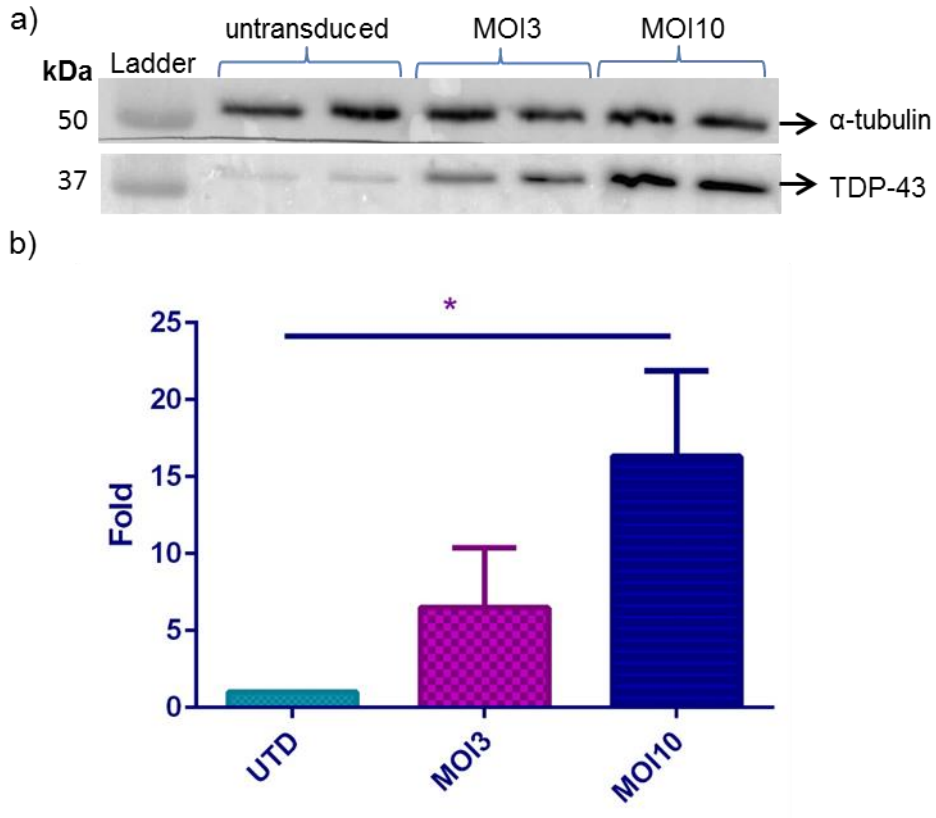

Figure 3.10: LV-TDP43 efficiently overexpresses TDP43 in HEK293T cells. a) HEK293T cells were transduced with different MOIs of LV-TDP43 virus. A representative western blot shows TDP-43 detected using anti-TDP43 antibody. b) The overexpression level (Mean ± SEM) was determined by densitometry of western blot. The TDP-43 expression level was compared between transduced and untransduced samples after normalisation with α-tubulin. Statistical analysis was done using one-way ANOVA test. n=3. * ; p <0.05

3.3.2.3 LV-based viral vectors efficiently express proteins of interest in motor neurons

As a further validation of the LV-based vector efficiency, primary motor neurons were transduced with the viruses and harvested 5 days post transduction for protein analysis. Western blots were probed as above. Figures 3.11, 3.12 and 3.13 show that FL-ARFIP2, HC-ARFIP2 and TDP43, respectively, were successfully expressed at high levels compared to untransduced samples.

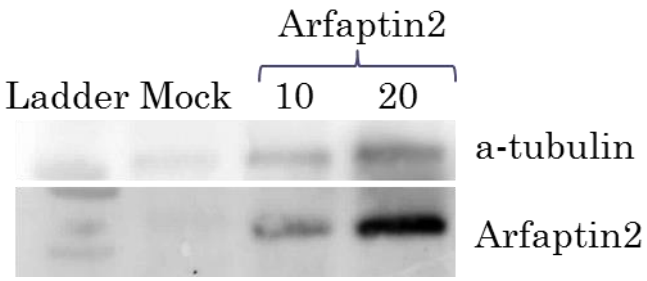

Figure 3.11: LV-ARFIP2 expresses FL-ARFIP2 in motor neurons. Primary motor neurons were transduced with two different MOI levels of LV-ARFIP2 virus. FL-ARFIP2 detected by mouse anti-HA-tag antibody. There is abundant expression of FL-ARFIP2 with both MOIs.

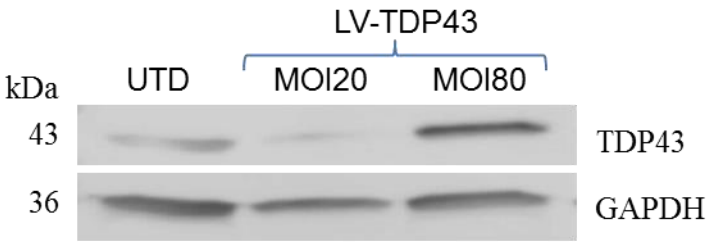

Figure 3.12: LV-TDP43 overexpresses TDP43 in motor neurons. Primary motor neurons were transduced with two different MOI levels of LV-TDP43 virus. TDP43 was detected by rabbit anti-TDP43 antibody, which also detects endogenous TDP43.

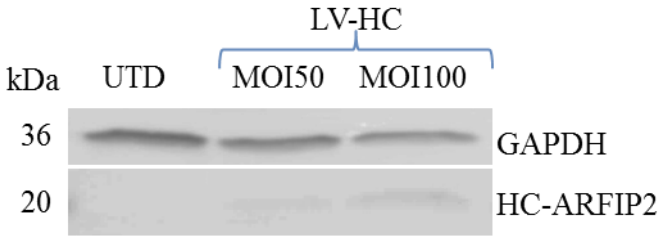

Figure 3.13: LV-HC expresses HC-ARFIP2 in motor neurons. Primary motor neurons were transduced with two different MOI levels of LV-HC virus. HC-ARFIP2 detected by mouse anti-HA-tag antibody.

3.3.3 Increased primary motor neuron survival with HC-ARFIP2 expression

The effect of HC-ARFIP2 over expression on motor neuron survival was determined by propidium iodide (PI) exclusion experiment. The principle of the assay is that PI intercalates between DNA bases and it is a fluorescent molecule that when excited shows red fluorescence. However, it is membrane impermeable. Therefore, viable cells which have intact membrane will be PI negative while dead cells will be PI permeable and therefore will show red nuclei. In other word, cell death was detected by positive PI staining. On the other hand, Hoechst 33342 is a membrane permeable intercalating agent and produces blue fluorescence when excited. Therefore, Hoechst will stain the nuclei of both live and dead cells.

Primary motor neurons from NTG and SOD1G93A TG mouse embryos were extracted and cultured, using immunopanning technique. Cells were transduced with LV-ARFIP2, LV-HC or LV-TDP43 viruses. Five days post transduction, half the culture plates were induced with 10mM H_2O_2 for 50 min to investigate the effect of oxidative stress. Afterwards, all cell cultures were treated with PI for 10 min, and then washed and fixed directly.

Cells expressing FL-ARFIP2 and HC-ARFIP2 were detected by immunofluorescent staining with anti HA-tag antibody, while TDP43 overexpression was detected by anti TDP43 antibody. Untransduced control cells were labelled with TUJ1 antibody, which recognises beta-III-tubluin. The nuclei were stained with Hoechst 33342.

Figure 3.14 is an example taken at low magnification for a successful motor neuron culture immunostained with HA antibody for FL-ARFIP2 detection. However, the PI staining was only obvious at higher magnification. Figure 3.15 shows an example of live and dead cells, which are PI positive or PI negative, respectively, from

a control slide taken at 63x magnification power. In addition, Hoechst 33342 staining was used as a confirmation to differentiate the dead cells as their nuclei show chromatin condensation. This has been widely used for detection of apoptotic cells (Antonelli et al., 2008, Kameswaran and Ramanibai, 2009). Figure 3.15 shows that PI positive dead cells also have DNA condensation with the Hoechst 33342 staining compared to the nuclei of cells that are PI negative.

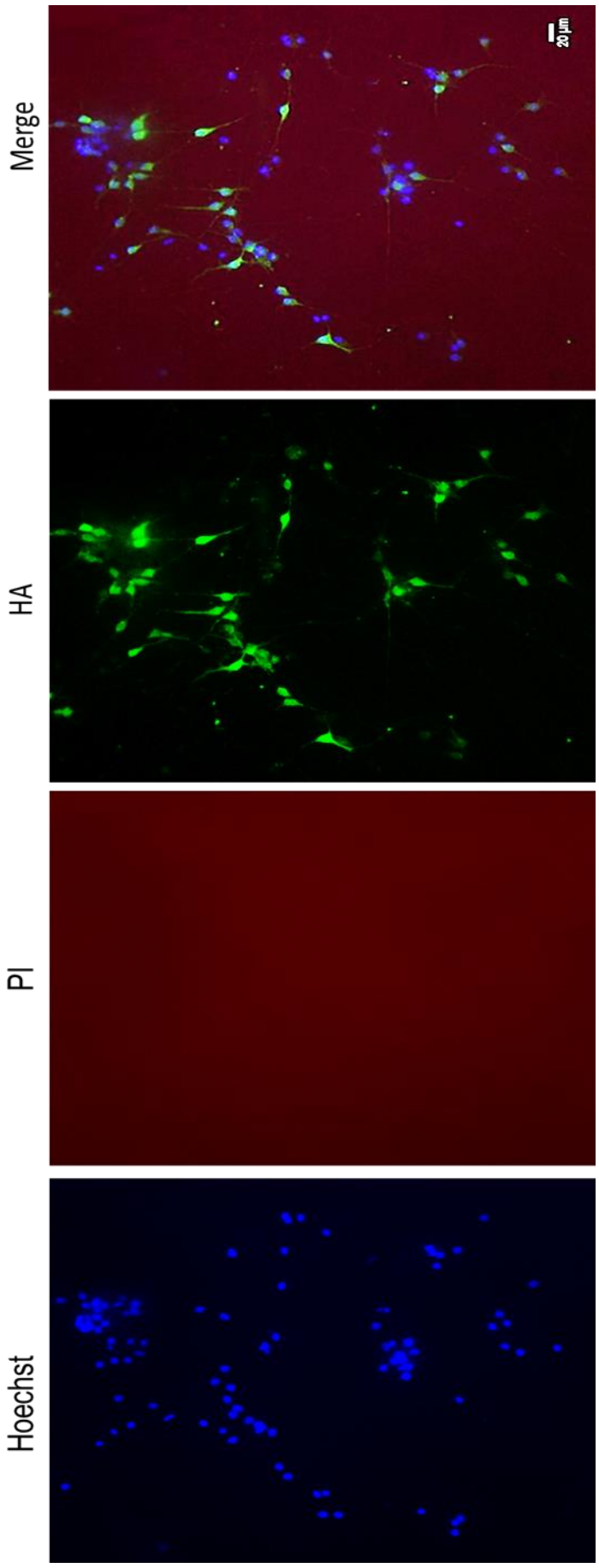

Figure 3.14: Example of a successful primary motor neuron culture and staining. Primary motor neurons from mouse embryos were extracted and cultured. The cells were transduced with LV-ARFIP2 for 5 days then were treated with PI. Cells were fixed and immunolabelled with Hoechst 33342 for nuclear staining and anti-HA-tag antibody to detect transduced cells.

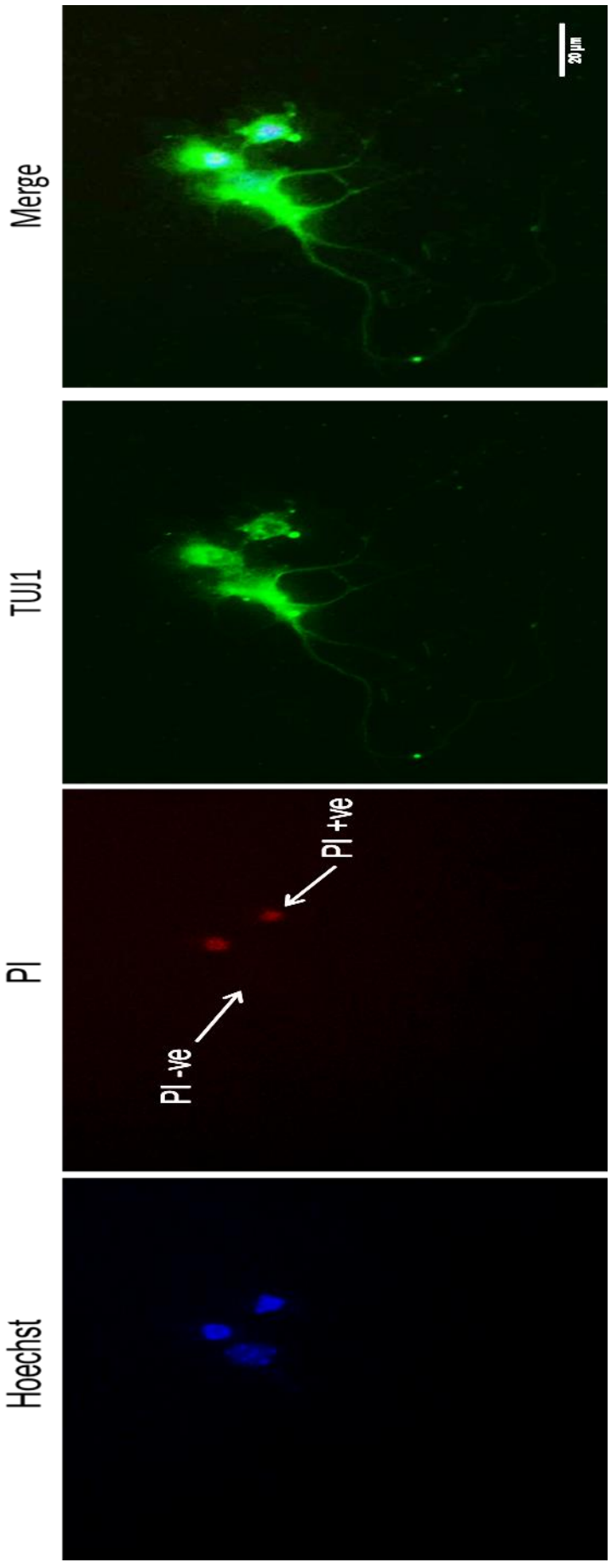

Figure 3.15: Example of live and dead primary motor neurons. Primary motor neurons from mouse embryos were extracted and cultured. These cells were mock transduced for 5 days then were treated with PI. Cells were fixed and immunolabelled with Hoechst 33342 for nuclear staining and anti-TUJ1 antibody to detect motor neurons.

PI positive and negative cells were counted blindly from four fields, in which each shows at least one motor neuron, of each coverslip. An average of 90 cells was counted per sample. The percentage of cell survival was determined from the total number of cells counted from each sample. The experiment was repeated on 3 independent experimental repeats. Each repeat consisted of at least two TG and NTG embryos. Statistical analysis was performed on Graphpad Prism and the statistical significance was calculated using one-way ANOVA test.

The results show that HC-ARFIP2 expression significantly increases motor neuron survival of the TG embryos compared to the overexpression of TDP43, FL-ARFIP2 and the untransduced control by around 20% (n=3; $p<0.05$). This is true in both non-stressed and H_2O_2 stressed cells (Figures 3.16). Comparing 3.16 a and 3.16 b, there is approximately 10% more cell death in the samples stressed with H_2O_2, which is expected.

NTG motor neurons also show similar results with significant difference between HC-ARFIP2 expression and other treatments and controls in non-stressed motor neurons (n=3; $p<0.05$), while H_2O_2 stressed motor neurons showed only significant difference between HC-ARFIP2 overexpressing cells and other samples excluding control (n=3; $p<0.05$) (Figure 3.17).

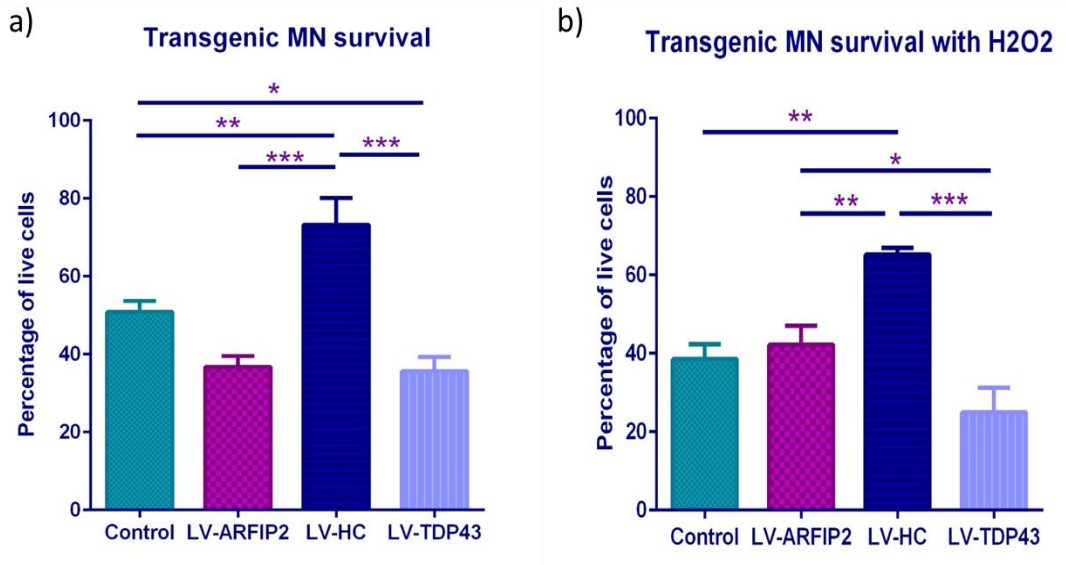

Figure 3.16: SOD1G93A transgenic motor neuron survival. Primary motor neurons were cultured and transduced with different LV vectors. Cells were treated with PI and fixed 5 days post transduction. Live and dead cells were identified by PI positive or PI negative staining respectively. a) Cells were not treated with H_2O_2. b) Cells were treated with H_2O_2 five days post transduction. Statistical analysis was performed using one-way ANOVA test (Mean ± SEM). n=3. *; $p < 0.05$, **; $p < 0.01$, ***; $p < 0.001$

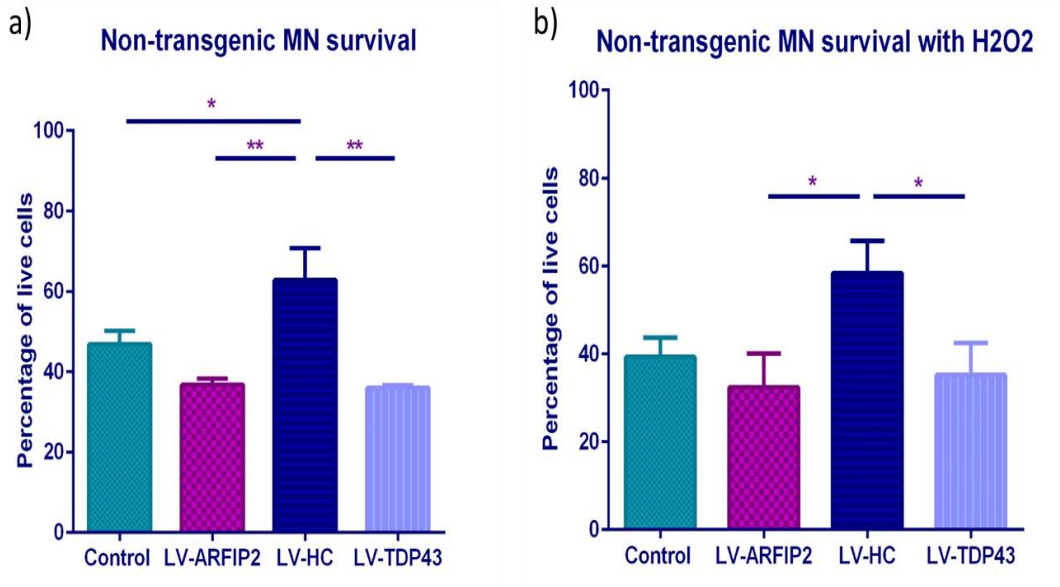

Figure 3.17: Non-transgenic motor neuron survival. Primary motor neurons were cultured and transduced with different LV-vectors. Cells were treated with PI and fixed 5 days post transduction. Live and dead cells were identified by PI positive or PI negative staining respectively. a) Cells were not treated with H_2O_2. b) Cells were treated with H_2O_2 five days post transduction. Statistical analysis was performed using one-way ANOVA test (Mean ± SEM). n=3. *; $p < 0.05$, **; $p < 0.01$

4.4 Discussion

LV vectors are suitable gene transfer vectors for *in vitro* experiments as they mediate long-term sustained gene expression with low toxicity (Blomer et al., 1997). This was specifically important for experiments on primary motor neurons as they are very sensitive cells and transfection buffers were shown to be causing tremendous cell death. Therefore, LV-based vectors were designed and produced at high titres. *HC-ARFIP2* was the main gene of interest as our hypothesis was that HC-ARFIP2 could promote motor neuron survival. LV-based vectors expressing FL-ARFIP2 and TDP43 were produced to be used as controls.

Though LV subcloning and production is a preparatory step, it was crucial in order to achieve the aim of this chapter. The procedure for producing a virus expressing our gene of interest was time consuming and involved many steps, in which the gene of interest was cloned by PCR to add the restriction sites required for the subcloning. The LV-backbone was digested using enzymes corresponding to the restriction sites expressed on the PCR products. Then the PCR products and the LV-backbone were ligated to produce the LV-plasmid. The plasmid was validated by sequencing and transfection for efficiency. After that, it was used for viral production using the 4 plasmids transfection method. The viral product was titered by p24 ELISA kit and validated by transduction and western blotting. The results showed that efficient viruses have been produced with high titres suitable for *in vitro* studies.

The HA-tag facilitated the evaluation of protein expression in western blot and the identification of cells overexpressing our genes of interest in immunostaining. Measuring the overexpression level of FL-ARFIP2 and HC-ARFIP2 is not required, as they were detected through a specific tag.

The aim to achieve efficient gene transfer with minimal neuronal toxicity was achieved by using LV-based vectors as shown in figure 3.14. It also revealed that good expression efficiency was accomplished, as substantial number of cells were HA positive.

Though immunostaining of cells using anti-HA-tag antibody was successful, the fluorescence intensity was quite low and bleached quickly. This made it hard to capture good high-resolution pictures using the confocal microscope. Counting the cells using fluorescent microscope, led to some level of bleaching of the fluorescence signal. This also made it challenging to obtain high-resolution images.

Propidium iodide (PI) exclusion assay was performed to investigate the effect of Arfaptin2 or HC-ARFIP2 expression on cell viability. PI binds to nucleic acids (DNA and RNA) by intercalating between bases. It is membrane-impermeable; therefore, it is excluded from viable cells. PI gives red fluorescence upon excitation. PI was used in combination with Hoechst 33342 dye, which is a nucleic acid stain that binds to double stranded DNA and emits blue fluorescence upon excitation. In contrast to PI, Hoechst is membrane permeable. Therefore, Hoechst is used to identify viable cells while the PI is used to identify apoptotic cells. This method was used due to its simplicity and economical use.

Results presented in figures 3.16 and 3.17 supported the hypothesis that expression of HC-ARFIP2 significantly increase cell survival compared to other treatments and controls even in the presence of oxidative stress. This allows us to conclude that HC-ARFIP2 expression increases motor neuron survival regardless of oxidative stress and SOD1 mutation. This also corroborates with the findings generated by a previous MSc student in our team (Kong, 2011) which demonstrated

that HC-ARFIP2 expression enhances survival of NSC34 cell line regardless of H_2O_2 or SOD1G93A expression.

H_2O_2 treatment was used to investigate whether HC-ARFIP2 can protect against oxidative stress. Previous detailed investigation of H_2O_2-induced primary neuron survival showed that short; as little as 30 min, exposure to H_2O_2 is enough to induce significant cell death in a dose-dependent manner. The effective dose was from 100 µM (Whittemore et al., 1995, Fan et al., 2012, Konyalioglu et al., 2013). Therefore, we used a high concentration of H_2O_2 with a short exposure for 50 min to induce oxidative stress. However, comparison of figures 3.16a and 3.17a with 3.16b and 3.17b shows that there is roughly 10% cell death induced in H_2O_2 treated cells, which was much lower than expected. This could be due to two reasons. Firstly, it could due to the short time delay between the treatment and the fixation in which cells were fixed ~20 min after H_2O_2 treatment. Many experimental procedures incubate the cell-lines in medium for around 24 hours after the treatment, which allows the cytotoxic effect to be more obvious and detectable (Abdo et al., 2010, Park et al., 2015, Zhu et al., 2015). However, it should be noted that primary neurons are more sensitive than neuronal cell lines (Fan et al., 2012); therefore, we preferred the short time delay. Secondly, this low cell death could be due to low H_2O_2 potency. It was shown previously that a delay of more than 5 min between the preparation and the application of H_2O_2 reduces its efficacy and cytotoxic effect (Whittemore et al., 1995). In this project, a diluted H_2O_2 solution was prepared at least one hour before the treatment, which could have affected its efficiency.

In figure 3.17, although the difference in survival between HC-ARFIP2 expressing motor neurons and control was not significant, it was significant in all other experiments, and there was a noticeable trend of increased survival of NTG motor

neurons overexpressing HC-ARFIP2. The lack of significant difference might be due to high variability between samples, technical issues or insufficient number of repeats.

TDP43 overexpression was used as a positive control for cell death and was expected to decrease cell survival compared to control as it has been shown that TDP43 overxpression is toxic to cells (Ash et al., 2010). However, a significant decrease in cell survival transduced with LV-TDP43 was only observed with TG motor neurons. The insignificant difference in other experiments might be due to the fact that TDP43 induced cytotoxicity is dose dependent (Wu et al., 2013). Therefore, an optimisation of TDP43 expression level and cytotoxic effect could have altered the outcome of the experiment.

Our data served as a proof of concept that HC-ARFIP2 expression can increase motor neuron survival *in vitro*. These results achieved the aims of this chapter and provided confidence to move forward to investigate the downstream effectors by which HC-ARFIP2 exerts its pro-survival effect.

CHAPTER 4: HC-ARFIP2 mediates neuroprotection through the Akt pathway

4.1 Introduction

A previous study showed that ARFIP2 is involved in Huntingtin protein aggregation through the Akt pathway (Rangone et al., 2005). In addition, Akt is a known downstream effector of Rac1 (Stankiewicz and Linseman, 2014). Akt, also known as protein kinase B (PKB), has many downstream effectors that exert different functions. It is a pro-survival kinase involved in many cellular processes including cell survival, protein synthesis and degradation, and RNA transcription (Figure 4.1). *Akt1, Akt2 and Akt3* genes produce three closely related kinases, Akt1, Akt2 and Akt3, respectively. Akt1 and 2 are ubiquitously expressed in different types of cells while Akt3 is predominantly expressed in the brain.

The involvement of Akt pathway in ALS has been implicated in several studies (Wagey et al., 1998, Yin et al., 2012, Peviani et al., 2014). Phosphorylated Akt (Phospho-Akt), which is the active form, was found to be drastically decreased in ALS patients' post mortem spinal cord, despite their variable disease backgrounds (Dewil et al 2007). In addition, Akt expression was found to be downregulated in muscles of ALS patients compared to normal and spinal muscular atrophy (SMA) individuals and therefore it has been suggested to use Akt as a biomarker for ALS (Yin et al., 2012). This downregulation of phospho-Akt seems to occur early in the disease process, as phospho-Akt was downregulated in large motor neurons of pre-symptomatic SOD1G93A mouse model as well (Dewil et al., 2007). Taken together, these observations indicate the importance of this pathway in the pathogenesis of ALS in general, regardless of the genetic background. In addition, its involvement in ALS seems to be in both motor neurons and muscles, which are among the affected cells and tissues in ALS. Therefore, the Akt pathway seemed an interesting and logical target to investigate the downstream effectors of HC-ARFIP2.

4.2 Aim

The aim of this chapter is to understand the pathway by which HC-ARFIP2 exerts its neuroprotective effect by looking at downstream effectors. In this Chapter, we focused on proteins in the Akt pathway (Figure 4.1).

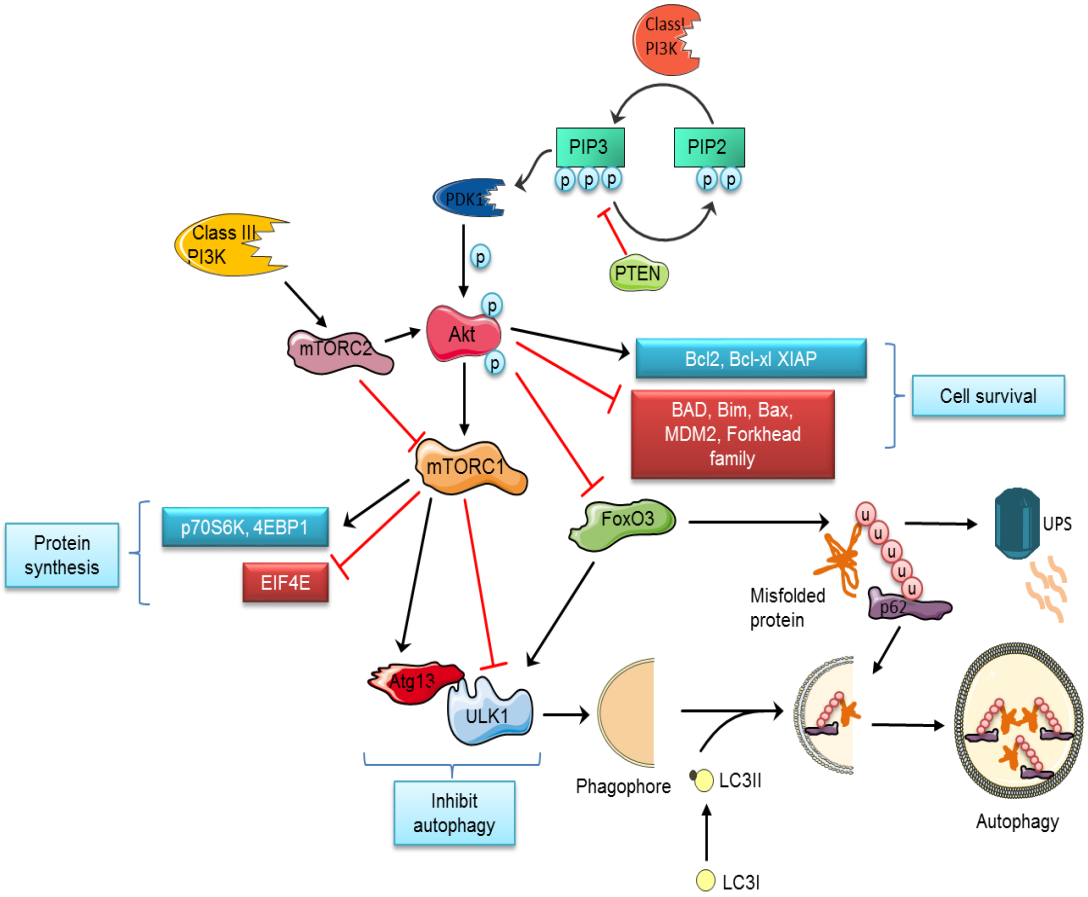

Figure 4.1: Schematic presentation of Akt/mTOR pathway and their role in protein degradation. After stimulation, Phosphoinositol 3 kinase phosphorylates phosphoinositol bisphosphate (PIP2) into phosphoinositol trisphosphate (PIP3). PIP3 induces phosphoinositide-dependent kinase-1 (PDK1) which then phosphorylates Akt at Ser473 and Thr308. Activated Akt can induce cell survival by direct effect on Bcl2 pro-survival proteins family or by inhibition of Bcl2 pro-apoptotic and the forkhead pro-apoptotic proteins families. In addition, phospho-Akt activates the mTORC1 pathway, which induces protein synthesis and inhibits protein degradation by inhibiting autophagy. On the other hand, Akt can induce protein degradation in an mTORC1 independent manner in which inhibition of FoxO3 induces protein degradation. LC3II binds to the inner and outer layer of the phagophore for elongation of the autophagic membrane and recruits p62. p62 carries the ubiquitinated unfolded protein to the phagophore. Proteins then are degraded in the autophagosome after fusing with lysosomes.

4.3 Results

4.3.1 HC-ARFIP2 increases phospho-Akt

HEK293T cells were transduced with LV-HC at MOI40 or MOI80 to study its downstream effectors. In addition, cells were transduced with LV-GFP and LV-ARFIP2 as controls beside the untransduced control. As Figure 3.9 showed efficient expression of FL-ARFIP2 in HEK293 cells using MOI30 and as we observed constantly that LV-ARFIP2 leads to more expression compared to LV-HC, MOI40 was used for LV-ARFIP2. Tests using LV-GFP within our group showed that MOI10 is highly efficient and therefore MOI10 was used for this virus throughout. Cell lysates were collected 5 days post-transduction and western blot analysis was performed to detect different proteins within the Akt pathway. First, the total Akt and the phospho-Akt expression levels were investigated using anti-Akt and anti-phospho-Akt at Ser473, respectively. Band densities were determined using densitometry. Readings from 3 independent experimental repeats were obtained.

After normalisation against GAPDH, Figure 4.2a and b show that LV-HC transduction induced phospho-Akt expression significantly compared to the untransduced control and the LV-GFP and LV-ARFIP2 controls. Phospho-Akt levels were increased to approximately 2.5 fold with both MOIs ($n=3$; $p<0.01$). On the other hand, LV transduction did not seem to have effect on the overall Akt expression level (Figure 4.2c and d).

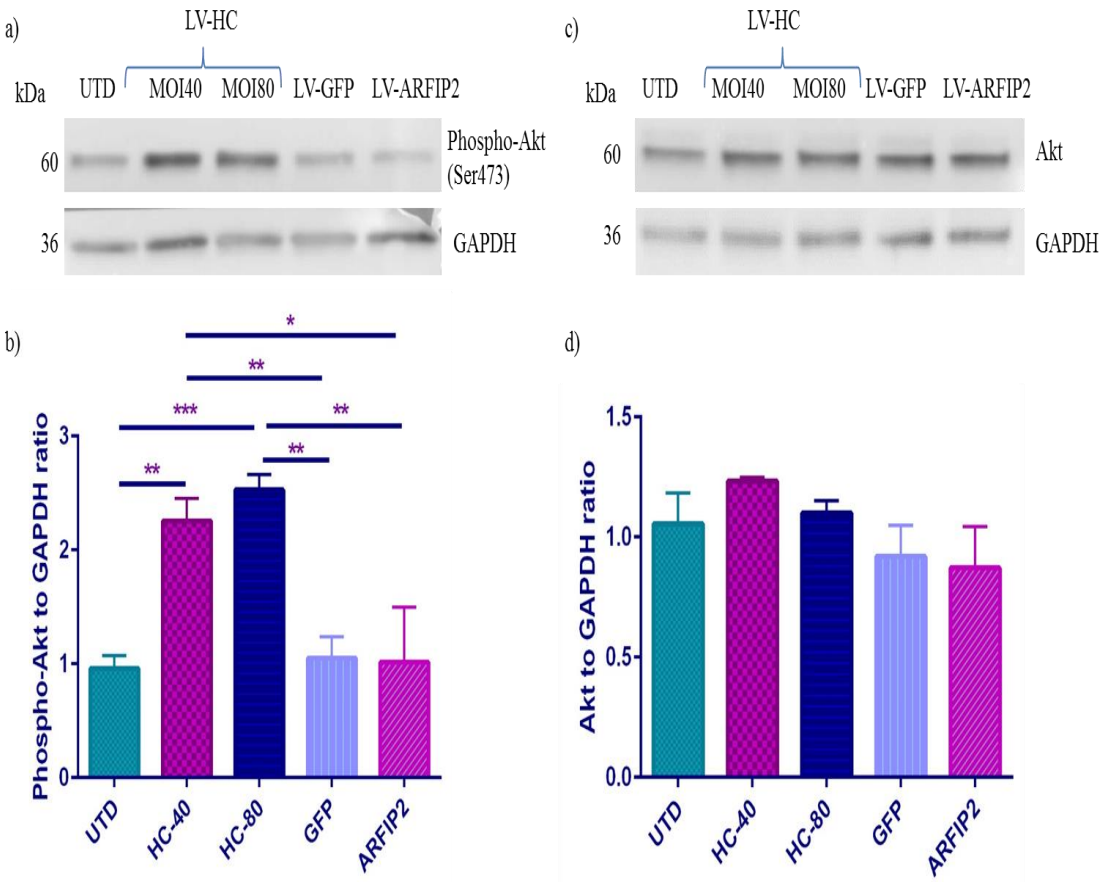

Figure 4.2: LV-HC transduction effect on Akt and phospho-Akt. a) Western blot membrane showing phospho-Akt detected using Ser473 phosphorylation specific antibody. b) The phospho-Akt expression level was compared between samples after normalisation with GAPDH. c) Western blot membrane showing the total Akt detected using anti-Akt antibody. d) The Akt expression level was determined as above. Statistical analysis was done using One-way ANOVA test (Mean ± SEM). n=3. * p <0.05. ** p <0.01. ***p <0.001

4.3.2 HC-ARFIP2 induces p62 expression

Downstream of phospho-Akt we looked at the expression of p62, which is involved in both protein degradation pathways; UPS and autophagy. The same lysates described in section 4.3.1 were used to evaluate changes in p62. Results in figure 4.3 reveal that, although not significant, there is a noticeable increase in p62 expression in cells transduced with LV-HC at both MOIs compared to UTD controls. However, interestingly LV-GFP transduced cell lysates also show increased p62 expression, which could question the reliability of GFP as a control, for which LV-ARFIP2 served as an extra control.

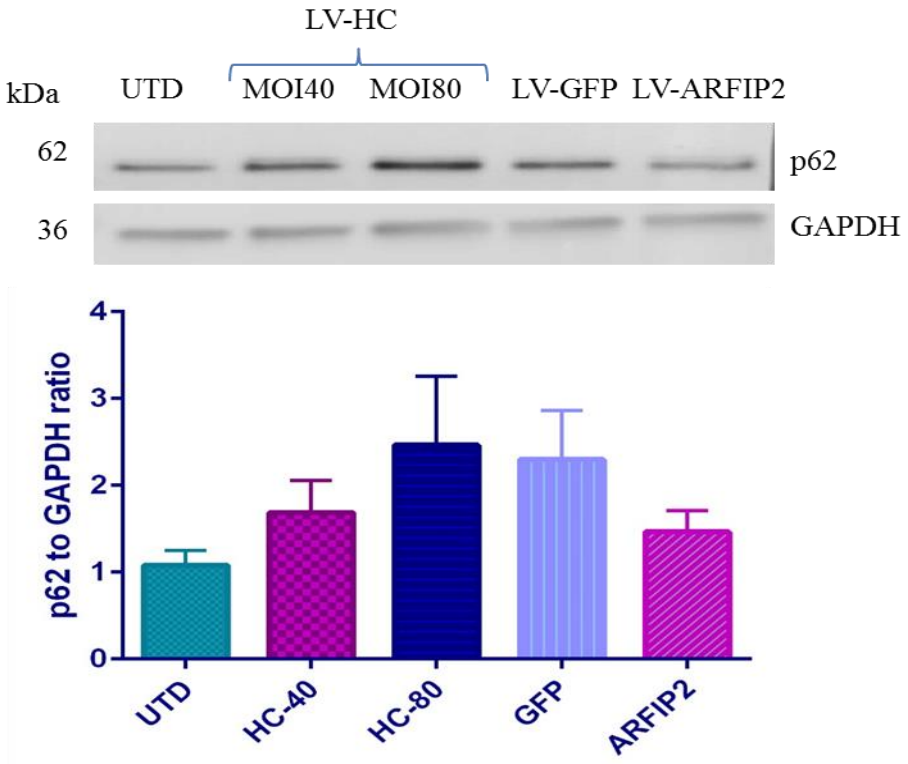

Figure 4.3: LV-HC transduction effect on p62 expression in HEK293T cells. Western blot shows the expression of p62 at 62kDa and the GAPDH loading control at 36kDa. The protein expression levels were determined by densitometry of the bands. The p62 expression level was compared between samples after normalisation with GAPDH. Statistical analysis was done using One-way ANOVA test (Mean ± SEM). n=3.

4.3.3 HC-ARFIP2 increases autophagy markers

We also looked at three autophagy markers in which LC3II and ULK1 activation indicates the activation of autophagy, while phospho-Akt inhibits Atg13, which is an inhibitor of autophagy. LC3 is a widely used marker for autophagosome formation. There are two forms of LC3, which are LC3I the inactive cytoplasmic form and LC3II which is the active lipid bound form and is involved in the elongation of the autophagosome membrane (Kabeya et al., 2000). Figure 4.4 shows that LV-HC transduction of HEK293T cells induces LC3-II expression significantly, at least at MOI80, compared to controls (n=3; $p<0.05$). HC-ARFIP2 modulation had no significant effect on LC3I expression.

In addition, Figure 4.5a and b shows that HC-ARFIP2 significantly increased ULK1 expression at high MOI. However, no significant change in the expression of Atg13 was observed (Figure 4.5c and d).

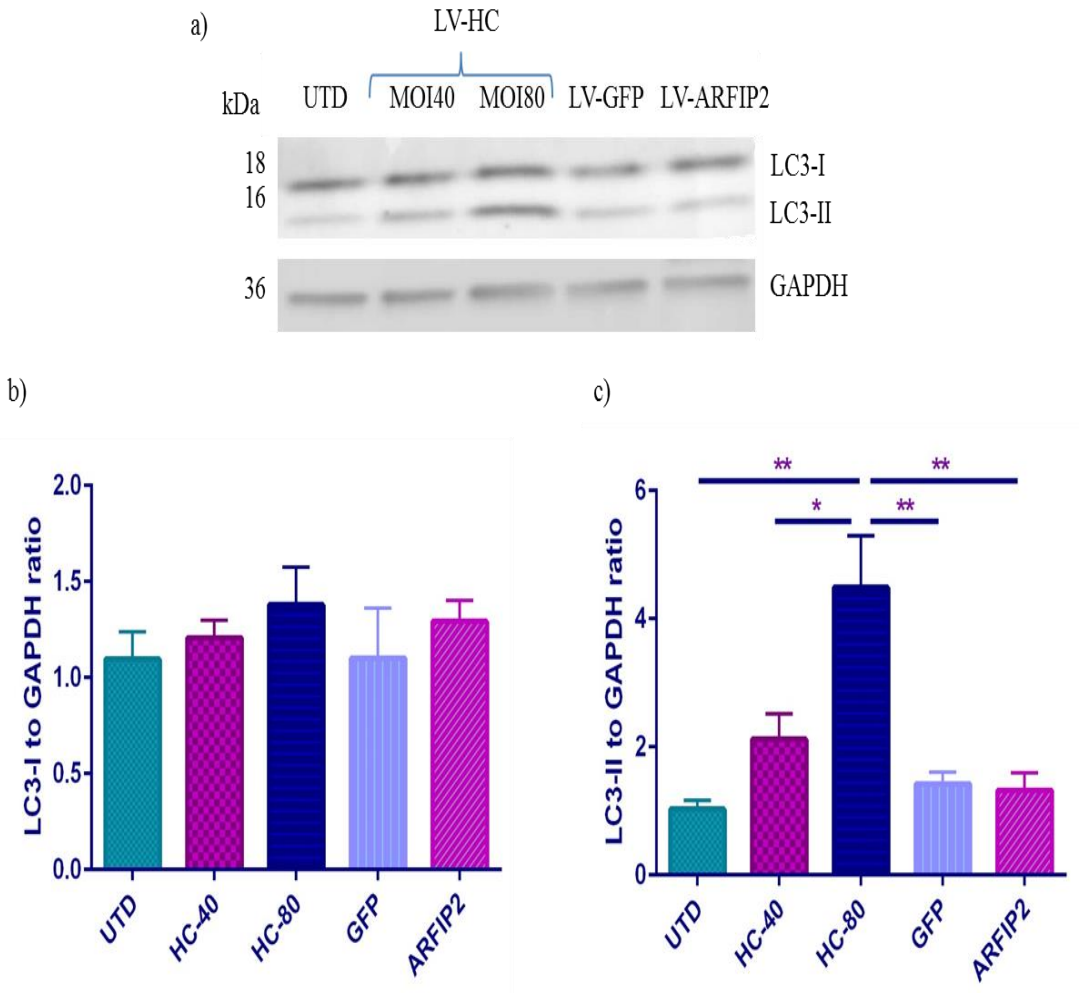

Figure 4.4: LV-HC transduction effect on LC3I/II expression in HEK293T cells. a) Representative western blot from one repeat showing the two bands of LC3I and II at 18 and 16kDa, respectively. b and c show the expression level of LC3I and II, respectively, after normalisation to GAPDH expression. Statistical analysis was done using One-way ANOVA test (Mean ± SEM). n=3. * p <0.05. ** p <0.01.

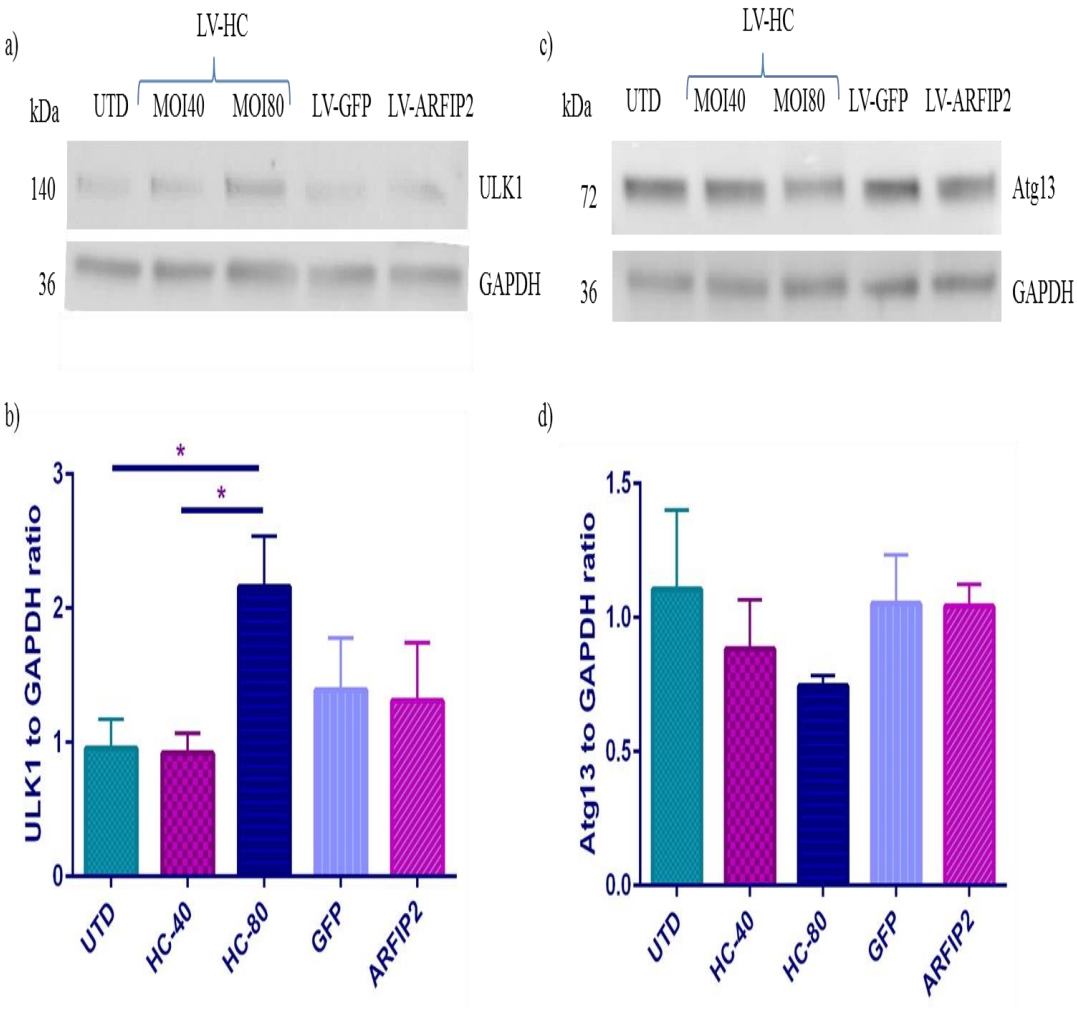

Figure 4.5: LV-HC transduction effect on ULK1 and Atg13 expression in HEK293T cells. Western blots are representative from one repeat. a and b) ULK1 expression level was measured by densitometry and normalised to GAPDH from 3 repeats and represented in the bar chart. c-d) Atg13 expression on western blot was measured by densitometry and normalised to GAPDH. Statistical analysis was done using One-way ANOVA test (Mean ± SEM). n=3. * $p < 0.05$

4.3.4 HC-ARFIP2 has no effect on 4E-BP1 phosphorylation

To investigate the effect of HC expression on mTORC1 pathway, we looked at the expression of the phosphorylated 4E-binding protein 1 (p-4EBP1), which is the active form and is a downstream target for mTORC1. When phosphorylated, p-4EBP1 is involved in the stimulation of protein synthesis. The same cell samples described in section 4.3.1 were used for p-4EBP1 analysis. p-4EBP1 isoforms are detected as a ladder of bands between 15 and 20 kDa (Gingras et al., 1999, Livingstone and Bidinosti, 2012). There was no significant difference in p-4EBP1 expression between treatments (Figure 4.6).

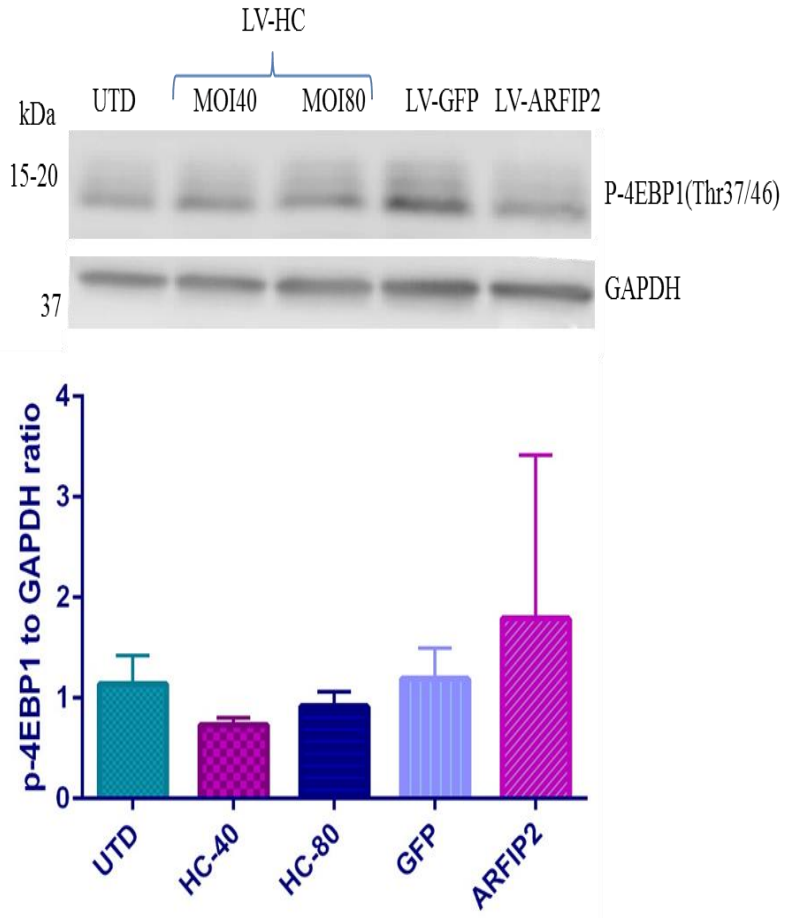

Figure 4.6: LV-HC transduction effect on p-4EBP1 expression in HEK293T cells. Representative western blot shows p-4EBP1 detected between 15-20 kDa. p-4EBP1 expression was normalised to GAPDH expression. The p-4EBP1 expression level was determined by densitometry of western blot. The p-4EBP1 expression level was compared between samples after normalisation with GAPDH. Statistical analysis was done using One-way ANOVA test (Mean ± SEM). n=3.

4.3.5 HC-ARFIP2 decrease PTEN expression

We wanted to look upstream of Akt to determine whether HC acted via PI3K or not. Therefore, we looked at the PTEN protein expression in the same cell lysates mentioned in section 4.3.1. Figure 4.7 revealed that the expression of PTEN significantly decreased to less than 50% in the presence of LV-HC treatment at MOI80 compared to control and other treatments ($n=3$; $p<0.01$). However, there was no change in the expression of PTEN with LV-HC treatment at MOI40.

Interestingly, PTEN was consistently detected at ~100kDa in all samples of the three repeats, although the actual protein size is 54kDa. The fact that no other bands were observed using this antibody questions the specificity of this antibody.

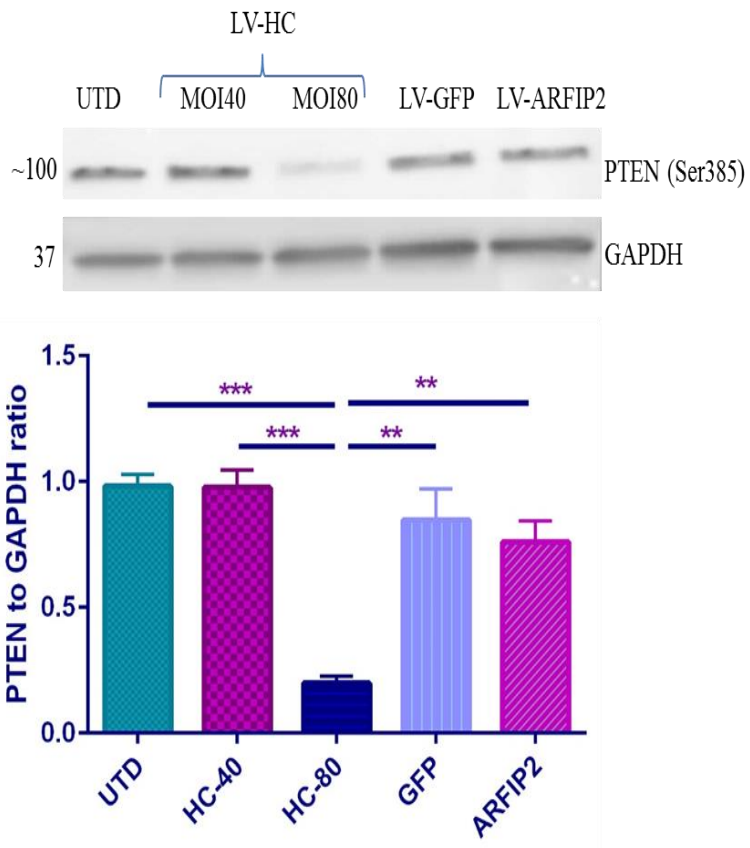

Figure 4.7: LV-HC transduction effect on PTEN expression in HEK293T cells. Representative western blot membrane shows PTEN expression in parallel to GAPDH. The PTEN expression level was determined by densitometry and was compared between samples after normalisation with GAPDH. Statistical analysis was done using One-way ANOVA test (Mean ± SEM). n=3. ** p <0.01. *** p <0.001

4.3.6 Validation by immunocytochemistry

In immunocytochemistry, colocalisation is defined as the observation of two or more different molecules labelled with different fluorophores overlapping in the same physical location in a cell. The colocalisation of the molecules might indicate an interaction between those molecules *in vivo* (Berggard et al., 2007). To investigate the effect of HC-ARFIP2 modulation on the distribution of the proteins investigated in this Chapter by western blotting, HEK293T cells were plated on 10mm coverslips and transduced with LV-HC or LV-ARFIP2 vectors. Cells were fixed 5 days post transduction. Figure 4.8 shows HEK293T cells labelled with anti-phospho-Akt (red) and anti-HA (green) to compare intensity and localisation of phospho-Akt in the two treatment conditions (LV-ARFIP2 and LV-HC). There were no obvious changes in phospho-Akt expression or localisation between the treatments.

Neither FL-ARFIP2 nor HC-ARFIP2 shows significant effect on PTEN immunoflourescence intensity and intracellular distribution in HEK293T cells (Figure 4.9).

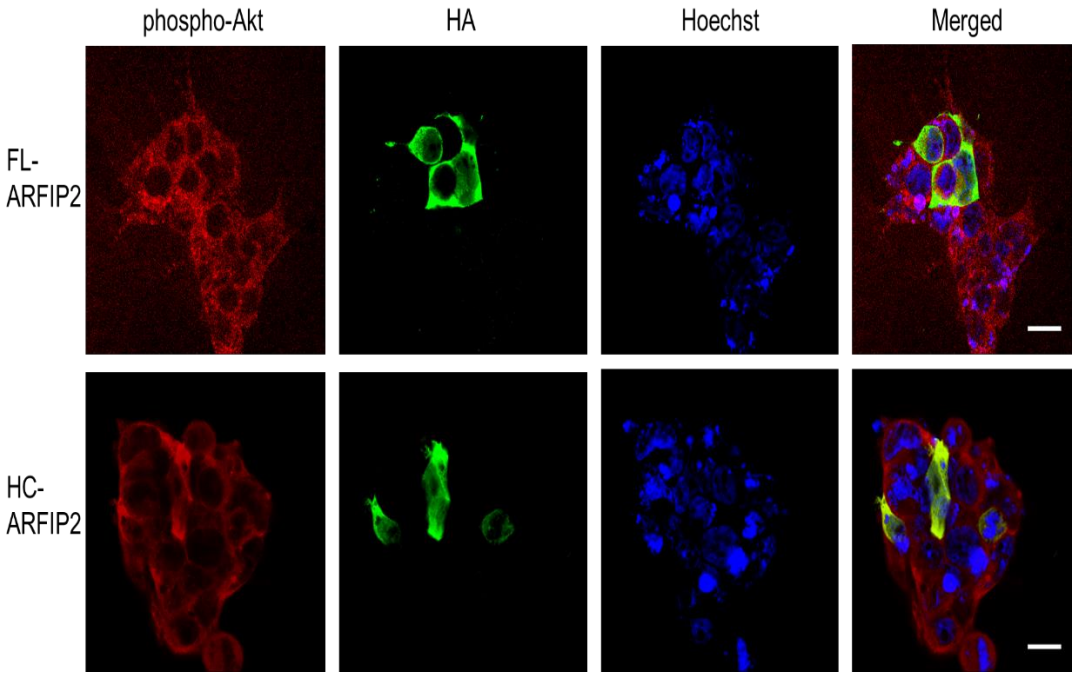

Figure 4.8: Immunostaining for overexpressed FL-ARFIP2 and HC-ARFIP2 with phospho-Akt in HEK293T cells. HEK293T cells were transduced with LV-ARFIP2 or -HC viruses. The overexpressed FL- and HC-ARFIP2 were detected using anti-HA antibody (green), while phospho-Akt in (red). Scale bar = 20µm

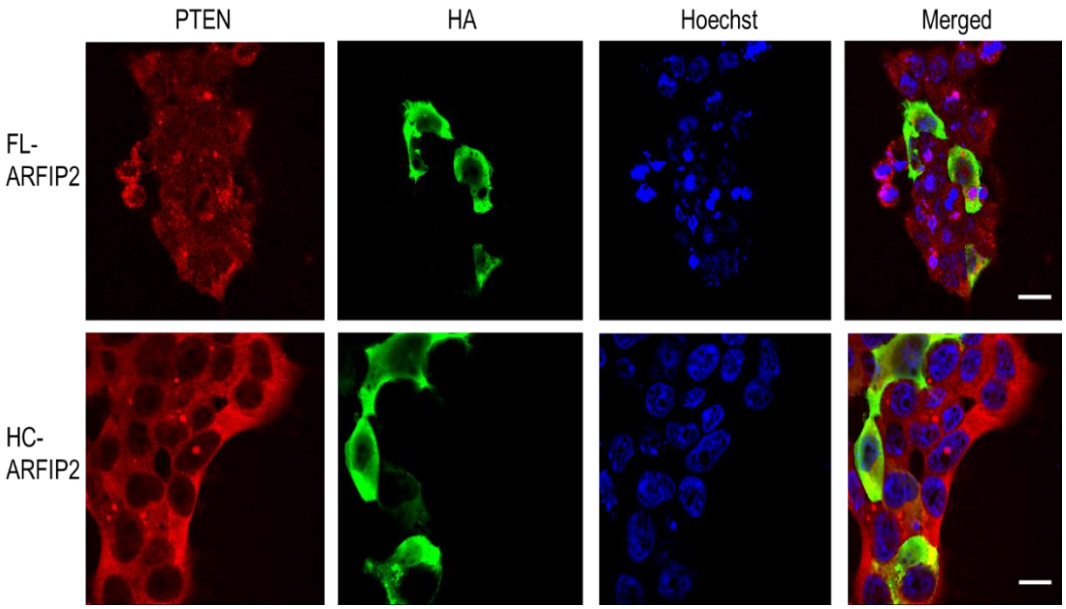

Figure 4.9: PTEN immunostaining in cells overexpressing FL-ARFIP2 or HC-ARFIP2. HEK293T cells were transduced with LV-ARFIP2 or -HC viruses. The overexpressed FL- and HC-ARFIP2 were detected using anti-HA antibody (green) while PTEN was detected with anti-PTEN (red). Scale bar = 20µm

Similarly, none of the autophagy markers used (LC3 and ULK1) were expressed differently between FL-ARFIP2 expressing and HC-ARFIP2 expressing cells based on immunoflourescent labelling (Figure 4.10).

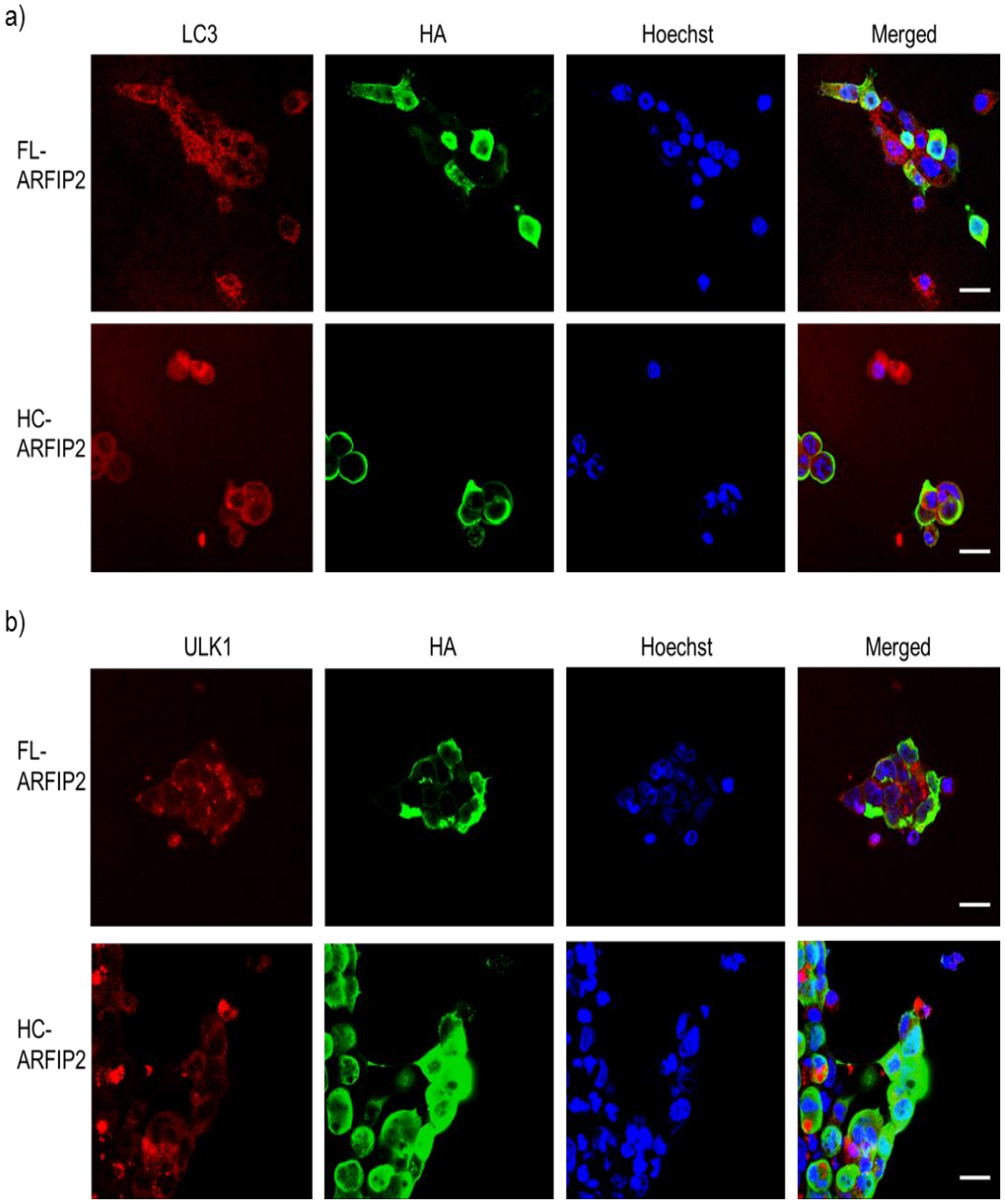

Figure 4.10: FL-ARFIP2 and HC-ARFIP2 has no effect on autophagy markers in immunostaining. HEK293T cells were transduced with LV-ARFIP2 or -HC viruses. The overexpressed FL- and HC-ARFIP2 were detected using anti-HA antibody (green). a and b shows endogenous LC3 and ULK1, respectively (red). Scale bar = 20µm

A previous study using plasmid transfection in the NSC34 cell line showed that overexpressed Arfaptin2 colocalised with SOD1 in aggregates while HC-ARFIP2 colocalised with SOD1 distributed throughout the cytoplasm (Kong, 2011). To check whether the same observation was seen using LV-transduction, we transduced HEK293T cells with LV-ARFIP2 or LV-HC and immunolabled them with anti-SOD1 and anti-HA antibodies. Notably, both FL-ARFIP2 and HC-ARFIP2 colocalise with endogenous SOD1 in HEK293T cells (Figure 4.11). In addition, FL-ARFIP2 colocalised with SOD1 in aggregates in cells overexpressing FL-ARFIP2. On the other hand, HC-ARFIP2 colocalised with SOD1 in a diffuse manner in the cytoplasm of cells expressing HC-ARFIP2, which was expected based on findings reported previously in our group using the NSC34 cell line (Kong, 2011).

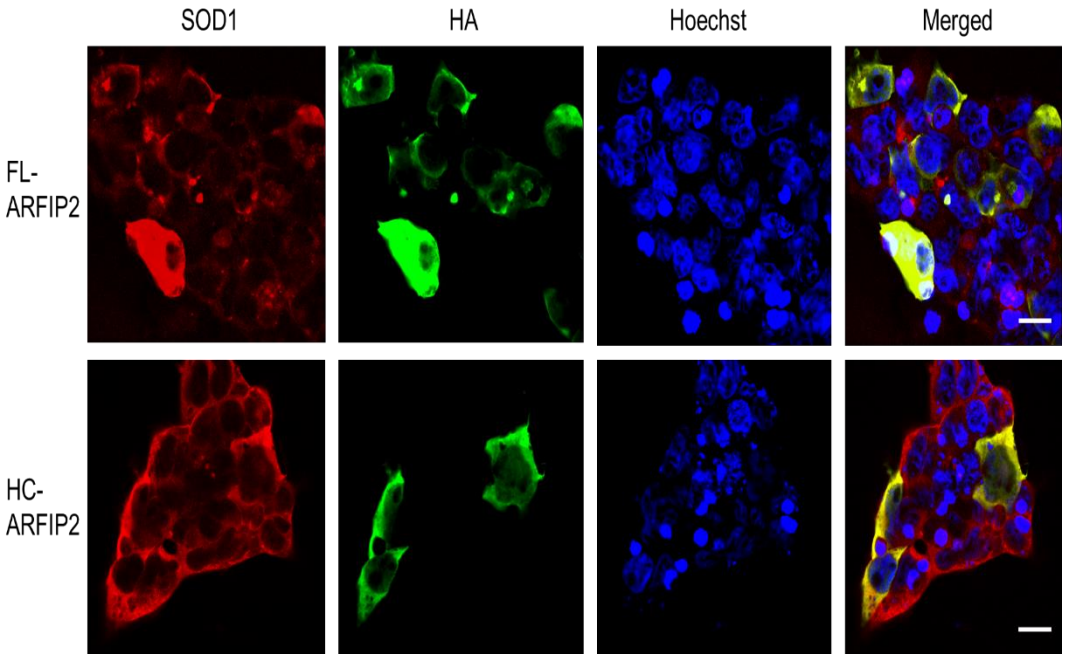

Figure 4.11: HA-tagged ARFIP2 colocalises with SOD1. HEK293T cells were transduced with LV-ARFIP2 or -HC viruses. The overexpressed FL- and HC-ARFIP2 were detected using anti-HA antibody (green). Endogenous SOD1 was detected by anti-SOD1 antibody (red). Scale bar = 20µm

4.4 Discussion

Accumulating evidence shows that activation of Akt pathway could induce motor neuron survival *in vitro* and *in vivo* (Dewil et al., 2007, Takata et al., 2013, Tsai et al., 2013, Peviani et al., 2014). Phospho-Akt loss has been also described in Alzheimer's disease (AD) and PD in addition to ALS, which stresses its importance for neuronal survival.

Our results show that HC-ARFIP2 works on the Akt pathway by decreasing active PTEN and hence increases Akt activation. Although PTEN was consistently detected at ~100 kDa on western blots, PTEN dimerization is normal and it has been reported that homo-dimerization does not affect the activity of PTEN. In fact, dimeric PTEN showed increased activity compared to monomeric PTEN (Papa et al., 2014). The inability to detect PTEN monomer might be due to inefficient denaturation. However, there was no other band detected in the background, which supports the antibody specificity.

HC-ARFIP2 increases Akt activation without effecting its expression. This finding is supported by the outcome of a previous study showing that decreased phospho-Akt expression was not linked to changes in Akt expression, as Akt expression was the same in SOD1G93A and control mice. This indicates that a defect in the activation of Akt occurs rather than loss of Akt expression (Dewil et al., 2007). These results are promising as they support a previous study, which showed that increased activation of Akt3 *in vitro* and *in vivo* increases neuronal survival (Dewil et al., 2007). In addition, motor neurons had increased survival in response to 7,8-Dihydroxyflavone through activation of the Akt pathway (Tsai et al., 2013). Interestingly, the Alsin protein, which is linked to FALS, consists of a GEF domain, which activates Rac1. It has been shown that overexpression of Alsin protein has a

neurprotective effect that is Rac1-dependent and PI3K/Akt-mediated (Kanekura et al., 2005).

p62 protein is involved in UPS and autophagy protein degradation pathways. It binds to ubiquitinated proteins and carries the misfolded protein to the proteasome subunit for degradation. In addition, p62 drives the misfolded protein to the autophagosome by binding to the LC3II units that are bound to the inner side of the phagophore during the autophagosome membrane elongation. As p62 is correlated with protein degradation, we sought to check its expression after HC-ARFIP2 modulation. No statistically significant difference was observed in the expression of p62 when HC-ARFIP2 is expressed. This statistical insignificance could be due to low number of experimental repeats.

Autophagy and UPS are cooperating mechanisms in which one can compensate for any defect in the other one. Therefore, it was interesting to look at the effect of HC-ARFIP2 expression on autophagy markers. HC-ARFIP2 seems to increase autophagy markers as well, at least with high MOI. This might indicate that HC-ARFIP2 works in an mTOR-independent pathway. To confirm our hypothesis, we looked at mTORC1 pathway downstream effectors. Two of the known downstream effectors of mTORC1 are P70S6K and 4E-BP1. With p70S6K we could not detect any expression. Regarding 4E-BP1, there was no change in protein expression. This suggests that HC-ARFIP2 promotes protein degradation without affecting protein synthesis. Future validation of the involvement of mTORC1 pathway in HC-ARFIP2 effect could be studied using known mTORC1 inhibitors.

Our results revealed that markers of autophagy (ULK1 and LC3II) were upregulated in response to HC-ARFIP2 expression, at least at MOI80. These indicate that HC-ARFIP2 might exert its neuroprotective effect by inducing protein

degradation, at least partially, by autophagy. Indeed, a previous study suggested autophagy activation as a therapeutic target for neurodegenerative diseases (Wang et al., 2012). It was demonstrated that activation of autophagy by inhibiting mTOR using rapamycin (mTOR-dependent pathway) or autophagy activation in an mTOR-independent pathway using spermidine or carbamazepine, both rescued MND phenotype and enhanced cognitive performance of FTLD mouse model with TDP43 proteinopathy. This rescue was accompanied by increased LC3II expression and decreased protein aggregation (Wang et al., 2012). These findings are further supported by a recent study on primary neurons and human stem cell-derived neurons and astrocytes carrying TDP43 mutation (Barmada et al., 2014).

Increased PI3K expression and activity in post mortem spinal cord of ALS patients was reported, while no change in Akt and mTOR (P70s6k) activity might indicate a disrupted pathway that could lead to neuronal death (Wagey et al., 1998)

The effect of Akt signalling pathway on autophagy and its role in neurodegeneration or survival is still controversial. Activation of PI3K/Akt pathway is important for cell survival. However, inhibition of autophagy by mTORC1, which is a downstream effector of Akt activation, might compromise cell viability and cause cell death. On the other hand, in response to stress, autophagy has been reported to induce autophagic-programmed cell death (Shimizu et al., 2004). Several studies showed that autophagic machinery is disrupted in neurodegenerative diseases. Therefore, the balance between activation of Akt and autophagy is vital and it is crucial to understand the mechanism behind it.

Although LC3II expression is used as a marker of autophagy, whether it means there is increased protein degradation by autophagy or there is an increased autophagosome formation without increasing protein degradation needs to be

elucidated by measuring the protein turnover or autophagic flux using known autophagy activator or inhibitor. Thus, we are cautious about interpreting the results as they stand.

In addition, it would be interesting to investigate HC-ARFIP2 effects on the expression of anti-apoptotic proteins downstream of Akt, such as Bcl-2, Bcl-xl and XIAP. This could elucidate whether HC-ARFIP2 works strictly on protein degradation or has multiple downstream targets. However, due to time restriction during the current PhD project, the expression of these proteins was not investigated.

Furthermore, it would be interesting, and probably more accurate, to investigate the effect of HC-ARFIP2 expression in neuronal cell lines, primary motor neurons and mixed primary cultures and observe if there is a differential effect between cell types.

To conclude, the prosurvival effect of LV-HC seems to occur through the PI3K/Akt pathway and may involve activation of autophagy. Although HEK293T cells are not the best model for MND investigation, the above results are encouraging and support, at least partially, our hypothesis.

CHAPTER 5: Self-complementary adeno-associated Virus design and production for Arfaptin2, HC-ARFIP2 and TDP43 overexpression *in vivo*

5.1 Introduction

Gene therapy is the treatment of a disease by introducing a nucleic acid to the cells to modulate the defective gene, which is replaced, deleted, upregulated or repaired. There has been a huge improvement in the field of gene therapy. However, gene therapy for CNS diseases presents more challenges due to its complexity and the presence of the blood brain barrier (BBB), which is a highly selective permeable barrier that protects the CNS from changes in the blood, infections and toxins and hence maintain the homeostasis of the CNS. Substances such as water, gases and lipid-soluble molecules cross the BBB by passive diffusion. Other nutrients enter the CNS through active transport via receptors on the endothelial cells. Although the BBB protects against infiltration of microbes to the CNS, some bacteria release cytotoxins that effect the tight junctions and allow the infiltration of these microbes to the CNS (Turowski and Kenny, 2015). Hence, the BBB stands in the way of treatments to reach the target cells of the CNS. Therefore, to be an efficient therapy, vector-mediated gene transfer has to reach the CNS effectively, have long-term expression, very low toxicity and high specificity to the target cells. In addition, gene therapy for ALS has to be effective even when introduced after the onset of clinical symptoms, as it is usually undiagnosed until clear symptoms have appeared.

Adeno-associated virus (AAV) is from the *Parvoviridae* family. It consists of a single-stranded DNA genome, which requires a helper virus or a cellular stress to promote the production of the complementary strand and replication. This causes slow onset of expression. In order to eliminate this step, a self- complementary adeno-associated virus (scAAV) was generated, in which the two ends of the single-stranded DNA complement each other and produce an intra-molecular double strand upon release from the viral particle (McCarty et al., 2001, McCarty et al., 2003). scAAV

showed significantly quicker and much higher transduction efficiency compared to conventional single-stranded AAV (McCarty et al., 2001, McCarty et al., 2003, Wang et al., 2003, Duque et al., 2009, Gray et al., 2011, Aschauer et al., 2013).

CNS exposed to AAV vectors showed no or low immune response and no toxicity, which indicates the likely safety of AAV vectors for long-term treatment. Furthermore, AAV vectors showed the ability to transduce quiescent cells, which is beneficial for motor neuron transduction (Duque et al., 2009, Aschauer et al., 2013).

AAV can infect a broad range of cells of the CNS, and AAV serotype 9 (AAV9) showed generally higher transduction efficiency compared to other serotypes (Aschauer et al., 2013). However, different AAV serotypes have different cellular tropism, for example, AAV9 transduced cortical neurons with higher efficiency compared to other serotypes, while AAV5 had higher transduction efficiency in the striatum, especially for astrocytes (Aschauer et al., 2013).

Mounting evidence suggests that scAAV9 is able to transduce cells of the CNS with high efficiency, safety and long-term expression (Kaspar et al., 2003, Duque et al., 2009, Foust et al., 2009, Foust et al., 2010, Valori et al., 2010, Gray et al., 2011, Aschauer et al., 2013, Benkhelifa-Ziyyat et al., 2013, Yamashita et al., 2013). Another advantage for scAAV9 is that it can be introduced to the CNS using non-invasive techniques, which is ideal for patients to improve their quality of life. scAAV9 has the ability to cross the blood brain barrier as intravenous injection of scAAV9 vector expressing the survival motor neuron (*SMN*) gene was able to transduce motor neurons without the requirement of BBB disrupting agents, upregulate SMN protein expression and improve the survival of the SMA mice, cats and nonhuman primate models (Duque et al., 2009, Foust et al., 2010, Valori et al., 2010). Furthermore, gene silencing in the CNS is achievable using scAAV9 as a vector (Little et al., 2014). The

ability to cross the blood brain barrier was demonstrated even in well-developed adult animal models (Duque et al., 2009, Foust et al., 2009, Foust et al., 2010). This is an important aspect when choosing a gene therapy vector for ALS as it is mostly an adult onset disease. However, the exact mechanism of how scAAV gains access through the blood brain barrier is still unknown. Although, the highest percentage of transduced cells in adult mice were astrocytes (Foust et al., 2009), scAAV9 cannot be ruled out as an option of ALS gene therapy as astrocytes have been implicated in the pathogenesis of ALS (Haidet-Phillips et al., 2011, Pirooznia et al., 2014).

In addition, scAAV9 is able to undergo retrograde axonal transport upon intramuscular injection. Intramuscular injection of scAAV9-SMN virus demonstrated that it was possible to transduce cells of the CNS using this method of virus delivery, not just motor neurons which innervated the injected muscle, and significantly improve the survival of the SMN mouse model (Benkhelifa-Ziyyat et al., 2013).

In ALS, at disease onset intramuscular injection of AAV vector carrying neurotrophic factors, such as insulin growth factor 1 (IGF-1) or glial cell line-derived neurotrophic factor (GDNF), showed the ability to undergo retrograde transfer and transduce motor neurons in the lumbar and thoracic spinal cord and hence slowed the disease progression and induced survival of SOD1G93A mice (Kaspar et al., 2003). However, the effectiveness of those proteins was modest as they extended the life span by 22 days with IGF-1 and 7 days with GDNF compared to controls. In addition, the controls used were injected with GFP-expressing virus, which is known to be toxic; therefore, this effect on life span might be negligible if compared to non-treated controls (Kaspar et al., 2003).

A study targeting another aspect of ALS using AAV9 as a vector and intravenous injection as mode of administration, found that controlling the calcium permeability

through AMPA receptor increased the motor neuron survival. However, the effect on motor neuron survival was just around 15% and the effect on life span was not investigated (Yamashita et al., 2013).

5.2 Aim

Based on the results in Chapter 4, we aim to investigate the effect of HC-ARFIP2 expression on an *in vivo* ALS mouse model. Hence, for the above reasons, we chose scAAV9 as a vector to deliver HC-ARFIP2 to the CNS of SOD1G93A mice as those advantages could not be accomplished using LV vector (Kaspar et al., 2003). This will help to efficiently express the protein of interest *in vivo*. In addition, our aim is to introduce the gene of interest using a non-invasive technique as the scAAV9 showed the capability to cross the blood brain barrier and efficiently transduce the cells of the CNS. Using this method of virus delivery, the ultimate aim is to improve the quality of life of ALS patients.

5.3 Results

5.3.1 Construction of scAAV-ARFIP2, scAAV-HC-ARFIP2 and scAAV-TDP43 plasmid vectors

5.3.1.1 Amplification of FL-ARFIP2, HC-ARFIP2 and TDP43 DNA by PCR

All genes that were used in viral subcloning were amplified by PCR as mentioned in section 2.2.3, using different primers. FL-ARFIP2 and HC-ARFIP2 primers were designed with AgeI on their 5'end and HA-tag and XbaI on their 3'end. The primers for TDP43 contained AgeI restriction site on their 5'end and XbaI on their 3'end. The PCR products were run on a 1% agarose gel (Figure 5.1). FL-ARFIP2 is 1kbp, HC-ARFIP2 is 0.5kbp, TDP43 is 1.25kbp. The desired bands were purified by DNA-gel extraction kit. The inserts are ready to be subcloned into scAAV backbone.

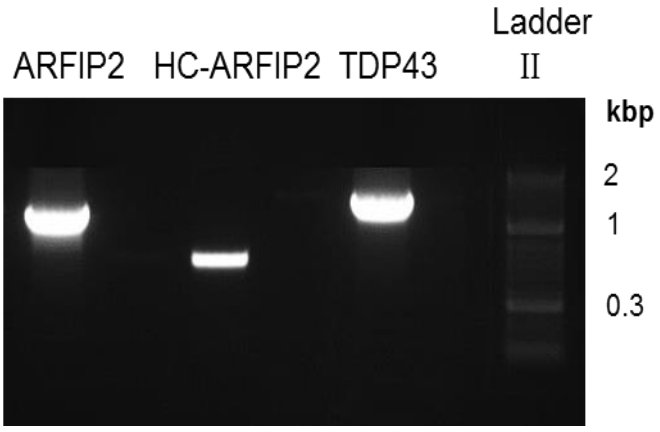

Figure 5.1: FL-ARFIP2, HC-ARFIP2 and TDP43 PCR products for scAAV subcloning. PCR products were run on 1% agarose gel for each gene. The FL-ARFIP2 DNA is at 1kbp. The HC-ARFIP2 DNA is at ~0.5kbp. The TDP43 DNA is at 1.25kbp.

5.3.1.2 Digestion of scAAV-backbone

The scAAV-CMV-GFP plasmid was digested with the same restriction enzymes (AgeI and XbaI) to remove the GFP cassette to be replaced with the desired inserts (Figure 5.2). scAAV-backbone was gel extracted and purified by gel extraction kit.

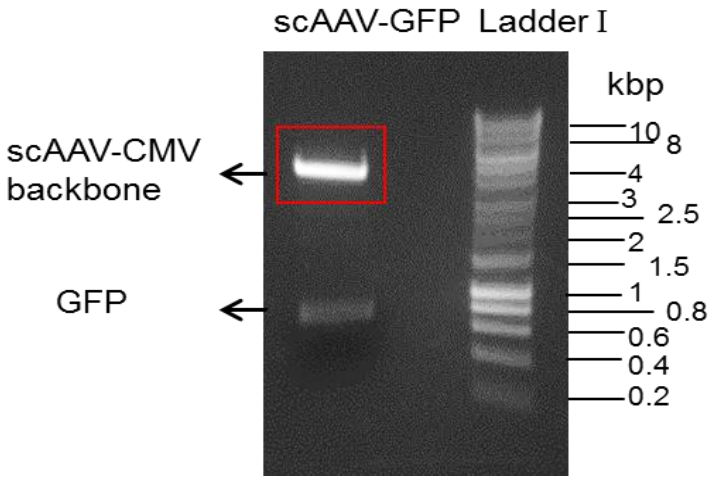

Figure 5.2: scAAV-CMV-GFP plasmid. scAAV-CMV-GFP plasmid cut by AgeI and XbaI. The scAAV-CMV backbone is ~4kbp the GFP size is ~0.7kbp.

5.3.1.3 Ligation of scAAV-backbone with the inserts

The target inserts (FL-ARFIP2, HC-ARFIP2 and TDP43) were ligated into the scAAV-backbone using the T4 DNA ligase. XL10-gold cells were transformed with the ligation mix. Several colonies were picked and the plasmids were extracted. Successful ligations were analysed using AgeI and XbaI restriction enzymes and visualised on agarose gel. The expected size for FL-ARFIP2 is 1kbp and the size of HC-ARFIP2 is ~0.5kbp. However, the XbaI site appeared to be blocked by methylation as AgeI single digestion linearized the plasmid and XbaI did not cut the plasmid (Figure 5.3). Therefore, SbfI and PsiI restriction sites were used instead of XbaI to validate the insertion of FL-ARFIP2 and HC-ARFIP2 into the backbone of scAAV vector. Figure 5.4 shows plasmid maps of scAAV-ARFIP2 and scAAV-HC. It also shows successful double digestion of scAAV-ARFIP2 and scAAV-HC using AgeI with SbfI which is 11bp before XbaI, or PsiI, which is 89bp before XbaI. Therefore, the expected size of FL-ARFIP2 cut by AgeI and SbfI is 1079bp while FL-ARFIP2 cutted by AgeI and PsiI is 1154bp. The size of HC-ARFIP2 cut by AgeI and SbfI is 572bp while AgeI and PsiI cut fragment size 647bp.

Figure 5.5 shows representative plasmid map of scAAV vector with the TDP43. It also shows the successful insertion of the TDP43 to the scAAV backbone as validated by digestion showing scAAV-backbone at ~4kbp and TDP43 at 1.25kbp. The plasmid was further validated by sequencing.

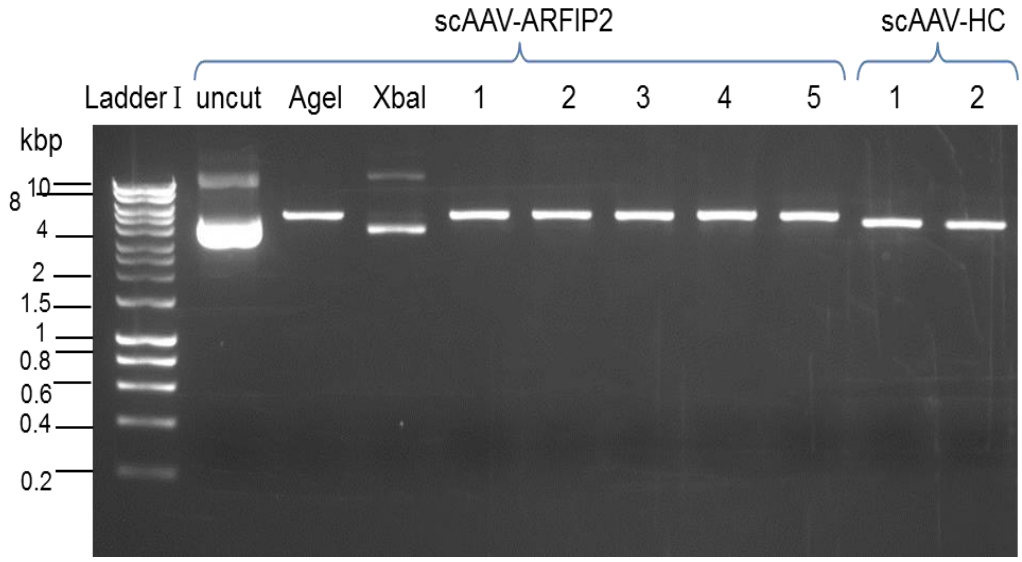

Figure 5.3: scAAV-ARFIP2 and scAAV-HC plasmid validation. scAAV-ARFIP2 and scAAV-HC plasmids were digested with AgeI and XbaI to detect successful ligation. AgeI single digestion shows linearized plasmid while XbaI did not linearize the plasmid. Therefore, double digestion of the plasmids in lanes 5-11 did not show expected bands of scAAV backbone (~4 kbp), ARFIP2 (1 kbp) and HC-ARFIP2 (0.5kbp).

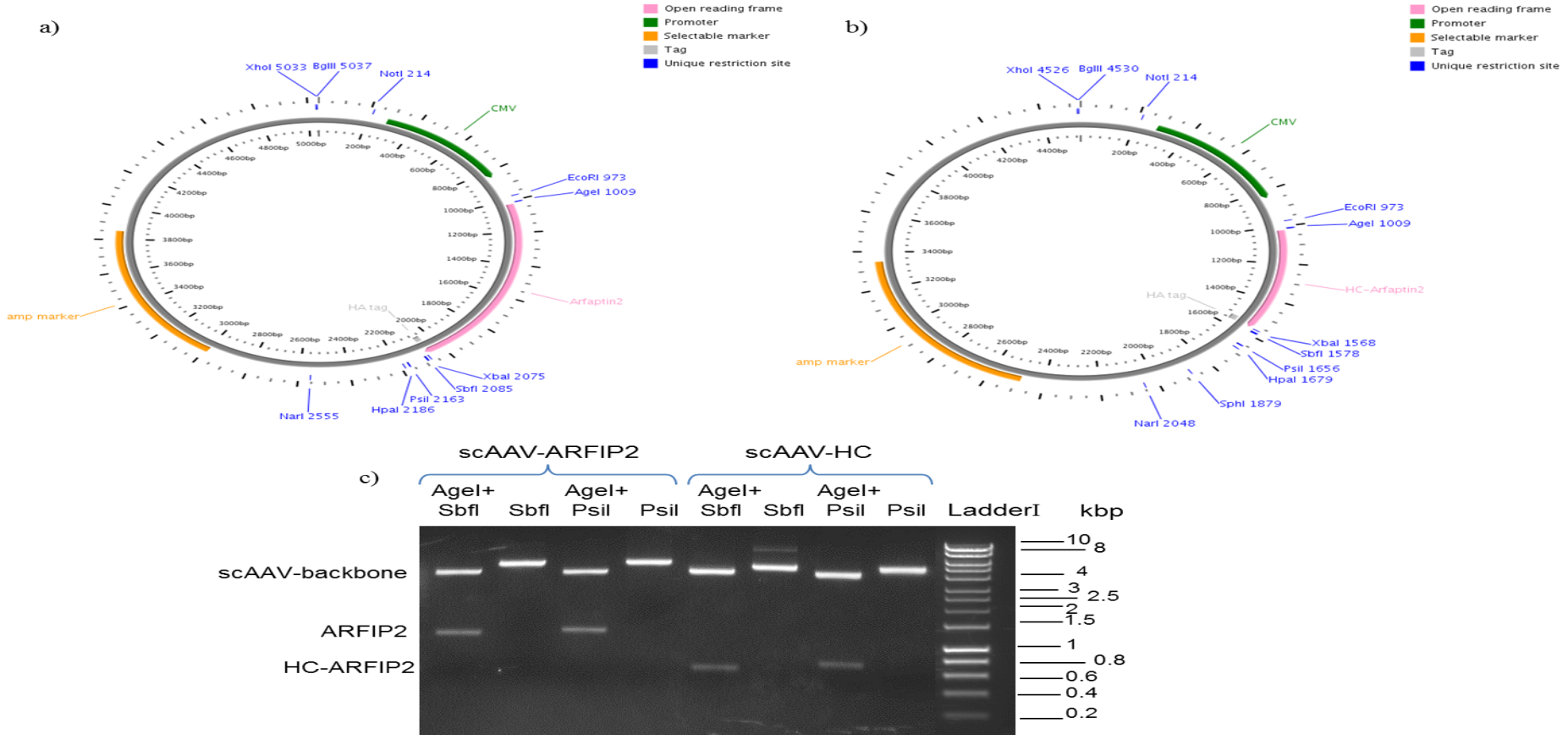

Figure 5.4: Validation of scAAV-ARFIP2 and scAAV-HC successful ligation. A) Plasmid map of scAAV-ARFIP2. b) Plasmid map of scAAV-HC. Plasmid maps were produced by Plasmapper website version 2.0. c) scAAV-ARFIP2 and scAAV-HC were double digested with AgeI and SbfI or PsiI to validate the successful ligation, also plasmids were single digested with SbfI or PsiI to check their ability to linearize the plasmids.

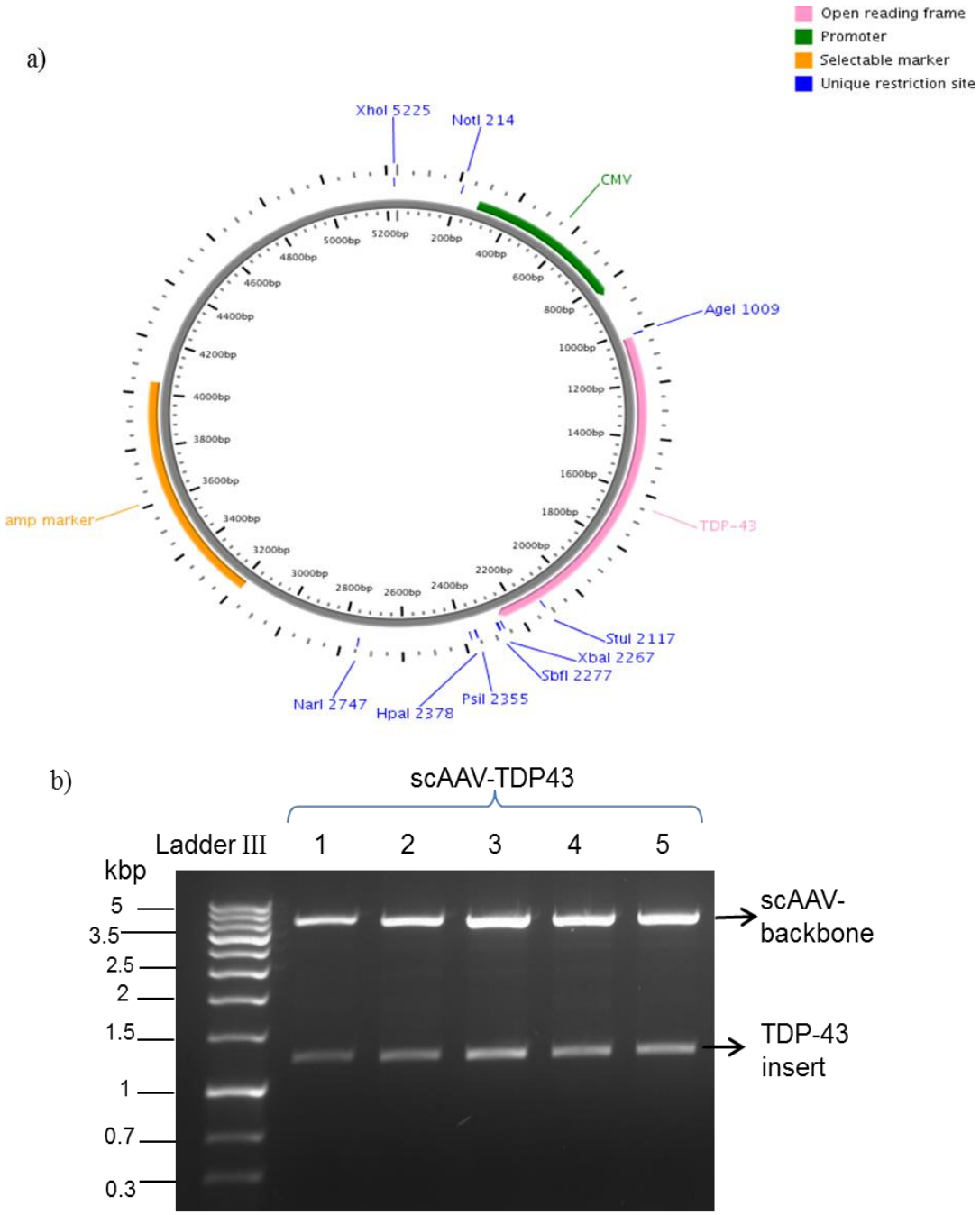

Figure 5.5: Validation of scAAV-TDP43 successful ligation. a) Plasmid map represents the scAAV-TDP43 sequence with unique restriction sites. b) TDP-43 was ligated to the scAAV backbone and transformed into XL10-gold cells. Plasmid extracts from several colonies were digested with AgeI and XbaI. All samples show successful digestion at the right sites (scAAV backbone at 4kbp and TDP-43 at ~1.25kbp)

5.3.2 scAAV-based vectors efficiency testing and purification

5.3.2.1 scAAV-based plasmids efficiently overexpress the proteins of interest

HEK293T cells were transfected with scAAV-ARFIP2, scAAV-HC or scAAV-TDP43 plasmids in order to confirm the efficiency of the plasmids prior to virus production. After 3 days of transfection, the proteins were harvested and concentrations were determined by BCA protein assay. Western blot was performed to determine the expression of FL-ARFIP2, HC-ARFIP2 and TDP43. The FL-ARFIP2 and HC-ARFIP2 were detected using mouse anti-HA antibody as a primary antibody. The successful expression of FL-ARFIP2 or HC-ARFIP2 was evaluated by the presence of bands at 38kDa and 19kDa, respectively, in the transfected samples compared to the untransfected controls. Figure 5.6 shows successful expression of FL-ARFIP2 and HC-ARFIP2 as they were detected by anti-HAtag antibody.

The TDP43 was detected using rabbit anti-TDP43 antibody as a primary antibody and then stained with HRP-conjugated goat anti-rabbit antibody as a secondary antibody. The successful overexpression of TDP43 was evaluated by comparison of band densities between the transfected and untransfected cells. The densities of the bands were determined using Gene tools software from Syngene. Comparing the band densities of the scAAV-TDP43 transfected samples with the untransfected control, the result shows successful overexpression of TDP43 by over 70 fold (see Figure 5.7).

Following successful validation of the vector genomes, we then started virus production and purification of scAAV-HC.

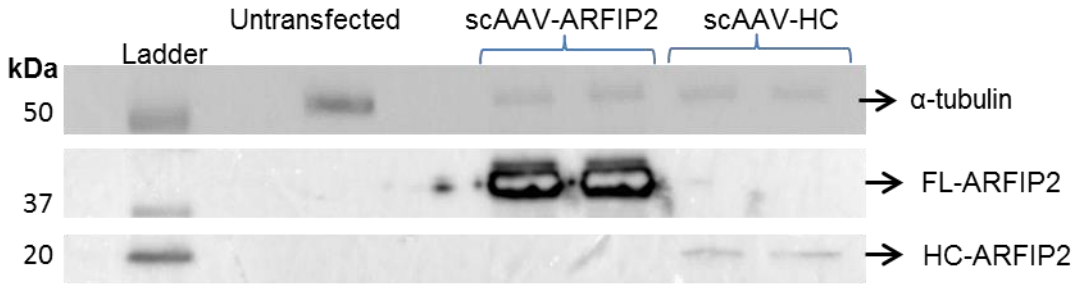

Figure 5.6: Validation of the scAAV-based plasmids expressing FL-ARFIP2 or HC-ARFIP2. HEK293T cells were transfected with the scAAV-based plasmids expressing FL-ARFIP2 or HC-ARFIP2 using the PEI transfection method. FL-ARFIP2 and HC-ARFIP2 expression was detected on a western blot by mouse anti-HA antibody. FL-ARFIP2 is detected at ~38kDa while the HC-ARFIP2 is detected around 20kDa. α-tubulin was used as loading control.

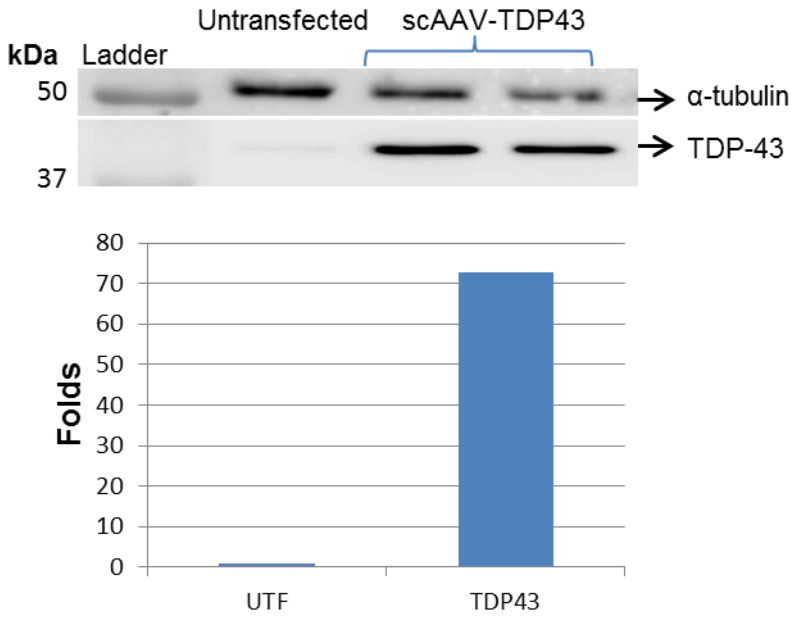

Figure 5.7: Validation of the scAAV-based vector genome expressing TDP43. HEK293T cells were transfected with the scAAV-TDP43 plasmid using the PEI transfection method. TDP43 overexpression was detected on a western blot by rabbit anti-TDP43 antibody. TDP43 is detected at 43kDa. α-tubulin was used as loading control. Densitometry shows over 70 fold increase in the expression of TDP43 compared to the untransfected (UTF) sample.

5.3.2.2 scAAV-HC virus production and purification

Once plasmid was validated, scAAV-HC virus was produced by transfecting HEK293T cells with the scAAV-HC vector genome and packaging plasmids (pAAV-2/9 and pHelper) using the PEI transfection method. After 5 days, the media was collected and purified as described in Section 2.2.6.2.5. Aliquots of the 40% fraction containing purified virus were collected. A sample of each aliquot was run on SDS-PAGE for purity analysis. SDS-PAGE gels were stained using SYPRO-Ruby protein gel stain. Figure 5.8 shows fractions of purified scAAV-HC virus showing the three bands representing the virus capsid proteins VP1, VP2 and VP3. Clean high-quality (HQ) fractions that showed no other bands were pooled, re-concentrated and desalted. HQ prep was re-run on SDS-PAGE to validate the purity (Figure 5.9)

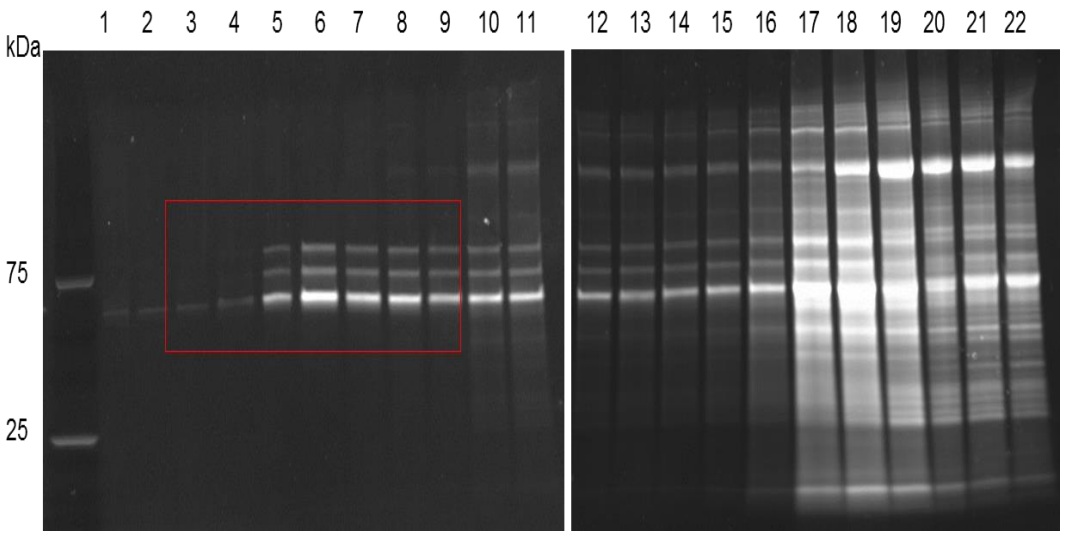

Figure 5.8: scAAV-HC fractions analysis. Samples were run on SDS-PAGE and stained using SYPRO-Ruby protein gel. Sample numbers 3-9 showing three capsid bands were pooled as high quality prep.

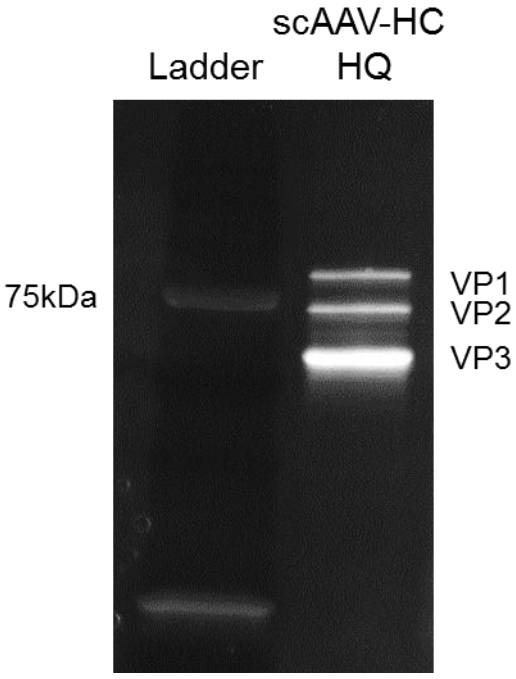

Figure 5.9: scAAV-HC high quality fraction analysis. HQ prep shows only 3 bands representing viral capsid proteins VP1, VP2 and VP3.

5.3.2.3 scAAV-HC efficiently overexpress HC-ARFIP2 in HEK293T cells

After production, concentration and purification of scAAV-HC, the viral titre was determined by qPCR using two different sets of primers for confirmation as described in Section 2.2.6.2.8. Viral titres ranged between 10^7-10^{10} viral genomes (vg/ml). To validate the efficiency of the produced virus, HEK293T cells were transduced with 50µl or 100µl of scAAV-HC of which the titre was $2.55*10^{10}$vg/ml. Cells were harvested 5 days post transduction and the protein was extracted and detected as above.

Figure 5.10 shows that the produced viruses were able to overexpress HC-ARFIP2. However, the achieved titres above are very low for *in vivo* applications. Our group and others have shown that titres around 10^{13}vg/ml are necessary to be able to administer doses ranging from $1x10^{11}$-$5x10^{11}$ vg in mice to achieve high level of gene transfer to CNS. After two runs, we could not generate scAAV-HC virus appropriate for use *in vivo*.

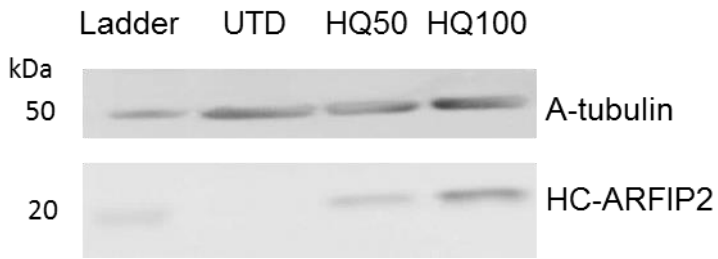

Figure 5.10: Validation of the scAAV-HC virus. HEK293T cells were transduced with 50µl or 100µl of scAAV-HC of which the titre was $2.55*10^{10}$vg/ml. HC-ARFIP2 expression was detected by mouse anti-HA antibody.

5.4 Discussion

The aim in this Chapter was to produce a vector that efficiently overexpresses HC-ARFIP2 in the CNS of an ALS-mouse model and use it to investigate the effect of HC-ARFIP2 expression on SOD1G93A mice survival. Therefore, it was necessary to produce high titre scAAV9-based vector that expressed HC-ARFIP2. The plan was to use this vector and run an efficacy pilot study in which virus would be administered by facial vain injection into WT mice. After 3 weeks, the spinal cord and brain tissues would be collected to detect the expression of HC-ARFIP2 using western blot and immunohistochemistry. Once expression had been validated, we would proceed with a survival study to determine the effect of HC-ARFIP2 expression on the symptoms and life span of SOD1G93A mice.

FL-ARFIP2, HC-ARFIP2 and TDP43 were successfully subcloned into scAAV9 vectors. As a priority, scAAV-HC production was performed first. scAAV-HC was produced successfully and the viral product efficiently transduced HEK293T cells. However, the titre of the resulting virus was too low to be used in *in vivo* experiments. The target titres mostly used for *in vivo* experiments are around 10^{13}-10^{14}vg/ml, which could not be accomplished after two attempts for scAAV-HC production, which generated virus preps with titres from 10^{7}-10^{10} vg/ml.

The scAAV production takes approximately 3 weeks from the production of plasmid mega prep until the titration of the virus. In addition, as scAAV production involves many materials and steps, any of those steps can be the reason of the reduced titre. It can be due to technical issues like HEK293T cell viability, plasmid purity, plasmid ratios or transfection efficiency. Our team also showed that the transgene could influence the titre achieved. Optimising scAAV-HC viral production and purification could take several months. Unfortunately, the lack of time as my PhD

studentship was ending and based on the outcome of scAAV production and purification, we decided not to proceed with the *in vivo* study.

CHAPTER 6: GENERAL DISCUSSION

6.1 Discussion

To date and despite the enormous amount of research on ALS, there is no effective treatment available for ALS. Finding a treatment for ALS is challenging due to the heterogeneity in the underlying pathogenesis of ALS. Although many pathogenic mechanisms have been suggested and studied, the primary trigger for the disease remains unknown.

Although very little is known about the exact function of Arfaptin2, its ability to bind to molecules involved in intracellular vesicular transport, indicates the possibility of its role in protein inclusion formation. Two independent groups have shown that Arfaptin2 is involved in polyQ-huntingtin aggregation in Huntington's disease (Peters et al., 2002, Rangone et al., 2005). To date and to our knowledge, the involvement of Arfaptin2 in ALS has not been studied. Accordingly, we sought to explore whether Arfaptin2 is involved in protein aggregation in ALS.

In this project we used primary motor neurons from mouse embryos as a follow up on the previous study on NSC34, which are immortalised motor neuron-like cells used as models for motor neurons (Kong, 2011). The current study has defined a number of important observations and issues that will be discussed in this chapter.

PI exclusion assay, represented in Chapter 3, was performed to investigate the effect of overexpressing FL-ARFIP2 or HC-ARFIP2 on cell viability. At first, transfection using Fugene as a transfection reagent was used to express FL-ARFIP2, HC-ARFIP2 or TDP43 in primary motor neurons. However, it was observed in some experiments that all cells were dead by the end of the incubation period. In some experiments where some cells survived, the number was much lower than expected and would not be sufficient for statistical analysis and completion of our study. This

was true for both transfected and mock transfected controls, which indicated that the cytotoxic effect was probably due to the transfection reagent rather than the transfected plasmids. In addition, as this reagent was used previously within our group to transfect NSC34 cell lines, our observations suggest that primary motor neurons are more sensitive to transfection reagents than neuronal cell lines. This also suggests that primary motor neurons are better models to investigate motor neuron reaction to treatments as they show closer resemblance to normal cells *in vivo*. On the other hand, as far as we know, there is no study investigating the expression level of Arfaptin2 in different developmental stages of the CNS. Therefore, it is unknown yet whether Arfaptin2 or HC-ARFIP2 expression would have different effects on adult cell lines compared to the embryonic cells that we used in this project. Hence, further validation of these results on adult cell lines might be required.

Subsequently, in Chapter 3 subcloning of FL-ARFIP2, HC-ARFIP2 and TDP43 into LV vector was conducted. LV-based viruses , which mediated expression of FL-ARFIP2, HC-ARFIP2 or TDP43, were successfully produced. The viral products efficiently express the desired proteins in primary motor neurons. Survival assays using these vectors showed that HC-ARFIP2 significantly increased motor neuron survival by approximately 20% compared to untransduced cells. This protective effect was observed clearly when compared to FL-ARFIP2 and TDP43 treated samples, where survival was increased by approximately 40% in some cases. This supports findings from our previous study (Kong, 2011), where it was shown that HC-ARFIP2 expression in NSC34 cells increased cell survival compared to controls. The findings were similar between WT NSC34 and stably transfected G93A-NSC34 cell lines, in both of which survival was increased by 10% when overexpressing HC-ARFIP2.

As neurodegenerative diseases share some common features, treatments for neurodegenerative diseases might be exchangeable; i.e. treatment for one neurodegenerative disease might be useful for another neurodegenerative disease as well. For example, Neuregulin1 was found to have a neuroprotective effect in AD as well as PD models (Carlsson et al., 2011, Ryu et al., 2012, Cui et al., 2013). Similarly, we showed in this project that the neuroprotective effect of HC-ARFIP2 that has been reported in HD models (Peters et al., 2002) is applicable to ALS *in vitro* models as well.

It is evident that activation of Akt by phosphorylation has a neuroprotective effect (Ning et al., 2004, Kanekura et al., 2005, Dewil et al., 2007, Ning et al., 2010, Takata et al., 2013, Tsai et al., 2013, Little et al., 2014, Peviani et al., 2014). Interestingly, previous studies showed that administering Fasudil, an inhibitor of the Rho pathway, to SOD1G93A mice delayed onset and prolonged survival through upregulation of phospho-Akt and downregulation of PTEN (Takata et al., 2013). In addition, Little *et al*. showed recently that knocking down PTEN in an SMA mouse model rescued motor neuron function and prolonged life span (Little et al., 2014). These and other observations emphasise the importance of this pathway in the development and survival of motor neurons. Results in Chapter 4 support those findings, as we showed that HC-ARFIP2 expression in HEK293T cells downregulated PTEN, and hence upregulated phospho-Akt expression. The enhancement in Akt phosphorylation induced the autophagic markers, LC3II and ULK1, suggesting activation of a protein degradation pathway. There were no differences observed in activity of 4EBP1, which induces protein synthesis and is downstream of the mTORC pathway. Taken together, these results indicate that the prosurvival effect of HC-ARFIP2 is through the Akt pathway and involves protein degradation. This effect is independent from the

mTORC pathway. In this study, we used HEK293T cells, as they are easy to maintain and transduce. In addition, they yield sufficient amounts of protein to be used for western blotting.

The importance of the results presented in this thesis lies in the possibility to apply this concept to other proteinopathies. Some neurodegenerative diseases share features such as accumulation of misfolded proteins. In addition, Akt dysregulation has been implicated in different neurodegenerative diseases. For example, Prion disease is a neurodegenerative disease and a proteinopathy that is characterised by the accumulation of misfolded prion protein. Research showed that the Akt pathway is dysregulated in *in vivo* and *in vitro* models of Prion disease (Shott et al., 2014, Simon et al., 2014). It was shown that activation of Akt ameliorates toxicity in cells expressing mutant prion protein (Simon et al., 2014). One of the histopathological characteristics of AD is the accumulation of β-amyloid peptides. A combination of microRNA (miRNA) sequencing and miRNA-target prediction methods used to compare microRNA expression levels in the brain of an AD mouse model and controls showed that the biggest numbers of differentially expressed miRNAs were affecting the PI3K/Akt pathway (Luo et al., 2014). In addition, it was shown that activation of the PI3K/Akt pathway in *in vitro* and *in vivo* AD models using Neuregulin1beta1 improved neuronal survival by increasing the expression of Bcl-2, which is a downstream anti-apoptotic effector to Akt (Ryu et al., 2012, Cui et al., 2013). Similarly, reduction in Akt activity was found in PD models (Wang et al., 2013). Targeting the Akt pathway using Fasudil, which is a Rho inhibitor, increased neuronal survival in a PD *in vivo* model (Zhao et al., 2015). Collectively, these findings support the significance of the Akt pathway in neurodegenerative diseases and support the idea that Akt modulation could rescue from neurodegeneration.

Impaired autophagy has also been reported in AD, PD and HD (Boland et al., 2008, Martinez-Vicente et al., 2010, Ciechanover and Kwon, 2015, De Rosa et al., 2015). Therapeutic strategies involving induction of autophagy in these diseases showed that rescuing autophagy leads to rescue of neurodegeneration (Ciechanover and Kwon, 2015). Therefore, the application of HC-ARFIP2 expression to other neurodegenerative disease models with featuring protein aggregation could rescue Akt dysregulation, increase autophagy and subsequently decrease aggregate formation and neurotoxicity.

Different defects within the autophagy pathway have been described in different neurodegenerative diseases. For instance, in HD, defective recognition and engulfment of mutant polyQ-huntingtin by autophagosomes was observed rather than impaired autophagosome-lysosomal degradation (Martinez-Vicente et al., 2010). In an AD model it was demonstrated that AD-linked aggregates are caused by impaired autophagosome clearance rather than impaired autophagy activation. This indicates that activation of autophagy does not necessarily increase protein degradation (Boland et al., 2008). As we showed that HC-ARFIP2 increases some autophagy markers, it is necessary to investigate the effect of HC-ARFIP2 on autophagosome formation, components and clearance as well; i.e autophagy flux.

Chapter 5 of the current PhD project outlines the procedure followed for scAAV9-based virus production. One of the down sides of using viruses as a method of gene transfer is the laborious work that needs to be done to obtain these viruses. Though the virus design, subcloning and production are preparatory steps rather than “real” experiments, they were time consuming and necessary to achieve the aims of the study. Finally, an efficient virus was successfully produced, however the viral yield was

lower than desired for usage in mouse model studies. Therefore, high titre viral stocks will need to be produced for subsequent studies.

6.2 Conclusion

In conclusion, the results partially support the theory of involvement of Arfaptin2 in protein degradation pathways. In addition, HC-ARFIP2 can promote motor neuron survival through Akt pathway activation, which indicates that modulation of Arfaptin2 can be a target for therapeutic strategies for ALS.

One of the disadvantages of using viruses as a DNA transfer vector is that a "one size fits all" concept cannot be applied. As observed in Chapter 3, different constructs led to different expression levels using the same MOI. Therefore, a standardised MOI cannot be used for all viruses. A more detailed optimisation of the MOI used of each virus for each type of cell line might give a more accurate conclusion.

6.3 Future perspectives

Firstly, as a subsequent step to this study, the effect of HC-ARFIP2 expression needs to be studied *in vivo*. This could be done using systemic or cerebrospinal fluid (CSF) delivery of scAAV9-based vectors. Plasmids produced in this study can be used for subsequent future studies as well. In addition, due to the emerging evidence showing the role of glial cells in the pathogenesis of ALS, a co-culture study could be conducted to determine the effect of Arfaptin2 modulation on motor neuron survival. This could determine whether the neuroprotective effect of HC-ARFIP2 is cell type-dependent.

Secondly, although primary motor neurons are hard to extract and the protein lysate yield is low, it is still necessary toconfirm the downstream effectors of HC-ARFIP2 in primary motor neurons. In addition, as HC-ARFIP2 showed induction of

autophagic markers, autophagy flux should be studied to determine if protein degradation is accomplished. Finally, it would be interesting to investigate the interaction between Arfaptin2 and SOD1, TDP43 and p62 using immunoprecipitation. Additionally, as the colocalisation study did not lead to firm conclusions, it might be worth re-investigating the colocalisation of Arfaptin2 with the aforementioned proteins to validate their interaction. Furthermore, it would be interesting to investigate the colocalisation of Arfaptin2 with other ALS-linked proteins to understand whether Arfaptin2 could be a therapeutic target for a broad spectrum of ALS subtypes.

REFERENCES

Abdo H, Derkinderen P, Gomes P, Chevalier J, Aubert P, Masson D, Galmiche JP, Vanden Berghe P, Neunlist M, Lardeux B (2010) Enteric glial cells protect neurons from oxidative stress in part via reduced glutathione. FASEB J 24:1082-1094.

Agosta F, Weiler M, Filippi M (2015) Propagation of Pathology through Brain Networks in Neurodegenerative Diseases: From Molecules to Clinical Phenotypes. CNS Neurosci Ther.

Al-Saif A, Al-Mohanna F, Bohlega S (2011) A mutation in sigma-1 receptor causes juvenile amyotrophic lateral sclerosis. Annals of neurology 70:913-919.

Alexander GM, Deitch JS, Seeburger JL, Del Valle L, Heiman-Patterson TD (2000) Elevated cortical extracellular fluid glutamate in transgenic mice expressing human mutant (G93A) Cu/Zn superoxide dismutase. Journal of neurochemistry 74:1666-1673.

Antonelli T, Tomasini MC, Fournier J, Mazza R, Tanganelli S, Pirondi S, Fuxe K, Ferraro L (2008) Neurotensin receptor involvement in the rise of extracellular glutamate levels and apoptotic nerve cell death in primary cortical cultures after oxygen and glucose deprivation. Cereb Cortex 18:1748-1757.

Armon C (2005) Acquired nucleic acid changes may trigger sporadic amyotrophic lateral sclerosis. Muscle & nerve 32:373-377.

Aschauer DF, Kreuz S, Rumpel S (2013) Analysis of transduction efficiency, tropism and axonal transport of AAV serotypes 1, 2, 5, 6, 8 and 9 in the mouse brain. PloS one 8:e76310.

Ash PE, Zhang YJ, Roberts CM, Saldi T, Hutter H, Buratti E, Petrucelli L, Link CD (2010) Neurotoxic effects of TDP-43 overexpression in C. elegans. Human molecular genetics 19:3206-3218.

Ayala V, Granado-Serrano AB, Cacabelos D, Naudi A, Ilieva EV, Boada J, Caraballo-Miralles V, Llado J, Ferrer I, Pamplona R, Portero-Otin M (2011) Cell stress induces TDP-43 pathological changes associated with ERK1/2 dysfunction: implications in ALS. Acta neuropathologica 122:259-270.

Baens M, Noels H, Broeckx V, Hagens S, Fevery S, Billiau AD, Vankelecom H, Marynen P (2006) The dark side of EGFP: defective polyubiquitination. PloS one 1:e54.

Balch WE, Kahn RA, Schwaninger R (1992) ADP-ribosylation factor is required for vesicular trafficking between the endoplasmic reticulum and the cis-Golgi compartment. The Journal of biological chemistry 267:13053-13061.

Baldwin MA, Pan KM, Nguyen J, Huang Z, Groth D, Serban A, Gasset M, Mehlhorn I, Fletterick RJ, Cohen FE, et al. (1994) Spectroscopic characterization of conformational differences between PrPC and PrPSc: an alpha-helix to beta-sheet transition. Philosophical transactions of the Royal Society of London Series B, Biological sciences 343:435-441.

Baloh RH (2011) TDP-43: the relationship between protein aggregation and neurodegeneration in amyotrophic lateral sclerosis and frontotemporal lobar degeneration. The FEBS journal 278:3539-3549.

Barmada SJ, Serio A, Arjun A, Bilican B, Daub A, Ando DM, Tsvetkov A, Pleiss M, Li X, Peisach D, Shaw C, Chandran S, Finkbeiner S (2014) Autophagy induction enhances TDP43 turnover and survival in neuronal ALS models. Nature chemical biology 10:677-685.

Bender FL, Fischer M, Funk N, Orel N, Rethwilm A, Sendtner M (2007) High-efficiency gene transfer into cultured embryonic motoneurons using recombinant lentiviruses. Histochemistry and cell biology 127:439-448.

Benkhelifa-Ziyyat S, Besse A, Roda M, Duque S, Astord S, Carcenac R, Marais T, Barkats M (2013) Intramuscular scAAV9-SMN injection mediates widespread gene delivery to the spinal cord and decreases disease severity in SMA mice. Molecular therapy : the journal of the American Society of Gene Therapy 21:282-290.

Berggard T, Linse S, James P (2007) Methods for the detection and analysis of protein-protein interactions. Proteomics 7:2833-2842.

Biljan I, Giachin G, Ilc G, Zhukov I, Plavec J, Legname G (2012) Structural basis for the protective effect of the human prion protein carrying the dominant-negative E219K polymorphism. The Biochemical journal 446:243-251.

Bilsland LG, Sahai E, Kelly G, Golding M, Greensmith L, Schiavo G (2010) Deficits in axonal transport precede ALS symptoms in vivo. Proceedings of the National Academy of Sciences of the United States of America 107:20523-20528.

Blomer U, Naldini L, Kafri T, Trono D, Verma IM, Gage FH (1997) Highly efficient and sustained gene transfer in adult neurons with a lentivirus vector. Journal of virology 71:6641-6649.

Boland B, Kumar A, Lee S, Platt FM, Wegiel J, Yu WH, Nixon RA (2008) Autophagy induction and autophagosome clearance in neurons: relationship to autophagic pathology in Alzheimer's disease. The Journal of neuroscience : the official journal of the Society for Neuroscience 28:6926-6937.

Bosco DA, Morfini G, Karabacak NM, Song Y, Gros-Louis F, Pasinelli P, Goolsby H, Fontaine BA, Lemay N, McKenna-Yasek D, Frosch MP, Agar JN, Julien JP, Brady ST, Brown RH, Jr. (2010) Wild-type and mutant SOD1 share an aberrant conformation and a common pathogenic pathway in ALS. Nature neuroscience 13:1396-1403.

Bradley WG, Daroff RB, Fenichel G, Jankovic J (2003) Neurology in Clinical Practice e-dition: Butterworth Heinemann.

Burd CG, Strochlic TI, Setty SRG (2004) Arf-like GTPases: not so Arf-like after all. Trends Cell Biol 14:687-694.

Cargnello M, Roux PP (2011) Activation and function of the MAPKs and their substrates, the MAPK-activated protein kinases. Microbiology and molecular biology reviews : MMBR 75:50-83.

Carlsson T, Schindler FR, Hollerhage M, Depboylu C, Arias-Carrion O, Schnurrbusch S, Rosler TW, Wozny W, Schwall GP, Groebe K, Oertel WH, Brundin P, Schrattenholz A, Hoglinger GU (2011) Systemic administration of neuregulin-1beta1 protects dopaminergic neurons in a mouse model of Parkinson's disease. Journal of neurochemistry 117:1066-1074.

Chalasani ML, Kumari A, Radha V, Swarup G (2014) E50K-OPTN-induced retinal cell death involves the Rab GTPase-activating protein, TBC1D17 mediated block in autophagy. PloS one 9:e95758.

Chattopadhyay M, Valentine JS (2009) Aggregation of copper-zinc superoxide dismutase in familial and sporadic ALS. Antioxidants & redox signaling 11:1603-1614.

Cheah BC, Vucic S, Krishnan AV, Kiernan MC (2010) Riluzole, neuroprotection and amyotrophic lateral sclerosis. Current medicinal chemistry 17:1942-1199.

Chen AK, Lin RY, Hsieh EZ, Tu PH, Chen RP, Liao TY, Chen W, Wang CH, Huang JJ (2010) Induction of amyloid fibrils by the C-terminal fragments of TDP-43 in amyotrophic lateral sclerosis. J Am Chem Soc 132:1186-1187.

Chen YZ, Bennett CL, Huynh HM, Blair IP, Puls I, Irobi J, Dierick I, Abel A, Kennerson ML, Rabin BA, Nicholson GA, Auer-Grumbach M, Wagner K, De Jonghe P, Griffin JW, Fischbeck KH, Timmerman V, Cornblath DR, Chance PF (2004) DNA/RNA helicase gene mutations in a form of juvenile amyotrophic lateral sclerosis (ALS4). American journal of human genetics 74:1128-1135.

Chia R, Tattum MH, Jones S, Collinge J, Fisher EM, Jackson GS (2010) Superoxide dismutase 1 and tgSOD1 mouse spinal cord seed fibrils, suggesting a propagative cell death mechanism in amyotrophic lateral sclerosis. PloS one 5:e10627.

Cho GW, Kim GY, Baek S, Kim H, Kim T, Kim HJ, Kim SH (2011) Recombinant human erythropoietin reduces aggregation of mutant Cu/Zn-binding superoxide dismutase (SOD1) in NSC-34 cells. Neuroscience letters 504:107-111.

Chow CY, Landers JE, Bergren SK, Sapp PC, Grant AE, Jones JM, Everett L, Lenk GM, McKenna-Yasek DM, Weisman LS, Figlewicz D, Brown RH, Meisler MH (2009) Deleterious variants of FIG4, a phosphoinositide phosphatase, in patients with ALS. American journal of human genetics 84:85-88.

Ciechanover A, Kwon YT (2015) Degradation of misfolded proteins in neurodegenerative diseases: therapeutic targets and strategies. Exp Mol Med 47:e147.

Clague MJ, Urbe S (2010) Ubiquitin: same molecule, different degradation pathways. Cell 143:682-685.

Corbetta S, Gualdoni S, Albertinazzi C, Paris S, Croci L, Consalez GG, de Curtis I (2005) Generation and characterization of Rac3 knockout mice. Molecular and cellular biology 25:5763-5776.

Cruz-Garcia D, Ortega-Bellido M, Scarpa M, Villeneuve J, Jovic M, Porzner M, Balla T, Seufferlein T, Malhotra V (2013) Recruitment of arfaptins to the trans-Golgi network by PI(4)P and their involvement in cargo export. The EMBO journal 32:1717-1729.

Cui W, Tao J, Wang Z, Ren M, Zhang Y, Sun Y, Peng Y, Li R (2013) Neuregulin1beta1 antagonizes apoptosis via ErbB4-dependent activation of PI3-kinase/Akt in APP/PS1 transgenic mice. Neurochem Res 38:2237-2246.

Czubryt MP, Austria JA, Pierce GN (2000) Hydrogen peroxide inhibition of nuclear protein import is mediated by the mitogen-activated protein kinase, ERK2. The Journal of cell biology 148:7-16.

D'Souza-Schorey C, Boshans RL, McDonough M, Stahl PD, Van Aelst L (1997) A role for POR1, a Rac1-interacting protein, in ARF6-mediated cytoskeletal rearrangements. The EMBO journal 16:5445-5454.

De Matteis MA, Wilson C, D'Angelo G (2013) Phosphatidylinositol-4-phosphate: The Golgi and beyond (vol 35, pg 612, 2013). BioEssays : news and reviews in molecular, cellular and developmental biology 35:756-756.

De Rosa P, Marini ES, Gelmetti V, Valente EM (2015) Candidate genes for Parkinson disease: Lessons from pathogenesis. Clin Chim Acta.

Deglon N, Tseng JL, Bensadoun JC, Zurn AD, Arsenijevic Y, De Almeida LP, Zufferey R, Trono D, Aebischer P (2000) Self-inactivating lentiviral vectors with enhanced transgene expression as potential gene transfer system in Parkinson's disease. Hum Gene Ther 11:179-190.

DeJesus-Hernandez M, Kocerha J, Finch N, Crook R, Baker M, Desaro P, Johnston A, Rutherford N, Wojtas A, Kennelly K, Wszolek ZK, Graff-Radford N, Boylan K, Rademakers R (2010) De novo truncating FUS gene mutation as a cause of sporadic amyotrophic lateral sclerosis. Human mutation 31:E1377-1389.

DeJesus-Hernandez M, Mackenzie IR, Boeve BF, Boxer AL, Baker M, Rutherford NJ, Nicholson AM, Finch NA, Flynn H, Adamson J, Kouri N, Wojtas A, Sengdy P, Hsiung GY, Karydas A, Seeley WW, Josephs KA, Coppola G, Geschwind DH, Wszolek ZK, Feldman H, Knopman DS, Petersen RC, Miller BL, Dickson DW, Boylan KB, Graff-Radford NR, Rademakers R (2011) Expanded GGGGCC hexanucleotide repeat in noncoding region of C9ORF72 causes chromosome 9p-linked FTD and ALS. Neuron 72:245-256.

Deng HX, Bigio EH, Zhai H, Fecto F, Ajroud K, Shi Y, Yan J, Mishra M, Ajroud-Driss S, Heller S, Sufit R, Siddique N, Mugnaini E, Siddique T (2011a) Differential involvement of optineurin in amyotrophic lateral sclerosis with or without SOD1 mutations. Arch Neurol 68:1057-1061.

Deng HX, Chen W, Hong ST, Boycott KM, Gorrie GH, Siddique N, Yang Y, Fecto F, Shi Y, Zhai H, Jiang H, Hirano M, Rampersaud E, Jansen GH, Donkervoort S, Bigio EH, Brooks BR, Ajroud K, Sufit RL, Haines JL, Mugnaini E, Pericak-Vance MA, Siddique T (2011b) Mutations in UBQLN2 cause dominant X-linked juvenile and adult-onset ALS and ALS/dementia. Nature 477:211-215.

Deng HX, Zhai H, Bigio EH, Yan J, Fecto F, Ajroud K, Mishra M, Ajroud-Driss S, Heller S, Sufit R, Siddique N, Mugnaini E, Siddique T (2010) FUS-immunoreactive inclusions are a common feature in sporadic and non-SOD1 familial amyotrophic lateral sclerosis. Annals of neurology 67:739-748.

Dewil M, Lambrechts D, Sciot R, Shaw PJ, Ince PG, Robberecht W, Van den Bosch L (2007) Vascular endothelial growth factor counteracts the loss of phospho-Akt preceding motor neurone degeneration in amyotrophic lateral sclerosis. Neuropathology and applied neurobiology 33:499-509.

Diaz-Amarilla P, Olivera-Bravo S, Trias E, Cragnolini A, Martinez-Palma L, Cassina P, Beckman J, Barbeito L (2011) Phenotypically aberrant astrocytes that promote motoneuron damage in a model of inherited amyotrophic lateral sclerosis. Proceedings of the National Academy of Sciences of the United States of America 108:18126-18131.

Dibaj P, Steffens H, Zschuntzsch J, Nadrigny F, Schomburg ED, Kirchhoff F, Neusch C (2011) In Vivo imaging reveals distinct inflammatory activity of CNS microglia versus PNS macrophages in a mouse model for ALS. PloS one 6:e17910.

Duque S, Joussemet B, Riviere C, Marais T, Dubreil L, Douar AM, Fyfe J, Moullier P, Colle MA, Barkats M (2009) Intravenous administration of self-complementary AAV9 enables transgene delivery to adult motor neurons. Molecular therapy : the journal of the American Society of Gene Therapy 17:1187-1196.

Elden AC, Kim HJ, Hart MP, Chen-Plotkin AS, Johnson BS, Fang X, Armakola M, Geser F, Greene R, Lu MM, Padmanabhan A, Clay-Falcone D, McCluskey L, Elman L, Juhr D, Gruber PJ, Rub U, Auburger G, Trojanowski JQ, Lee VM, Van Deerlin VM, Bonini NM, Gitler AD (2010) Ataxin-2 intermediate-length polyglutamine expansions are associated with increased risk for ALS. Nature 466:1069-1075.

Esclaire F, Kisby G, Spencer P, Milne J, Lesort M, Hugon J (1999) The Guam cycad toxin methylazoxymethanol damages neuronal DNA and modulates tau mRNA expression and excitotoxicity. Experimental neurology 155:11-21.

Fan Y, Sun C, Gao X, Wang F, Li X, Kassim RM, Tai G, Zhou Y (2012) Neuroprotective effects of ginseng pectin through the activation of ERK/MAPK and Akt survival signaling pathways. Mol Med Rep 5:1185-1190.

Farg MA, Sundaramoorthy V, Sultana JM, Yang S, Atkinson RA, Levina V, Halloran MA, Gleeson PA, Blair IP, Soo KY, King AE, Atkin JD (2014) C9ORF72, implicated in amytrophic lateral sclerosis and frontotemporal dementia, regulates endosomal trafficking. Human molecular genetics 23:3579-3595.

Fecto F, Yan J, Vemula SP, Liu E, Yang Y, Chen W, Zheng JG, Shi Y, Siddique N, Arrat H, Donkervoort S, Ajroud-Driss S, Sufit RL, Heller SL, Deng HX, Siddique T (2011) SQSTM1 mutations in familial and sporadic amyotrophic lateral sclerosis. Archives of neurology 68:1440-1446.

Ferraiuolo L, Kirby J, Grierson AJ, Sendtner M, Shaw PJ (2011) Molecular pathways of motor neuron injury in amyotrophic lateral sclerosis. Nature reviews Neurology 7:616-630.

Field NC, Metcalf JS, Caller TA, Banack SA, Cox PA, Stommel EW (2013) Linking beta-methylamino-L-alanine exposure to sporadic amyotrophic lateral sclerosis in Annapolis, MD. Toxicon : official journal of the International Society on Toxinology 70:179-183.

Figueroa-Romero C, Hur J, Bender DE, Delaney CE, Cataldo MD, Smith AL, Yung R, Ruden DM, Callaghan BC, Feldman EL (2012) Identification of epigenetically altered genes in sporadic amyotrophic lateral sclerosis. PloS one 7:e52672.

Foust KD, Nurre E, Montgomery CL, Hernandez A, Chan CM, Kaspar BK (2009) Intravascular AAV9 preferentially targets neonatal neurons and adult astrocytes. Nature biotechnology 27:59-65.

Foust KD, Wang X, McGovern VL, Braun L, Bevan AK, Haidet AM, Le TT, Morales PR, Rich MM, Burghes AH, Kaspar BK (2010) Rescue of the spinal muscular atrophy phenotype in a mouse model by early postnatal delivery of SMN. Nature biotechnology 28:271-274.

Gerolami R, Uch R, Jordier F, Chapel S, Bagnis C, Brechot C, Mannoni P (2000) Gene transfer to hepatocellular carcinoma: transduction efficacy and transgene expression kinetics by using retroviral and lentiviral vectors. Cancer gene therapy 7:1286-1292.

Gillingham AK, Munro S (2007) The small G proteins of the arf family and their regulators. Annu Rev Cell Dev Bi 23:579-611.

Gingras AC, Gygi SP, Raught B, Polakiewicz RD, Abraham RT, Hoekstra MF, Aebersold R, Sonenberg N (1999) Regulation of 4E-BP1 phosphorylation: a novel two-step mechanism. Genes Dev 13:1422-1437.

Gitler AD, Shorter J (2011) RNA-binding proteins with prion-like domains in ALS and FTLD-U. Prion 5:179-187.

Graber DJ, Harris BT (2013) Purification and culture of spinal motor neurons from rat embryos. Cold Spring Harbor protocols 2013:319-326.

Gray SJ, Matagne V, Bachaboina L, Yadav S, Ojeda SR, Samulski RJ (2011) Preclinical differences of intravascular AAV9 delivery to neurons and glia: a comparative study of adult mice and nonhuman primates. Molecular therapy : the journal of the American Society of Gene Therapy 19:1058-1069.

Greenway MJ, Andersen PM, Russ C, Ennis S, Cashman S, Donaghy C, Patterson V, Swingler R, Kieran D, Prehn J, Morrison KE, Green A, Acharya KR, Brown RH, Jr., Hardiman O (2006) ANG mutations segregate with familial and 'sporadic' amyotrophic lateral sclerosis. Nature genetics 38:411-413.

Guareschi S, Cova E, Cereda C, Ceroni M, Donetti E, Bosco DA, Trotti D, Pasinelli P (2012) An over-oxidized form of superoxide dismutase found in sporadic amyotrophic lateral sclerosis with bulbar onset shares a toxic mechanism with mutant SOD1. Proceedings of the National Academy of Sciences of the United States of America 109:5074-5079.

Guo JL, Lee VM (2014) Cell-to-cell transmission of pathogenic proteins in neurodegenerative diseases. Nat Med 20:130-138.

Guo W, Chen Y, Zhou X, Kar A, Ray P, Chen X, Rao EJ, Yang M, Ye H, Zhu L, Liu J, Xu M, Yang Y, Wang C, Zhang D, Bigio EH, Mesulam M, Shen Y, Xu Q, Fushimi K, Wu JY (2011) An ALS-associated mutation affecting TDP-43 enhances protein aggregation, fibril formation and neurotoxicity. Nature structural & molecular biology 18:822-830.

Gurney ME (1997) The use of transgenic mouse models of amyotrophic lateral sclerosis in preclinical drug studies. Journal of the neurological sciences 152 Suppl 1:S67-73.

Gurney ME, Pu H, Chiu AY, Dal Canto MC, Polchow CY, Alexander DD, Caliendo J, Hentati A, Kwon YW, Deng HX, et al. (1994) Motor neuron degeneration in mice that express a human Cu,Zn superoxide dismutase mutation. Science 264:1772-1775.

Haidet-Phillips AM, Hester ME, Miranda CJ, Meyer K, Braun L, Frakes A, Song S, Likhite S, Murtha MJ, Foust KD, Rao M, Eagle A, Kammesheidt A, Christensen A, Mendell JR, Burghes AH, Kaspar BK (2011) Astrocytes from familial and sporadic ALS patients are toxic to motor neurons. Nature biotechnology 29:824-828.

Hakeda-Suzuki S, Ng J, Tzu J, Dietzl G, Sun Y, Harms M, Nardine T, Luo L, Dickson BJ (2002) Rac function and regulation during Drosophila development. Nature 416:438-442.

Hentati A, Bejaoui K, Pericak-Vance MA, Hentati F, Speer MC, Hung WY, Figlewicz DA, Haines J, Rimmler J, Ben Hamida C, et al. (1994) Linkage of recessive familial amyotrophic lateral sclerosis to chromosome 2q33-q35. Nature genetics 7:425-428.

Hortobagyi T, Troakes C, Nishimura AL, Vance C, van Swieten JC, Seelaar H, King A, Al-Sarraj S, Rogelj B, Shaw CE (2011) Optineurin inclusions occur in a minority of TDP-43 positive ALS and FTLD-TDP cases and are rarely observed in other neurodegenerative disorders. Acta neuropathologica 121:519-527.

Ishigaki S, Hishikawa N, Niwa J, Iemura S, Natsume T, Hori S, Kakizuka A, Tanaka K, Sobue G (2004) Physical and functional interaction between Dorfin and Valosin-containing protein that are colocalized in ubiquitylated inclusions in neurodegenerative disorders. The Journal of biological chemistry 279:51376-51385.

Ito H, Fujita K, Nakamura M, Wate R, Kaneko S, Sasaki S, Yamane K, Suzuki N, Aoki M, Shibata N, Togashi S, Kawata A, Mochizuki Y, Mizutani T, Maruyama H, Hirano A, Takahashi R, Kawakami H, Kusaka H (2011) Optineurin is co-localized with FUS in basophilic inclusions of ALS with FUS mutation and in basophilic inclusion body disease. Acta neuropathologica 121:555-557.

Jacquier A, Buhler E, Schafer MK, Bohl D, Blanchard S, Beclin C, Haase G (2006) Alsin/Rac1 signaling controls survival and growth of spinal motoneurons. Annals of neurology 60:105-117.

Jain A, Brady-Kalnay SM, Bellamkonda RV (2004) Modulation of Rho GTPase activity alleviates chondroitin sulfate proteoglycan-dependent inhibition of neurite extension. Journal of neuroscience research 77:299-307.

Jana NR, Zemskov EA, Wang G, Nukina N (2001) Altered proteasomal function due to the expression of polyglutamine-expanded truncated N-terminal huntingtin induces apoptosis by caspase activation through mitochondrial cytochrome c release. Human molecular genetics 10:1049-1059.

Jansen AH, Reits EA, Hol EM (2014) The ubiquitin proteasome system in glia and its role in neurodegenerative diseases. Frontiers in molecular neuroscience 7:73.

Johnson BS, Snead D, Lee JJ, McCaffery JM, Shorter J, Gitler AD (2009) TDP-43 is intrinsically aggregation-prone, and amyotrophic lateral sclerosis-linked mutations accelerate aggregation and increase toxicity. The Journal of biological chemistry 284:20329-20339.

Johnson JO, Mandrioli J, Benatar M, Abramzon Y, Van Deerlin VM, Trojanowski JQ, Gibbs JR, Brunetti M, Gronka S, Wuu J, Ding J, McCluskey L, Martinez-Lage M, Falcone D, Hernandez DG, Arepalli S, Chong S, Schymick JC, Rothstein J, Landi F, Wang YD, Calvo A, Mora G, Sabatelli M, Monsurro MR, Battistini S, Salvi F, Spataro R, Sola P, Borghero G, Consortium I, Galassi G, Scholz SW, Taylor JP, Restagno G, Chio A, Traynor BJ (2010a) Exome sequencing reveals VCP mutations as a cause of familial ALS. Neuron 68:857-864.

Johnson JO, Mandrioli J, Benatar M, Abramzon Y, Van Deerlin VM, Trojanowski JQ, Gibbs JR, Brunetti M, Gronka S, Wuu J, Ding J, McCluskey L, Martinez-Lage M, Falcone D, Hernandez DG, Arepalli S, Chong S, Schymick JC, Rothstein J, Landi F, Wang YD, Calvo A, Mora G, Sabatelli M, Monsurro MR, Battistini S, Salvi F, Spataro R, Sola P, Borghero G, Galassi G, Scholz SW, Taylor JP, Restagno G, Chio A, Traynor BJ (2010b) Exome sequencing reveals VCP mutations as a cause of familial ALS. Neuron 68:857-864.

Johnson JO, Pioro EP, Boehringer A, Chia R, Feit H, Renton AE, Pliner HA, Abramzon Y, Marangi G, Winborn BJ, Gibbs JR, Nalls MA, Morgan S, Shoai M, Hardy J, Pittman A, Orrell RW, Malaspina A, Sidle KC, Fratta P, Harms MB, Baloh RH, Pestronk A, Weihl

CC, Rogaeva E, Zinman L, Drory VE, Borghero G, Mora G, Calvo A, Rothstein JD, Consortium I, Drepper C, Sendtner M, Singleton AB, Taylor JP, Cookson MR, Restagno G, Sabatelli M, Bowser R, Chio A, Traynor BJ (2014) Mutations in the Matrin 3 gene cause familial amyotrophic lateral sclerosis. Nature neuroscience 17:664-666.

Johnston JA, Ward CL, Kopito RR (1998) Aggresomes: a cellular response to misfolded proteins. The Journal of cell biology 143:1883-1898.

Kabeya Y, Mizushima N, Ueno T, Yamamoto A, Kirisako T, Noda T, Kominami E, Ohsumi Y, Yoshimori T (2000) LC3, a mammalian homologue of yeast Apg8p, is localized in autophagosome membranes after processing. The EMBO journal 19:5720-5728.

Kamel F, Umbach DM, Munsat TL, Shefner JM, Sandler DP (1999) Association of cigarette smoking with amyotrophic lateral sclerosis. Neuroepidemiology 18:194-202.

Kameswaran TR, Ramanibai R (2009) Indirubin-3-monooxime induced cell cycle arrest and apoptosis in Hep-2 human laryngeal carcinoma cells. Biomedicine & pharmacotherapy = Biomedecine & pharmacotherapie 63:146-154.

Kanekura K, Hashimoto Y, Kita Y, Sasabe J, Aiso S, Nishimoto I, Matsuoka M (2005) A Rac1/phosphatidylinositol 3-kinase/Akt3 anti-apoptotic pathway, triggered by AlsinLF, the product of the ALS2 gene, antagonizes Cu/Zn-superoxide dismutase (SOD1) mutant-induced motoneuronal cell death. The Journal of biological chemistry 280:4532-4543.

Kanoh H, Williger BT, Exton JH (1997) Arfaptin 1, a putative cytosolic target protein of ADP-ribosylation factor, is recruited to Golgi membranes. The Journal of biological chemistry 272:5421-5429.

Karbowski M, Neutzner A (2011) Neurodegeneration as a consequence of failed mitochondrial maintenance. Acta Neuropathol.

Karra D, Dahm R (2010) Transfection techniques for neuronal cells. The Journal of neuroscience : the official journal of the Society for Neuroscience 30:6171-6177.

Kaspar BK, Llado J, Sherkat N, Rothstein JD, Gage FH (2003) Retrograde viral delivery of IGF-1 prolongs survival in a mouse ALS model. Science 301:839-842.

Kaufman RJ (2002) Orchestrating the unfolded protein response in health and disease. The Journal of clinical investigation 110:1389-1398.

Ko HS, Uehara T, Nomura Y (2002) Role of ubiquilin associated with protein-disulfide isomerase in the endoplasmic reticulum in stress-induced apoptotic cell death. The Journal of biological chemistry 277:35386-35392.

Ko HS, Uehara T, Tsuruma K, Nomura Y (2004) Ubiquilin interacts with ubiquitylated proteins and proteasome through its ubiquitin-associated and ubiquitin-like domains. FEBS letters 566:110-114.

Kong S (2011) Regulation of protein aggregation by Arfaptin2 in Amyotrophic lateral sclerosis. In: Medical school, vol. MSc Sheffield: The university of Sheffield.

Konyalioglu S, Armagan G, Yalcin A, Atalayin C, Dagci T (2013) Effects of resveratrol on hydrogen peroxide-induced oxidative stress in embryonic neural stem cells. Neural Regen Res 8:485-495.

Koppers M, van Blitterswijk MM, Vlam L, Rowicka PA, van Vught PW, Groen EJ, Spliet WG, Engelen-Lee J, Schelhaas HJ, de Visser M, van der Kooi AJ, van der Pol WL, Pasterkamp RJ, Veldink JH, van den Berg LH (2011) VCP mutations in familial and sporadic amyotrophic lateral sclerosis. Neurobiol Aging.

Kozin SA, Bertho G, Mazur AK, Rabesona H, Girault JP, Haertle T, Takahashi M, Debey P, Hoa GH (2001) Sheep prion protein synthetic peptide spanning helix 1 and beta-strand 2 (residues 142-166) shows beta-hairpin structure in solution. The Journal of biological chemistry 276:46364-46370.

Kuhle J, Lindberg RL, Regeniter A, Mehling M, Steck AJ, Kappos L, Czaplinski A (2009) Increased levels of inflammatory chemokines in amyotrophic lateral sclerosis. European journal of neurology : the official journal of the European Federation of Neurological Societies 16:771-774.

Kumar A, Al-Sammarraie N, DiPette DJ, Singh US (2014) Metformin impairs Rho GTPase signaling to induce apoptosis in neuroblastoma cells and inhibits growth of tumors in the xenograft mouse model of neuroblastoma. Oncotarget 5:11709-11722.

Kuner R, Groom AJ, Muller G, Kornau HC, Stefovska V, Bresink I, Hartmann B, Tschauner K, Waibel S, Ludolph AC, Ikonomidou C, Seeburg PH, Turski L (2005) Mechanisms of disease: motoneuron disease aggravated by transgenic expression of a functionally modified AMPA receptor subunit. Annals of the New York Academy of Sciences 1053:269-286.

Kwiatkowski TJ, Jr., Bosco DA, Leclerc AL, Tamrazian E, Vanderburg CR, Russ C, Davis A, Gilchrist J, Kasarskis EJ, Munsat T, Valdmanis P, Rouleau GA, Hosler BA, Cortelli P, de Jong PJ, Yoshinaga Y, Haines JL, Pericak-Vance MA, Yan J, Ticozzi N, Siddique T, McKenna-Yasek D, Sapp PC, Horvitz HR, Landers JE, Brown RH, Jr. (2009) Mutations in the FUS/TLS gene on chromosome 16 cause familial amyotrophic lateral sclerosis. Science 323:1205-1208.

Lai C, Xie C, McCormack SG, Chiang HC, Michalak MK, Lin X, Chandran J, Shim H, Shimoji M, Cookson MR, Huganir RL, Rothstein JD, Price DL, Wong PC, Martin LJ, Zhu JJ, Cai H (2006) Amyotrophic lateral sclerosis 2-deficiency leads to neuronal degeneration in amyotrophic lateral sclerosis through altered AMPA receptor trafficking. The Journal of neuroscience : the official journal of the Society for Neuroscience 26:11798-11806.

Levine TP, Daniels RD, Gatta AT, Wong LH, Hayes MJ (2013) The product of C9orf72, a gene strongly implicated in neurodegeneration, is structurally related to DENN Rab-GEFs. Bioinformatics 29:499-503.

Li HY, Yeh PA, Chiu HC, Tang CY, Tu BP (2011) Hyperphosphorylation as a defense mechanism to reduce TDP-43 aggregation. PloS one 6:e23075.

Linden R, Martins VR, Prado MA, Cammarota M, Izquierdo I, Brentani RR (2008) Physiology of the prion protein. Physiological reviews 88:673-728.

Little D, Valori CF, Mutsaers CA, Bennett EJ, Wyles M, Sharrack B, Shaw PJ, Gillingwater TH, Azzouz M, Ning K (2014) PTEN Depletion Decreases Disease Severity and Modestly Prolongs Survival in a Mouse Model of Spinal Muscular Atrophy. Molecular therapy : the journal of the American Society of Gene Therapy.

Livingstone M, Bidinosti M (2012) Rapamycin-insensitive mTORC1 activity controls eIF4E:4E-BP1 binding. F1000Res 1:4.

Lo WD, Akhmametyeva EM, Zhu L, Friesen PD, Chang LS (2003) Induction of apoptosis by the p53-related p73 and partial inhibition by the baculovirus-encoded p35 in neuronal cells. Brain research Molecular brain research 113:1-12.

Lock M, Alvira M, Vandenberghe LH, Samanta A, Toelen J, Debyser Z, Wilson JM (2010) Rapid, Simple, and Versatile Manufacturing of Recombinant Adeno-Associated Viral Vectors at Scale. Hum Gene Ther 21:1259-1271.

Luo H, Wu Q, Ye X, Xiong Y, Zhu J, Xu J, Diao Y, Zhang D, Wang M, Qiu J, Miao J, Zhang W, Wan J (2014) Genome-wide analysis of miRNA signature in the APPswe/PS1DeltaE9 mouse model of alzheimer's disease. PloS one 9:e101725.

Luty AA, Kwok JB, Dobson-Stone C, Loy CT, Coupland KG, Karlstrom H, Sobow T, Tchorzewska J, Maruszak A, Barcikowska M, Panegyres PK, Zekanowski C, Brooks WS, Williams KL, Blair IP, Mather KA, Sachdev PS, Halliday GM, Schofield PR (2010) Sigma nonopioid intracellular receptor 1 mutations cause frontotemporal lobar degeneration-motor neuron disease. Annals of neurology 68:639-649.

Man Z, Kondo Y, Koga H, Umino H, Nakayama K, Shin HW (2011) Arfaptins are localized to the trans-Golgi by interaction with Arl1, but not Arfs. The Journal of biological chemistry 286:11569-11578.

Maragakis NJ, Dykes-Hoberg M, Rothstein JD (2004) Altered expression of the glutamate transporter EAAT2b in neurological disease. Annals of neurology 55:469-477.

Martinez-Vicente M, Talloczy Z, Wong E, Tang G, Koga H, Kaushik S, de Vries R, Arias E, Harris S, Sulzer D, Cuervo AM (2010) Cargo recognition failure is responsible for inefficient autophagy in Huntington's disease. Nature neuroscience 13:567-576.

Maruyama H, Morino H, Ito H, Izumi Y, Kato H, Watanabe Y, Kinoshita Y, Kamada M, Nodera H, Suzuki H, Komure O, Matsuura S, Kobatake K, Morimoto N, Abe K, Suzuki N, Aoki M, Kawata A, Hirai T, Kato T, Ogasawara K, Hirano A, Takumi T, Kusaka H, Hagiwara K, Kaji R, Kawakami H (2010) Mutations of optineurin in amyotrophic lateral sclerosis. Nature 465:223-226.

McCarty DM, Fu H, Monahan PE, Toulson CE, Naik P, Samulski RJ (2003) Adeno-associated virus terminal repeat (TR) mutant generates self-complementary vectors to overcome the rate-limiting step to transduction in vivo. Gene therapy 10:2112-2118.

McCarty DM, Monahan PE, Samulski RJ (2001) Self-complementary recombinant adeno-associated virus (scAAV) vectors promote efficient transduction independently of DNA synthesis. Gene therapy 8:1248-1254.

Mead RJ, Bennett EJ, Kennerley AJ, Sharp P, Sunyach C, Kasher P, Berwick J, Pettmann B, Battaglia G, Azzouz M, Grierson A, Shaw PJ (2011) Optimised and rapid pre-clinical screening in the SOD1(G93A) transgenic mouse model of amyotrophic lateral sclerosis (ALS). PloS one 6:e23244.

Millhauser GL (2007) Copper and the prion protein: methods, structures, function, and disease. Annual review of physical chemistry 58:299-320.

Miquel J (1992) An update on the mitochondrial-DNA mutation hypothesis of cell aging. Mutation research 275:209-216.

Mitchell J, Paul P, Chen HJ, Morris A, Payling M, Falchi M, Habgood J, Panoutsou S, Winkler S, Tisato V, Hajitou A, Smith B, Vance C, Shaw C, Mazarakis ND, de Belleroche J (2010) Familial amyotrophic lateral sclerosis is associated with a mutation in D-amino acid oxidase. Proceedings of the National Academy of Sciences of the United States of America 107:7556-7561.

Mohammedeid AM, Lukashchuk V, Ning K (2014) Protein aggregation and Arfaptin2: A novel therapeutic target against neurodegenerative diseases. New Horizons in Translational Medicine 2:12-15.

Moreira LG, Pereira LC, Drummond PR, De Mesquita JF (2013) Structural and functional analysis of human SOD1 in amyotrophic lateral sclerosis. PloS one 8:e81979.

Munch C, Bertolotti A (2010) Exposure of hydrophobic surfaces initiates aggregation of diverse ALS-causing superoxide dismutase-1 mutants. Journal of molecular biology 399:512-525.

Munch C, O'Brien J, Bertolotti A (2011) Prion-like propagation of mutant superoxide dismutase-1 misfolding in neuronal cells. Proceedings of the National Academy of Sciences of the United States of America 108:3548-3553.

Munch C, Sedlmeier R, Meyer T, Homberg V, Sperfeld AD, Kurt A, Prudlo J, Peraus G, Hanemann CO, Stumm G, Ludolph AC (2004) Point mutations of the p150 subunit of dynactin (DCTN1) gene in ALS. Neurology 63:724-726.

Nagabhushana A, Chalasani ML, Jain N, Radha V, Rangaraj N, Balasubramanian D, Swarup G (2010) Regulation of endocytic trafficking of transferrin receptor by optineurin and its impairment by a glaucoma-associated mutant. BMC cell biology 11:4.

Naldini L, Blomer U, Gallay P, Ory D, Mulligan R, Gage FH, Verma IM, Trono D (1996) In vivo gene delivery and stable transduction of nondividing cells by a lentiviral vector. Science 272:263-267.

Nanou A, Higginbottom A, Valori CF, Wyles M, Ning K, Shaw P, Azzouz M (2013) Viral delivery of antioxidant genes as a therapeutic strategy in experimental models of amyotrophic lateral sclerosis. Molecular therapy : the journal of the American Society of Gene Therapy 21:1486-1496.

Neumann M, Sampathu DM, Kwong LK, Truax AC, Micsenyi MC, Chou TT, Bruce J, Schuck T, Grossman M, Clark CM, McCluskey LF, Miller BL, Masliah E, Mackenzie IR, Feldman H, Feiden W, Kretzschmar HA, Trojanowski JQ, Lee VM (2006) Ubiquitinated TDP-43 in frontotemporal lobar degeneration and amyotrophic lateral sclerosis. Science 314:130-133.

Ng J, Nardine T, Harms M, Tzu J, Goldstein A, Sun Y, Dietzl G, Dickson BJ, Luo L (2002) Rac GTPases control axon growth, guidance and branching. Nature 416:442-447.

Nijholt DA, De Kimpe L, Elfrink HL, Hoozemans JJ, Scheper W (2011) Removing protein aggregates: the role of proteolysis in neurodegeneration. Current medicinal chemistry 18:2459-2476.

Ning K, Drepper C, Valori CF, Ahsan M, Wyles M, Higginbottom A, Herrmann T, Shaw P, Azzouz M, Sendtner M (2010) PTEN depletion rescues axonal growth defect and improves survival in SMN-deficient motor neurons. Human molecular genetics 19:3159-3168.

Ning K, Pei L, Liao M, Liu B, Zhang Y, Jiang W, Mielke JG, Li L, Chen Y, El-Hayek YH, Fehlings MG, Zhang X, Liu F, Eubanks J, Wan Q (2004) Dual neuroprotective signaling mediated by downregulating two distinct phosphatase activities of PTEN. The Journal of neuroscience : the official journal of the Society for Neuroscience 24:4052-4060.

Nishimura AL, Mitne-Neto M, Silva HC, Richieri-Costa A, Middleton S, Cascio D, Kok F, Oliveira JR, Gillingwater T, Webb J, Skehel P, Zatz M (2004) A mutation in the vesicle-trafficking protein VAPB causes late-onset spinal muscular atrophy and amyotrophic lateral sclerosis. American journal of human genetics 75:822-831.

Nonaka T, Masuda-Suzukake M, Arai T, Hasegawa Y, Akatsu H, Obi T, Yoshida M, Murayama S, Mann DM, Akiyama H, Hasegawa M (2013) Prion-like properties of pathological TDP-43 aggregates from diseased brains. Cell Rep 4:124-134.

Novelli A, Reilly JA, Lysko PG, Henneberry RC (1988) Glutamate becomes neurotoxic via the N-methyl-D-aspartate receptor when intracellular energy levels are reduced. Brain research 451:205-212.

Nunziante M, Ackermann K, Dietrich K, Wolf H, Gadtke L, Gilch S, Vorberg I, Groschup M, Schatzl HM (2011) Proteasomal dysfunction and endoplasmic reticulum stress enhance trafficking of prion protein aggregates through the secretory pathway and increase accumulation of pathologic prion protein. The Journal of biological chemistry 286:33942-33953.

Orlacchio A, Babalini C, Borreca A, Patrono C, Massa R, Basaran S, Munhoz RP, Rogaeva EA, St George-Hyslop PH, Bernardi G, Kawarai T (2010) SPATACSIN mutations cause autosomal recessive juvenile amyotrophic lateral sclerosis. Brain : a journal of neurology 133:591-598.

Orrell RW (2000) Amyotrophic lateral sclerosis: copper/zinc superoxide dismutase (SOD1) gene mutations. Neuromuscular disorders : NMD 10:63-68.

Otomo A, Hadano S, Okada T, Mizumura H, Kunita R, Nishijima H, Showguchi-Miyata J, Yanagisawa Y, Kohiki E, Suga E, Yasuda M, Osuga H, Nishimoto T, Narumiya S, Ikeda JE (2003) ALS2, a novel guanine nucleotide exchange factor for the small GTPase

Rab5, is implicated in endosomal dynamics. Human molecular genetics 12:1671-1687.

Palfi S, Gurruchaga JM, Ralph GS, Lepetit H, Lavisse S, Buttery PC, Watts C, Miskin J, Kelleher M, Deeley S, Iwamuro H, Lefaucheur JP, Thiriez C, Fenelon G, Lucas C, Brugieres P, Gabriel I, Abhay K, Drouot X, Tani N, Kas A, Ghaleb B, Le Corvoisier P, Dolphin P, Breen DP, Mason S, Guzman NV, Mazarakis ND, Radcliffe PA, Harrop R, Kingsman SM, Rascol O, Naylor S, Barker RA, Hantraye P, Remy P, Cesaro P, Mitrophanous KA (2014) Long-term safety and tolerability of ProSavin, a lentiviral vector-based gene therapy for Parkinson's disease: a dose escalation, open-label, phase 1/2 trial. Lancet 383:1138-1146.

Papa A, Wan L, Bonora M, Salmena L, Song MS, Hobbs RM, Lunardi A, Webster K, Ng C, Newton RH, Knoblauch N, Guarnerio J, Ito K, Turka LA, Beck AH, Pinton P, Bronson RT, Wei W, Pandolfi PP (2014) Cancer-associated PTEN mutants act in a dominant-negative manner to suppress PTEN protein function. Cell 157:595-610.

Park HR, Lee H, Park H, Jeon JW, Cho WK, Ma JY (2015) Neuroprotective effects of Liriope platyphylla extract against hydrogen peroxide-induced cytotoxicity in human neuroblastoma SH-SY5Y cells. BMC Complement Altern Med 15:171.

Parkinson N, Ince PG, Smith MO, Highley R, Skibinski G, Andersen PM, Morrison KE, Pall HS, Hardiman O, Collinge J, Shaw PJ, Fisher EM, Study MRCPiA, Consortium FR (2006) ALS phenotypes with mutations in CHMP2B (charged multivesicular body protein 2B). Neurology 67:1074-1077.

Peter BJ, Kent HM, Mills IG, Vallis Y, Butler PJ, Evans PR, McMahon HT (2004) BAR domains as sensors of membrane curvature: the amphiphysin BAR structure. Science 303:495-499.

Peters PJ, Ning K, Palacios F, Boshans RL, Kazantsev A, Thompson LM, Woodman B, Bates GP, D'Souza-Schorey C (2002) Arfaptin 2 regulates the aggregation of mutant huntingtin protein. Nature cell biology 4:240-245.

Peviani M, Tortarolo M, Battaglia E, Piva R, Bendotti C (2014) Specific induction of Akt3 in spinal cord motor neurons is neuroprotective in a mouse model of familial amyotrophic lateral sclerosis. Molecular neurobiology 49:136-148.

Pirooznia SK, Dawson VL, Dawson TM (2014) Motor neuron death in ALS: programmed by astrocytes? Neuron 81:961-963.

Pizzi M, Spano P (2006) Distinct roles of diverse nuclear factor-kappaB complexes in neuropathological mechanisms. European journal of pharmacology 545:22-28.

Polymenidou M, Cleveland DW (2011) The seeds of neurodegeneration: prion-like spreading in ALS. Cell 147:498-508.

Ramalingam M, Kim SJ (2012) Reactive oxygen/nitrogen species and their functional correlations in neurodegenerative diseases. J Neural Transm.

Ramon-Cueto A, Nieto-Sampedro M (1992) Glial cells from adult rat olfactory bulb: immunocytochemical properties of pure cultures of ensheathing cells. Neuroscience 47:213-220.

Rangone H, Pardo R, Colin E, Girault JA, Saudou F, Humbert S (2005) Phosphorylation of arfaptin 2 at Ser260 by Akt Inhibits PolyQ-huntingtin-induced toxicity by rescuing proteasome impairment. The Journal of biological chemistry 280:22021-22028.

Re DB, Le Verche V, Yu C, Amoroso MW, Politi KA, Phani S, Ikiz B, Hoffmann L, Koolen M, Nagata T, Papadimitriou D, Nagy P, Mitsumoto H, Kariya S, Wichterle H, Henderson CE, Przedborski S (2014) Necroptosis drives motor neuron death in models of both sporadic and familial ALS. Neuron 81:1001-1008.

Reaume AG, Elliott JL, Hoffman EK, Kowall NW, Ferrante RJ, Siwek DF, Wilcox HM, Flood DG, Beal MF, Brown RH, Jr., Scott RW, Snider WD (1996) Motor neurons in Cu/Zn

superoxide dismutase-deficient mice develop normally but exhibit enhanced cell death after axonal injury. Nature genetics 13:43-47.

Renton AE, Majounie E, Waite A, Simon-Sanchez J, Rollinson S, Gibbs JR, Schymick JC, Laaksovirta H, van Swieten JC, Myllykangas L, Kalimo H, Paetau A, Abramzon Y, Remes AM, Kaganovich A, Scholz SW, Duckworth J, Ding J, Harmer DW, Hernandez DG, Johnson JO, Mok K, Ryten M, Trabzuni D, Guerreiro RJ, Orrell RW, Neal J, Murray A, Pearson J, Jansen IE, Sondervan D, Seelaar H, Blake D, Young K, Halliwell N, Callister JB, Toulson G, Richardson A, Gerhard A, Snowden J, Mann D, Neary D, Nalls MA, Peuralinna T, Jansson L, Isoviita VM, Kaivorinne AL, Holtta-Vuori M, Ikonen E, Sulkava R, Benatar M, Wuu J, Chio A, Restagno G, Borghero G, Sabatelli M, Consortium I, Heckerman D, Rogaeva E, Zinman L, Rothstein JD, Sendtner M, Drepper C, Eichler EE, Alkan C, Abdullaev Z, Pack SD, Dutra A, Pak E, Hardy J, Singleton A, Williams NM, Heutink P, Pickering-Brown S, Morris HR, Tienari PJ, Traynor BJ (2011) A hexanucleotide repeat expansion in C9ORF72 is the cause of chromosome 9p21-linked ALS-FTD. Neuron 72:257-268.

Ridley AJ, Paterson HF, Johnston CL, Diekmann D, Hall A (1992) The small GTP-binding protein rac regulates growth factor-induced membrane ruffling. Cell 70:401-410.

Rosen DR, Sapp P, O'Regan J, McKenna-Yasek D, Schlumpf KS, Haines JL, Gusella JF, Horvitz HR, Brown RH, Jr. (1994) Genetic linkage analysis of familial amyotrophic lateral sclerosis using human chromosome 21 microsatellite DNA markers. American journal of medical genetics 51:61-69.

Rosen DR, Siddique T, Patterson D, Figlewicz DA, Sapp P, Hentati A, Donaldson D, Goto J, O'Regan JP, Deng HX, et al. (1993) Mutations in Cu/Zn superoxide dismutase gene are associated with familial amyotrophic lateral sclerosis. Nature 362:59-62.

Ryu J, Yu HN, Cho H, Kim HS, Baik TK, Lee SJ, Woo RS (2012) Neuregulin-1 exerts protective effects against neurotoxicities induced by C-terminal fragments of APP via ErbB4 receptor. J Pharmacol Sci 119:73-81.

Sargsyan SA, Blackburn DJ, Barber SC, Monk PN, Shaw PJ (2009) Mutant SOD1 G93A microglia have an inflammatory phenotype and elevated production of MCP-1. Neuroreport 20:1450-1455.

Schink KO, Raiborg C, Stenmark H (2013) Phosphatidylinositol 3-phosphate, a lipid that regulates membrane dynamics, protein sorting and cell signalling. BioEssays : news and reviews in molecular, cellular and developmental biology 35:900-912.

Scotter EL, Vance C, Nishimura AL, Lee YB, Chen HJ, Urwin H, Sardone V, Mitchell JC, Rogelj B, Rubinsztein DC, Shaw CE (2014) Differential roles of the ubiquitin proteasome system and autophagy in the clearance of soluble and aggregated TDP-43 species. Journal of cell science 127:1263-1278.

Serafini T, Orci L, Amherdt M, Brunner M, Kahn RA, Rothman JE (1991) ADP-ribosylation factor is a subunit of the coat of Golgi-derived COP-coated vesicles: a novel role for a GTP-binding protein. Cell 67:239-253.

Shaw PJ (2005) Molecular and cellular pathways of neurodegeneration in motor neurone disease. Journal of neurology, neurosurgery, and psychiatry 76:1046-1057.

Shimizu S, Kanaseki T, Mizushima N, Mizuta T, Arakawa-Kobayashi S, Thompson CB, Tsujimoto Y (2004) Role of Bcl-2 family proteins in a non-apoptotic programmed cell death dependent on autophagy genes. Nature cell biology 6:1221-1228.

Shin OH, Exton JH (2001) Differential binding of arfaptin 2/POR1 to ADP-ribosylation factors and Rac1. Biochemical and biophysical research communications 285:1267-1273.

Shisheva A (2013) PtdIns5P: News and views of its appearance, disappearance and deeds. Arch Biochem Biophys 538:171-180.

Shott RH, Appanah C, Grenier C, Tremblay G, Roucou X, Schang LM (2014) Development of kinomic analyses to identify dysregulated signaling pathways in cells expressing cytoplasmic PrP. Virol J 11:175.

Simon D, Herva ME, Benitez MJ, Garrido JJ, Rojo AI, Cuadrado A, Torres JM, Wandosell F (2014) Dysfunction of the PI3K-Akt-GSK-3 pathway is a common feature in cell culture and in vivo models of prion disease. Neuropathology and applied neurobiology 40:311-326.

Sreedharan J, Blair IP, Tripathi VB, Hu X, Vance C, Rogelj B, Ackerley S, Durnall JC, Williams KL, Buratti E, Baralle F, de Belleroche J, Mitchell JD, Leigh PN, Al-Chalabi A, Miller CC, Nicholson G, Shaw CE (2008) TDP-43 mutations in familial and sporadic amyotrophic lateral sclerosis. Science 319:1668-1672.

Sta M, Sylva-Steenland RM, Casula M, de Jong JM, Troost D, Aronica E, Baas F (2011) Innate and adaptive immunity in amyotrophic lateral sclerosis: evidence of complement activation. Neurobiology of disease 42:211-220.

Stankiewicz TR, Linseman DA (2014) Rho family GTPases: key players in neuronal development, neuronal survival, and neurodegeneration. Frontiers in cellular neuroscience 8:314.

Sugihara K, Nakatsuji N, Nakamura K, Nakao K, Hashimoto R, Otani H, Sakagami H, Kondo H, Nozawa S, Aiba A, Katsuki M (1998) Rac1 is required for the formation of three germ layers during gastrulation. Oncogene 17:3427-3433.

Sun Z, Diaz Z, Fang X, Hart MP, Chesi A, Shorter J, Gitler AD (2011) Molecular determinants and genetic modifiers of aggregation and toxicity for the ALS disease protein FUS/TLS. PLoS biology 9:e1000614.

Suzukawa K, Miura K, Mitsushita J, Resau J, Hirose K, Crystal R, Kamata T (2000) Nerve growth factor-induced neuronal differentiation requires generation of Rac1-regulated reactive oxygen species. The Journal of biological chemistry 275:13175-13178.

Swarup V, Phaneuf D, Dupre N, Petri S, Strong M, Kriz J, Julien JP (2011) Deregulation of TDP-43 in amyotrophic lateral sclerosis triggers nuclear factor kappaB-mediated pathogenic pathways. The Journal of experimental medicine 208:2429-2447.

Swerdlow RH, Parks JK, Cassarino DS, Trimmer PA, Miller SW, Maguire DJ, Sheehan JP, Maguire RS, Pattee G, Juel VC, Phillips LH, Tuttle JB, Bennett JP, Jr., Davis RE, Parker WD, Jr. (1998) Mitochondria in sporadic amyotrophic lateral sclerosis. Experimental neurology 153:135-142.

Tada M, Coon EA, Osmand AP, Kirby PA, Martin W, Wieler M, Shiga A, Shirasaki H, Makifuchi T, Yamada M, Kakita A, Nishizawa M, Takahashi H, Paulson HL (2012) Coexistence of Huntington's disease and amyotrophic lateral sclerosis: a clinicopathologic study. Acta Neuropathol.

Tahirovic S, Hellal F, Neukirchen D, Hindges R, Garvalov BK, Flynn KC, Stradal TE, Chrostek-Grashoff A, Brakebusch C, Bradke F (2010) Rac1 regulates neuronal polarization through the WAVE complex. The Journal of neuroscience : the official journal of the Society for Neuroscience 30:6930-6943.

Takata M, Tanaka H, Kimura M, Nagahara Y, Tanaka K, Kawasaki K, Seto M, Tsuruma K, Shimazawa M, Hara H (2013) Fasudil, a rho kinase inhibitor, limits motor neuron loss in experimental models of amyotrophic lateral sclerosis. British journal of pharmacology 170:341-351.

Tonges L, Gunther R, Suhr M, Jansen J, Balck A, Saal KA, Barski E, Nientied T, Gotz AA, Koch JC, Mueller BK, Weishaupt JH, Sereda MW, Hanisch UK, Bahr M, Lingor P (2014) Rho kinase inhibition modulates microglia activation and improves survival in a model of amyotrophic lateral sclerosis. Glia 62:217-232.

Tsai T, Klausmeyer A, Conrad R, Gottschling C, Leo M, Faissner A, Wiese S (2013) 7,8-Dihydroxyflavone leads to survival of cultured embryonic motoneurons by activating intracellular signaling pathways. Molecular and cellular neurosciences 56:18-28.

Turner MR, Wotton C, Talbot K, Goldacre MJ (2011) Cardiovascular fitness as a risk factor for amyotrophic lateral sclerosis: indirect evidence from record linkage study. J Neurol Neurosurg Psychiatry.

Turowski P, Kenny BA (2015) The blood-brain barrier and methamphetamine: open sesame? Front Neurosci 9:156.

Valori CF, Ning K, Wyles M, Mead RJ, Grierson AJ, Shaw PJ, Azzouz M (2010) Systemic delivery of scAAV9 expressing SMN prolongs survival in a model of spinal muscular atrophy. Science translational medicine 2:35ra42.

Van Aelst L, Joneson T, Bar-Sagi D (1996) Identification of a novel Rac1-interacting protein involved in membrane ruffling. The EMBO journal 15:3778-3786.

Van Den Bosch L, Van Damme P, Bogaert E, Robberecht W (2006) The role of excitotoxicity in the pathogenesis of amyotrophic lateral sclerosis. Biochimica et biophysica acta 1762:1068-1082.

van Eersel J, Ke YD, Gladbach A, Bi M, Gotz J, Kril JJ, Ittner LM (2011) Cytoplasmic accumulation and aggregation of TDP-43 upon proteasome inhibition in cultured neurons. PloS one 6:e22850.

Van Maele B, De Rijck J, De Clercq E, Debyser Z (2003) Impact of the central polypurine tract on the kinetics of human immunodeficiency virus type 1 vector transduction. Journal of virology 77:4685-4694.

Van Valkenburgh H, Shern JF, Sharer JD, Zhu X, Kahn RA (2001) ADP-ribosylation factors (ARFs) and ARF-like 1 (ARL1) have both specific and shared effectors: characterizing ARL1-binding proteins. The Journal of biological chemistry 276:22826-22837.

Vance C, Rogelj B, Hortobagyi T, De Vos KJ, Nishimura AL, Sreedharan J, Hu X, Smith B, Ruddy D, Wright P, Ganesalingam J, Williams KL, Tripathi V, Al-Saraj S, Al-Chalabi A, Leigh PN, Blair IP, Nicholson G, de Belleroche J, Gallo JM, Miller CC, Shaw CE (2009) Mutations in FUS, an RNA processing protein, cause familial amyotrophic lateral sclerosis type 6. Science 323:1208-1211.

Verstraete E, Veldink JH, van den Berg LH, van den Heuvel MP (2014) Structural brain network imaging shows expanding disconnection of the motor system in amyotrophic lateral sclerosis. Hum Brain Mapp 35:1351-1361.

Wagey R, Pelech SL, Duronio V, Krieger C (1998) Phosphatidylinositol 3-kinase: increased activity and protein level in amyotrophic lateral sclerosis. Journal of neurochemistry 71:716-722.

Walker AK, Atkin JD (2011) Stress signaling from the endoplasmic reticulum: A central player in the pathogenesis of amyotrophic lateral sclerosis. IUBMB Life.

Wang H, Lim PJ, Karbowski M, Monteiro MJ (2009) Effects of overexpression of huntingtin proteins on mitochondrial integrity. Human molecular genetics 18:737-752.

Wang IF, Guo BS, Liu YC, Wu CC, Yang CH, Tsai KJ, Shen CK (2012) Autophagy activators rescue and alleviate pathogenesis of a mouse model with proteinopathies of the TAR DNA-binding protein 43. Proceedings of the National Academy of Sciences of the United States of America 109:15024-15029.

Wang Y, Liu W, He X, Zhou F (2013) Parkinson's disease-associated DJ-1 mutations increase abnormal phosphorylation of tau protein through Akt/GSK-3beta pathways. J Mol Neurosci 51:911-918.

Wang Z, Ma HI, Li J, Sun L, Zhang J, Xiao X (2003) Rapid and highly efficient transduction by double-stranded adeno-associated virus vectors in vitro and in vivo. Gene therapy 10:2105-2111.

Whittemore ER, Loo DT, Watt JA, Cotman CW (1995) A detailed analysis of hydrogen peroxide-induced cell death in primary neuronal culture. Neuroscience 67:921-932.

Wiedemann FR, Manfredi G, Mawrin C, Beal MF, Schon EA (2002) Mitochondrial DNA and respiratory chain function in spinal cords of ALS patients. Journal of neurochemistry 80:616-625.

Wiese S, Herrmann T, Drepper C, Jablonka S, Funk N, Klausmeyer A, Rogers ML, Rush R, Sendtner M (2010) Isolation and enrichment of embryonic mouse motoneurons from the lumbar spinal cord of individual mouse embryos. Nature protocols 5:31-38.

Williamson TL, Cleveland DW (1999) Slowing of axonal transport is a very early event in the toxicity of ALS-linked SOD1 mutants to motor neurons. Nature neuroscience 2:50-56.

Wood JD, Beaujeux TP, Shaw PJ (2003) Protein aggregation in motor neurone disorders. Neuropathology and applied neurobiology 29:529-545.

Wu CH, Fallini C, Ticozzi N, Keagle PJ, Sapp PC, Piotrowska K, Lowe P, Koppers M, McKenna-Yasek D, Baron DM, Kost JE, Gonzalez-Perez P, Fox AD, Adams J, Taroni F, Tiloca C, Leclerc AL, Chafe SC, Mangroo D, Moore MJ, Zitzewitz JA, Xu ZS, van den Berg LH, Glass JD, Siciliano G, Cirulli ET, Goldstein DB, Salachas F, Meininger V, Rossoll W, Ratti A, Gellera C, Bosco DA, Bassell GJ, Silani V, Drory VE, Brown RH, Jr., Landers JE (2012) Mutations in the profilin 1 gene cause familial amyotrophic lateral sclerosis. Nature 488:499-503.

Wu LS, Cheng WC, Shen CK (2013) Similar dose-dependence of motor neuron cell death caused by wild type human TDP-43 and mutants with ALS-associated amino acid substitutions. Journal of biomedical science 20:33.

Yamanaka K, Vande Velde C, Eymard-Pierre E, Bertini E, Boespflug-Tanguy O, Cleveland DW (2003) Unstable mutants in the peripheral endosomal membrane component ALS2 cause early-onset motor neuron disease. Proceedings of the National Academy of Sciences of the United States of America 100:16041-16046.

Yamashita T, Chai HL, Teramoto S, Tsuji S, Shimazaki K, Muramatsu S, Kwak S (2013) Rescue of amyotrophic lateral sclerosis phenotype in a mouse model by intravenous AAV9-ADAR2 delivery to motor neurons. EMBO molecular medicine 5:1710-1719.

Yang Y, Hentati A, Deng HX, Dabbagh O, Sasaki T, Hirano M, Hung WY, Ouahchi K, Yan J, Azim AC, Cole N, Gascon G, Yagmour A, Ben-Hamida M, Pericak-Vance M, Hentati F, Siddique T (2001) The gene encoding alsin, a protein with three guanine-nucleotide exchange factor domains, is mutated in a form of recessive amyotrophic lateral sclerosis. Nat Genet 29:160-165.

Yin F, Ye F, Tan L, Liu K, Xuan Z, Zhang J, Wang W, Zhang Y, Jiang X, Zhang DY (2012) Alterations of signaling pathways in muscle tissues of patients with amyotrophic lateral sclerosis. Muscle & nerve 46:861-870.

Zhang YJ, Jansen-West K, Xu YF, Gendron TF, Bieniek KF, Lin WL, Sasaguri H, Caulfield T, Hubbard J, Daughrity L, Chew J, Belzil VV, Prudencio M, Stankowski JN, Castanedes-Casey M, Whitelaw E, Ash PE, DeTure M, Rademakers R, Boylan KB, Dickson DW, Petrucelli L (2014) Aggregation-prone c9FTD/ALS poly(GA) RAN-translated proteins cause neurotoxicity by inducing ER stress. Acta neuropathologica 128:505-524.

Zhao Y, Zhang Q, Xi J, Xiao B, Li Y, Ma C (2015) Neuroprotective effect of fasudil on inflammation through PI3K/Akt and Wnt/beta-catenin dependent pathways in a mice model of Parkinson's disease. Int J Clin Exp Pathol 8:2354-2364.

Zhu A, Wu Z, Meng J, McGeer PL, Zhu Y, Nakanishi H, Wu S (2015) The Neuroprotective Effects of Ratanasampil on Oxidative Stress-Mediated Neuronal Damage in Human Neuronal SH-SY5Y Cells. Oxid Med Cell Longev 2015:792342.

Zhu G, Wu CJ, Zhao Y, Ashwell JD (2007) Optineurin negatively regulates TNFalpha- induced NF-kappaB activation by competing with NEMO for ubiquitinated RIP. Current biology : CB 17:1438-1443.

Zolotukhin S, Byrne BJ, Mason E, Zolotukhin I, Potter M, Chesnut K, Summerford C, Samulski RJ, Muzyczka N (1999) Recombinant adeno-associated virus purification using novel methods improves infectious titer and yield. Gene Ther 6:973-985.

Zufferey R, Dull T, Mandel RJ, Bukovsky A, Quiroz D, Naldini L, Trono D (1998) Self-inactivating lentivirus vector for safe and efficient in vivo gene delivery. Journal of virology 72:9873-9880.

APPENDICES

Image 1: Ethical approval form for human tissue

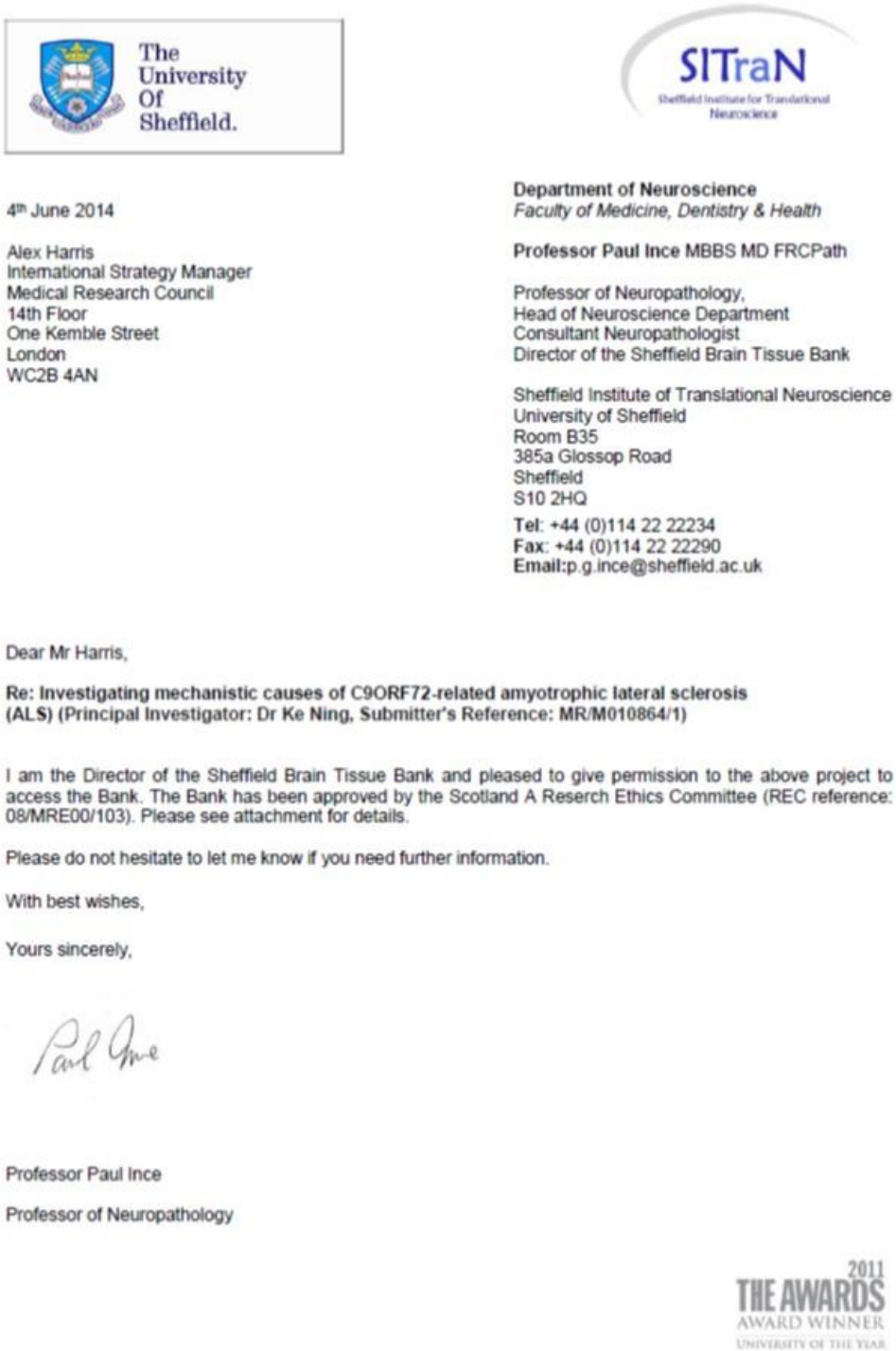

The University Of Sheffield.

SITraN
Sheffield Institute for Translational Neuroscience

4th June 2014

Alex Harris
International Strategy Manager
Medical Research Council
14th Floor
One Kemble Street
London
WC2B 4AN

Department of Neuroscience
Faculty of Medicine, Dentistry & Health

Professor Paul Ince MBBS MD FRCPath

Professor of Neuropathology,
Head of Neuroscience Department
Consultant Neuropathologist
Director of the Sheffield Brain Tissue Bank

Sheffield Institute of Translational Neuroscience
University of Sheffield
Room B35
385a Glossop Road
Sheffield
S10 2HQ

Tel: +44 (0)114 22 22234
Fax: +44 (0)114 22 22290
Email:p.g.ince@sheffield.ac.uk

Dear Mr Harris,

Re: Investigating mechanistic causes of C9ORF72-related amyotrophic lateral sclerosis (ALS) (Principal Investigator: Dr Ke Ning, Submitter's Reference: MR/M010864/1)

I am the Director of the Sheffield Brain Tissue Bank and pleased to give permission to the above project to access the Bank. The Bank has been approved by the Scotland A Reserch Ethics Committee (REC reference: 08/MRE00/103). Please see attachment for details.

Please do not hesitate to let me know if you need further information.

With best wishes,

Yours sincerely,

Paul Ince

Professor Paul Ince

Professor of Neuropathology

2011 THE AWARDS AWARD WINNER UNIVERSITY OF THE YEAR

Image 2: Permission to reprint publications

ELSEVIER

Dear Aida

Thank you for your permission request.

We hereby grant you permission to reprint the material below at no charge **in your thesis** subject to the following conditions:

1. If any part of the material to be used (for example, figures) has appeared in our publication with credit or acknowledgement to another source, permission must also be sought from that source. If such permission is not obtained then that material may not be included in your publication/copies.

2. Suitable acknowledgment to the source must be made, either as a footnote or in a reference list at the end of your publication, as follows:

"This article was published in Publication title, Vol number, Author(s), Title of article, Page Nos, Copyright Elsevier (or appropriate Society name) (Year)."

3. Your thesis may be submitted to your institution in either print or electronic form.

4. Reproduction of this material is confined to the purpose for which permission is hereby given.

5. This permission is granted for non-exclusive world **English** rights only. For other languages please reapply separately for each one required. Permission excludes use in an electronic form other than submission. Should you have a specific electronic project in mind please reapply for permission.

6. Should your thesis be published commercially, please reapply for permission.

Regards

Banita Samantray
Global Rights Department

Elsevier
(A division of Reed Elsevier India Pvt. Ltd.)

Ascendas International Tech Park | Crest Building - 12th Floor | Taramani Road | Taramani | Chennai 600 113 | India
Tel: +91 44 42994667 | Fax: +91 44 42994701
E-mail: b.samantray@reedelsevier.com | url: www.elsevier.com

From: aida M mohammedeid [mailto:mdq10amm@sheffield.ac.uk]
Sent: Wednesday, December 10, 2014 6:53 PM
To: Rights and Permissions (ELS)
Subject: table and figure permission

Image 3: FL-ARFIP2 sequence (top) alignment with LV-ARFIP2 forward sequencing result (middle) and LV-ARFIP2 reverse sequencing result (bottom)

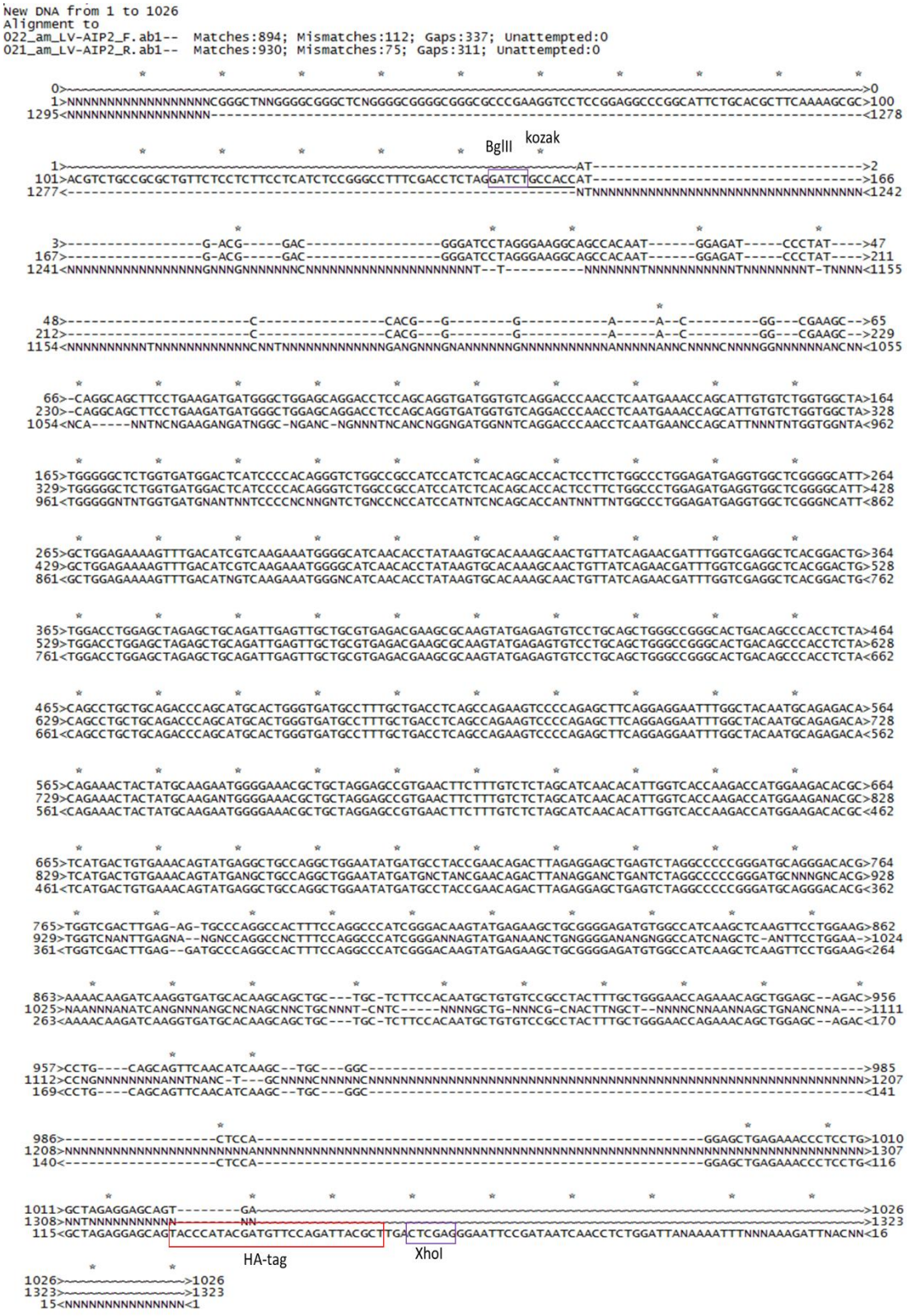

Image 4: FL-ARFIP2 sequence (top) alignment with LV-HC forward sequencing result (bottom)

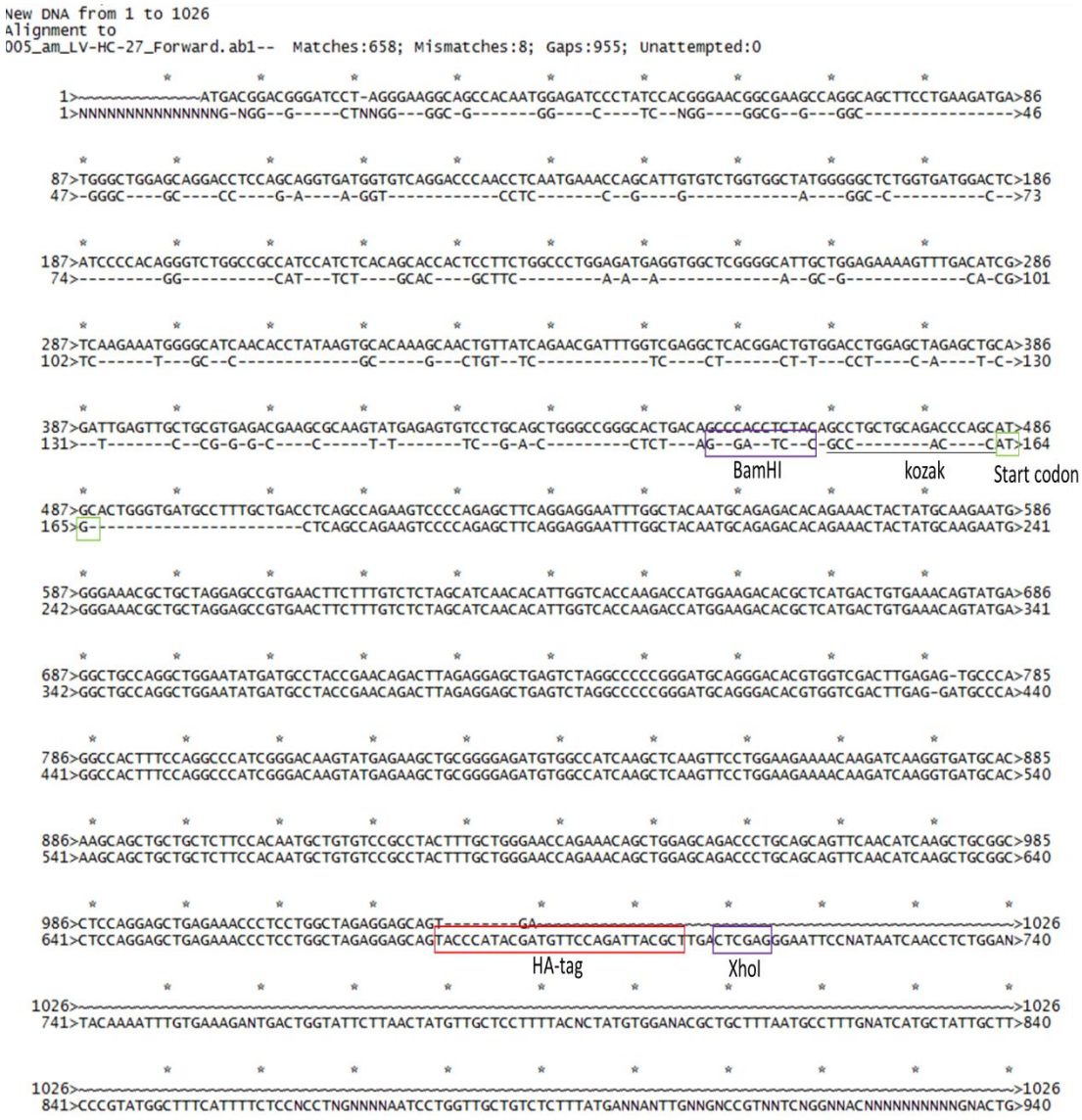

Image 5: TDP43 sequence (top) alignment with LV-TDP43 forward sequencing result (middle) and LV-TDP43 reverse sequencing result (bottom)

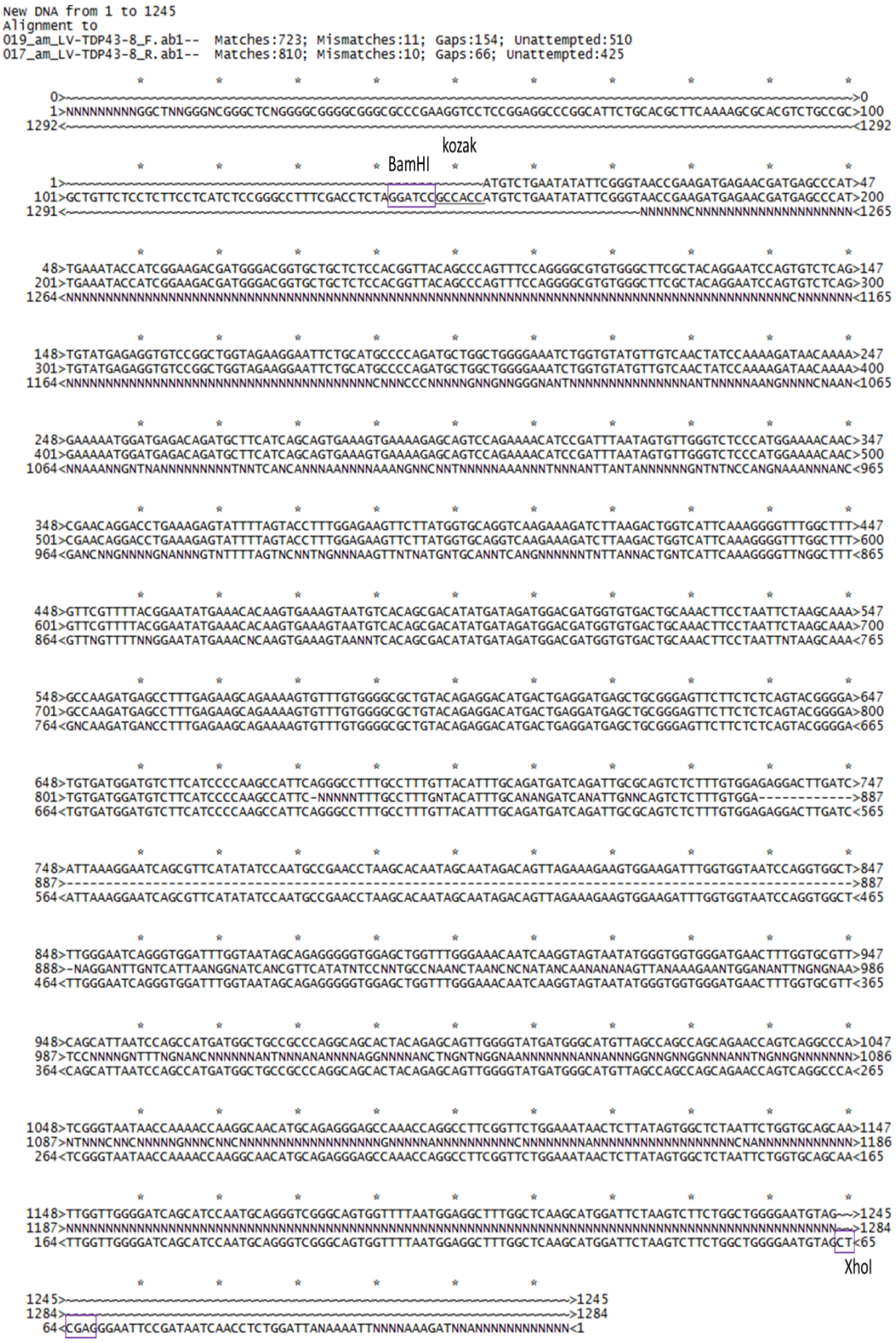

Image 6: FL-ARFIP2 sequence (top) alignment with scAAV-ARFIP2 forward sequencing result (middle) and scAAV-ARFIP2 reverse sequencing result (bottom)

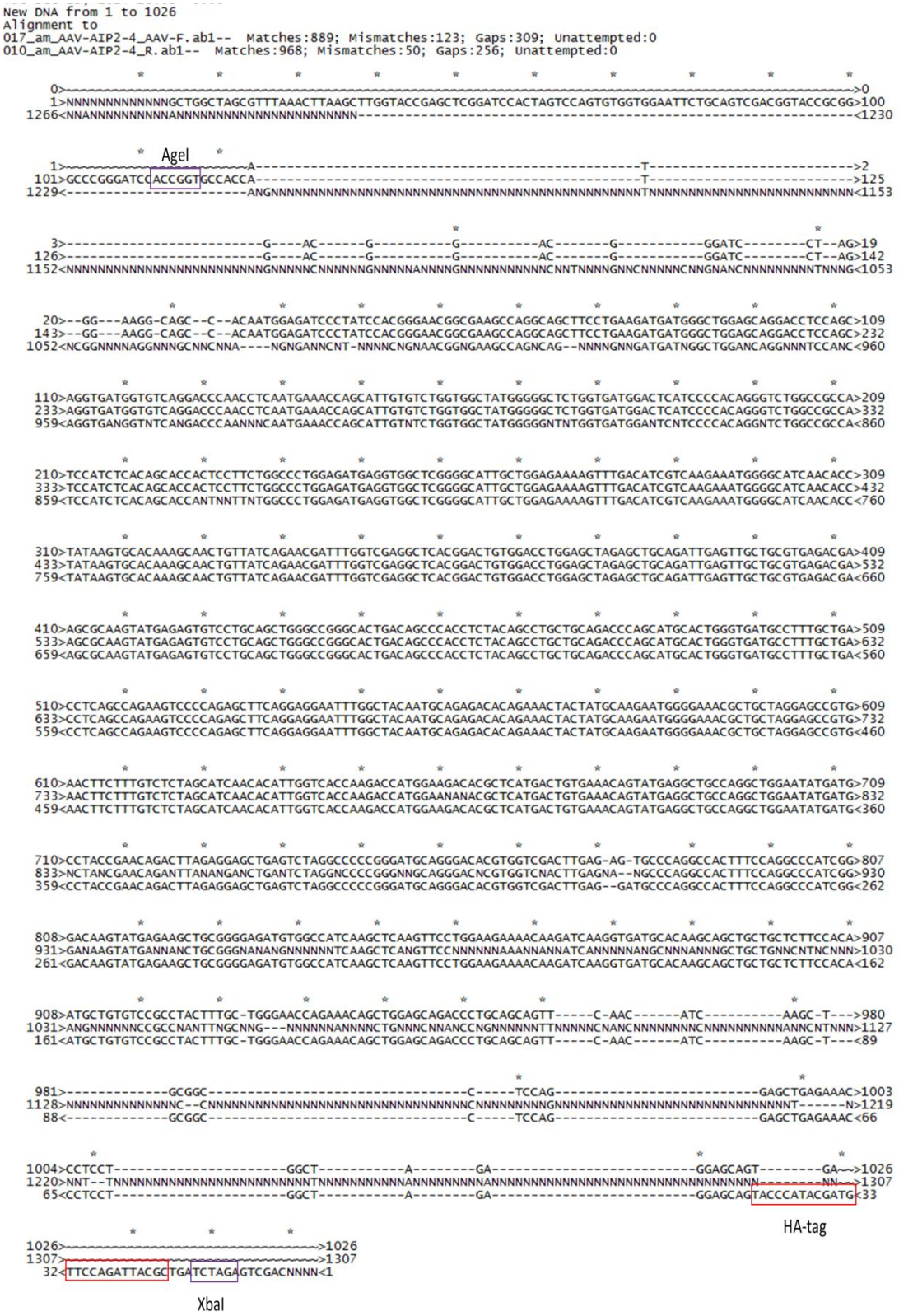

Image 7: FL-ARFIP2 sequence (top) alignment with scAAV-HC forward sequencing result (bottom)

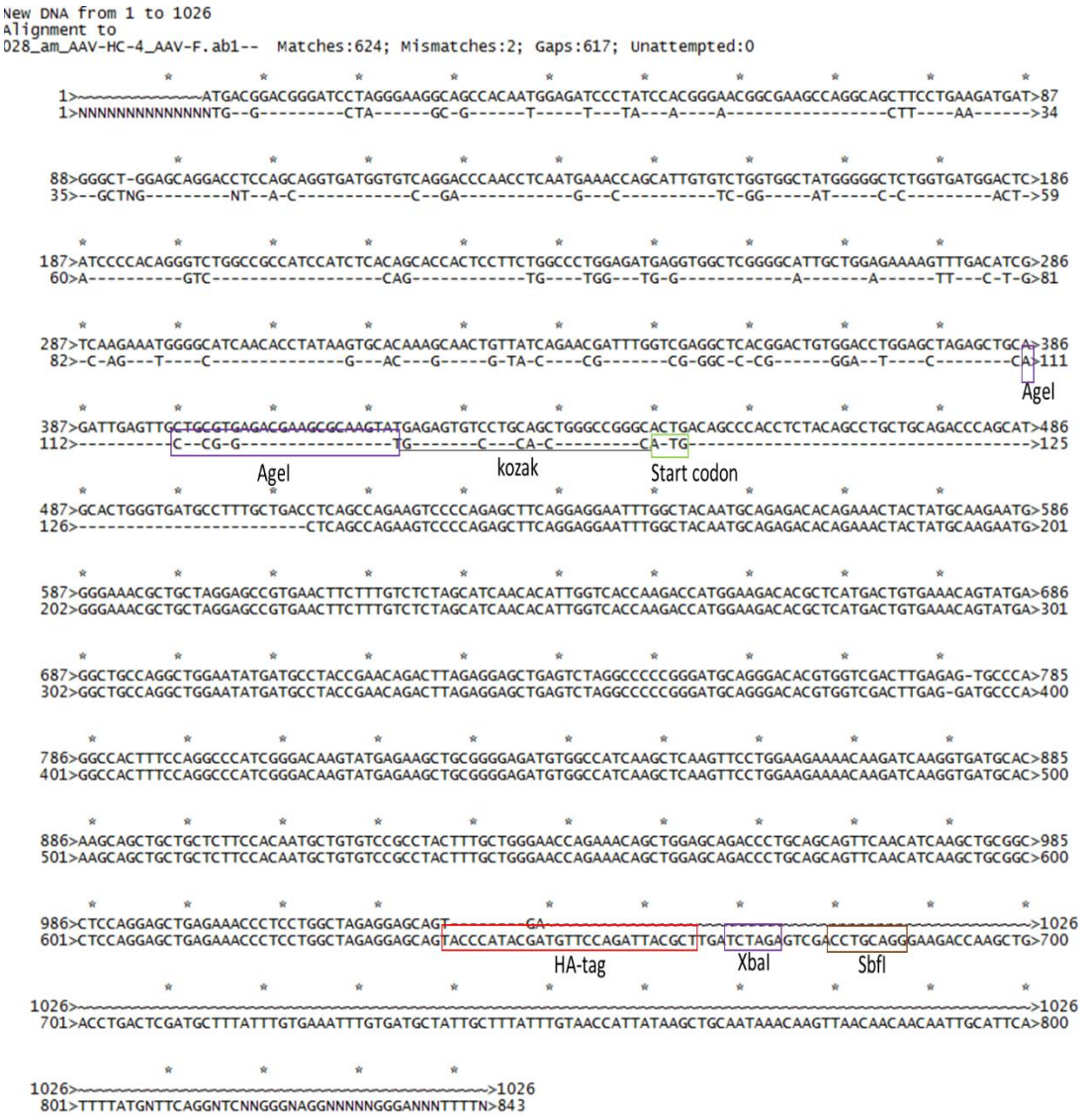

Image 8: TDP43 sequence (top) alignment with scAAV-TDP43 forward sequencing result (middle) and scAAV-TDP43 reverse sequencing result (bottom)

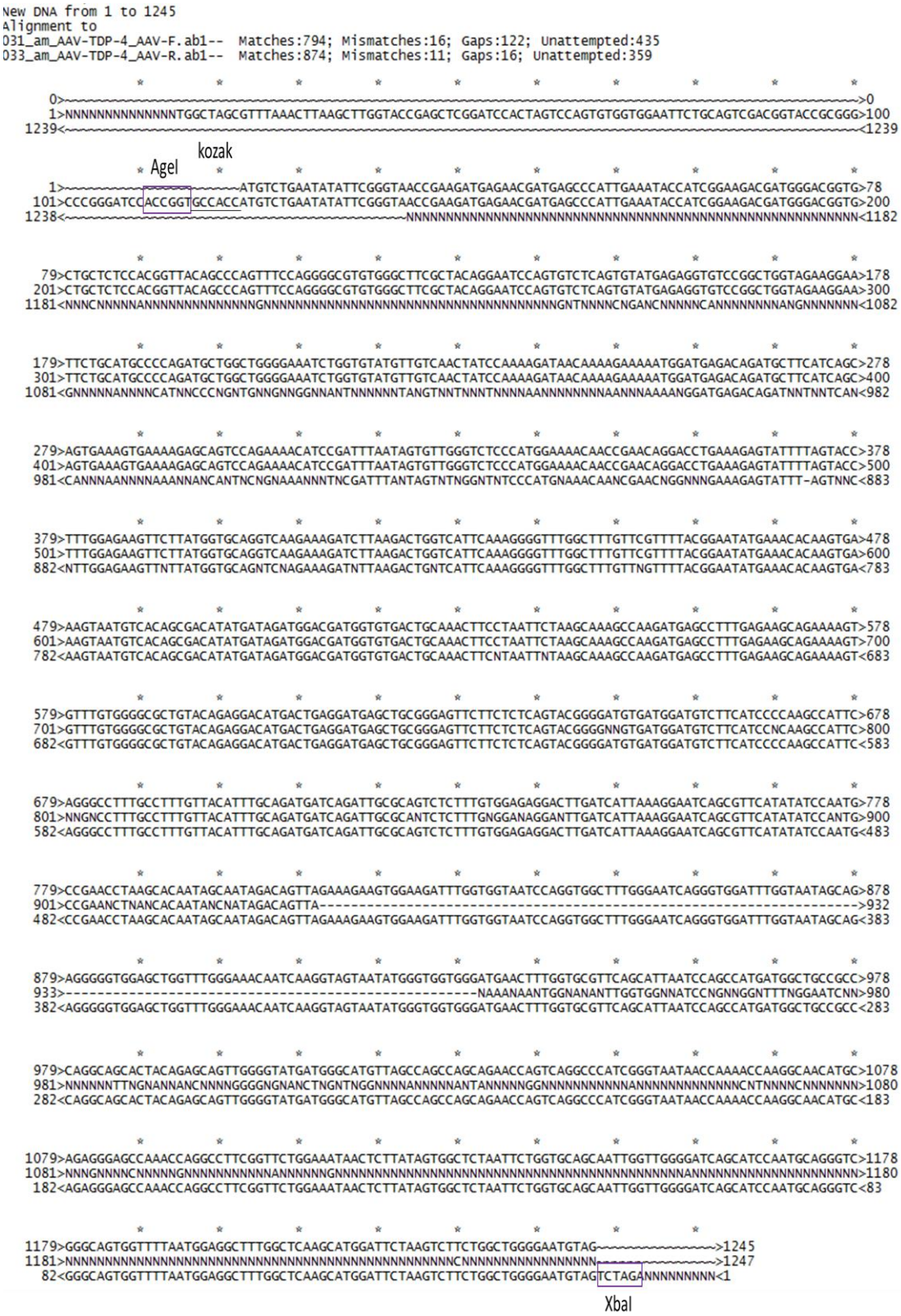

RE-PRINTS OF PUBLICATIONS

New Horizons in Translational Medicine 2 (2014) 12–15

Contents lists available at ScienceDirect

New Horizons in Translational Medicine

journal homepage: www.elsevier.com/locate/nhtm

Research Articles

Protein aggregation and Arfaptin2: A novel therapeutic target against neurodegenerative diseases

Aida M. Mohammedeid, Vera Lukashchuk, Ke Ning*

Sheffield Institute for Translational Neuroscience (SITraN), University of Sheffield, 385A Glossop Road, Sheffield S10 2HQ, UK

ARTICLE INFO

Available online 27 August 2014

Keywords:
Amyotrophic lateral sclerosis
Arfaptin2
Huntington's disease
Motor neuron disease
Neurodegenerative disease
Protein aggregation
Protein degradation
Therapeutic target

ABSTRACT

Therapeutic targets for neurodegenerative conditions are constantly emerging. Diseases such as amyotrophic lateral sclerosis and Huntington's disease are multifactorial and involve dysfunction of various cellular pathways. Protein aggregate formation is one of the crucial pathological signs of cellular dysfunction, and is characteristic of many neurodegenerative conditions. Proteins recruited to these aggregates are thought to play a role in formation of the pathogenic inclusions. This review aims at exploring the current evidence for protein aggregation and the role for Arfaptin2, as a candidate factor contributing to the formation of aggresomes and a potential therapeutic target in motor neuron disease.

Focal points:

- Bedside
  Understanding the multifactorial nature of the pathogenesis of neurodegenerative diseases will contribute to the research into the therapeutic targets of the disease, allowing more factors to be discovered in patients affected by the debilitating disorders of the nervous system.
- Benchside
  Collaborative efforts in investigating the causes and pathways of neurodegeneration are likely to increase the chance of discovering novel therapy approaches that may be utilised in more than one type of neurodegenerative disorders.
- Industry
  The application of the novel therapeutic target such as Arfaptin, and other proteins associated with protein aggregates, to the development of therapy approaches may open new avenues in drug discovery for neurodegenerative diseases.
- Community
  Diseases of central nervous system bear a great impact on the quality of life of the patients and their carers. Promoting the awareness through communicating the current state of the research provides a form of a mental support to those affected by these conditions.
- Regulatory agencies
  The need for funding the research into the basic understanding of the mechanisms involved in the pathogenesis of the neurodegenerative conditions must not be overlooked. The research into the cellular defects provides with invaluable findings about the healthy and diseased cell functioning.

1. Introduction

Neurodegenerative diseases constitute a class of disorders of the central nervous system characterised by progressive loss of neurons, which subsequently leads to death as a result of loss of vital physiological functions. Neurodegenerative diseases including amyotrophic lateral sclerosis (ALS), Alzheimer's (AD), Huntington's (HD) and Parkinson's (PD) diseases show some similarities in their pathogenesis. One of the common mechanisms causing neurodegeneration in these conditions is protein aggregation. Protein aggregates are a significant

*Corresponding author. Tel.: +44 114 2222245; fax: +44 114 2222290.
E-mail address: k.ning@sheffield.ac.uk (K. Ning).

http://dx.doi.org/10.1016/j.nhtm.2014.08.004
2307-5023/

pathological hallmark of many, if not all, neurodegenerative diseases. Protein aggregation is manifested in the form of protein inclusions, also known as aggresomes. These are non-membranous, stable, detergent-insoluble, β-sheet enriched, poly-ubiquitinated protein aggregates with high molecular weight, which are formed due to either overexpression of a protein which exceeds the degradation capacity or defective proteolytic pathways [12,25]. It is yet to be established what precise molecular mechanisms precede the formation of protein aggregates; however, ubiquitin-proteasome pathway plays one of the key roles. Therefore, components associated with the ubiquitin-proteasome machinery may be important players in the establishment of the disease pathogenesis. This review focuses on the general characteristics of protein aggregates in neurodegenerative diseases and their interference with proteasome-mediated degradation and presents Arfaptin2 as a modifier of the this pathway and a potential therapeutic target.

2. Types of protein aggregates

There are three common hypotheses regarding the role of protein aggregates in the pathology of neurodegenerative diseases. Firstly, protein aggregates have toxic effect on neurons and induce their death. Secondly, aggregates are formed as a defensive response to protect the cells against toxic abnormal proteins. Finally, the aggregates are formed as a result of other toxic effects [2].

Protein inclusions vary in structure, and may be characteristic of different neurodegenerative diseases. Four inclusion structures have been reported in neurodegenerative diseases which are skein-like inclusions, Lewy bodies, Bunina bodies and hyaline bodies. Skein-like inclusions are the most common in and specific to ALS [29]. The protein composition of these aggresomes can be detected by immunostaining, and may vary depending on the cause of the disease. Their appearance can range from small dot-like once they begin to form, to filament-like aggregates that increase in size by fusing with other aggregates [14]. The causative factors that may lead to protein aggresome formation and contribute to the pathology observed in neurodegenerative conditions may be speculated given the current evidence, which is discussed further onwards.

3. Protein degradation impairment in neurodegenerative diseases

There is mounting evidence showing that proteolytic machineries, such as ubiquitin-proteasomal system (UPS) and/or autophagy-lysosomal degradation, are impaired in neurodegenerative diseases, which causes cell toxicity and death [5,16,21,26,27]. For example, the inhibition of proteasome degradation pathways in primary motor neurons causes redistribution of the transactive response DNA-binding protein 43 kDa (TDP-43), which is involved in ALS pathogenesis, to the cytoplasm and aggregation, while other cellular stressors had no effect on its distribution. This redistribution was accompanied by increased insolubility, molecular weight (~50 kDa), ubiquitination and phosphorylation. Reduction in TDP-43 levels makes the neurons vulnerable, and knocking down TDP-43 increases their death rate. Therefore, it seems that TDP-43 distribution is controlled, at least partly, by the proteasome system and that a first hit, such as TDP-43 mutation, increases the cell vulnerability and a second hit, such as proteasome dysfunction, induces neurodegeneration and *vice versa* [27].

In addition, impaired ubiquitin proteasome activity plays role in tauopathies such as those representative of AD. Tau is a protein that is involved in microtubule formation, which has a direct impact on axonal transport. It has been shown that a phosphorylated form of a pro-survival kinase Akt phosphorylates tau at Ser214, thereby protecting it from aggregation. However, proteasome inhibition decreases phosphorylation of Akt leading to its decreased activity. This causes tau de-phosphorylation at normal site (Ser214) while inducing phosphorylation at other abnormal sites by Akt downstream effector protein glycogen synthase kinase-3β (GSK-3β) forming aggregate-prone protein, resulting in accumulation and aggregation of abnormal misfolded proteins [30].

4. Impaired endosomal trafficking and axonal transport

Given the highly polarised structure of neurons, functional endosomal trafficking and axonal transport are essential for neuron survival. Impairment of these functions is one of the pathological characteristics of ALS neurons, manifested by dysregulated protein and organelle transport between the dendrites, cell body and axon, and turnover of the membrane proteins [9]. Some of the evidence supporting this statement is discussed further. In one study, pre-symptomatic ALS-SOD1 (superoxide dismutase 1) mouse models showed impaired axonal transport signs such as decrease in speed and frequency of retrograde movement of endocytic carriers [3,28]. Alsin, a protein encoded by *ALS2* gene, which is involved in nuclear import and export, vesicle transport and endosomal trafficking, is a representative factor. ALS-related mutations of *ALS2* gene have been found in juvenile ALS cases causing loss of function of this protein (Yang et al., 2001). Dysfunction in axonal transport may therefore result in aggregation of proteins and contribute to the pathogenesis of ALS.

5. Arfaptin2 protein structure

ADP-ribosylation factor-interacting protein 2 (Arfaptin2), also known as partner of Rac1 (POR1), is a protein consisting of 341 amino acid (a.a) with a molecular weight of ~38.6 kDa that is ubiquitously expressed in different types of cells. It is expressed as a cytoplasmic protein that predominantly localises to the perinuclear region and is associated with microtubules-organising centre, and colocalises with the trans-Golgi marker TGN46 [15,17–19]. It shares 81% sequence homology with Arfaptin1. Though the exact function of Arfaptin2 is still unknown, its protein composition gives some clue of the possible cellular processes that it might be involved in. Arfaptin2 contains a leucine zipper which gives it a high positive charge that might have a function in DNA binding. The C-terminus contains the Bin/amphiphysin/Rvs (BAR) domain which is present in different proteins that are involved in membrane curvature and it is responsible for dimerisation, membrane binding and curvature sensing [13,17]. Arfaptin2 also contains a highly conserved amphipathic helix (AH) region (a.a 92–112) (Fig. 1). Both, BAR and AH, are believed to be essential for Arfaptin2 binding to the trans-Golgi network. This binding occurs via small GTPase and phoshatidylinositol 4-phosphatase (PI(4)P) binding [6].

It interacts with the ADP-ribosylation factor (ARF) family proteins, which are GTP-binding proteins that are involved in intracellular vesicular transport including formation of coated vesicle and cytoskeletal reorganisation [7,10,15,23] and transportation between the endoplasmic reticulum and Golgi [1,13] (Table 1). It also binds to

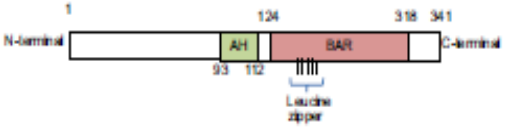

Fig. 1. Schematic presentation of known important Arfaptin2 domains. AH, amphipathic helix; BAR, Bin/amphiphysin/Rvs domain.

Table 1
List of molecules interacting with arfaptin2 and their functions.

Protein	Function	References
Rac1	Membrane ruffling and actin cytoskeleton rearrangement	[20]
Arf1–6	Membrane trafficking, recruit effectors to the Golgi apparatus, and cytoskeleton organisation	[7,10,15,23]
Arl-1	Formation of endosomes, endosome-to-Golgi trafficking, and trans-Golgi network protein sorting	[4]
PI(3)P	Endosome-derived transport vesicles, autophagy, trans-Golgi network protein sorting, and cytokinesis	[6,22]
PI(4)P	Vesicular trafficking, endoplasmic reticulum (ER) export, autophagy, cytokinesis, and actin cytoskeleton rearrangement	[6,8]
PI(5)P	Induce apoptosis, actin cytoskeleton rearrangement, vesicular trafficking, and glucose maintenance	[6,24]

Rac1, which is also a small GTP-binding protein that is involved in membrane ruffling, actin cytoskeleton rearrangement [20], generation of superoxide, transformation of oncogenic cells and activation of transcription factors in a GTP-dependent manner through its C-terminal.

6. Arfaptin2 role in Huntington's disease

A striking evidence for the involvement of Arfaptin2 in protein aggregation in neurodegenerative diseases came from a study of Huntington's disease. HD is a neurodegenerative disease, which is caused by a pathologic poly-glutamine (polyQ) repeat expansion in *huntingtin* gene giving rise to a protein product polyQ-huntingtin. The functions of huntingtin protein include cellular processes such as transcription, vesicular trafficking and mitosis. The polyQ-huntingtin pathogenic effect is through disruption of proteasomal activity [11]. Co-localisation of Arfaptin2 with huntingtin aggregates in HD cell models was suggestive of its potential role in aggresome formation. Evidence showed that both full length and the N-terminus of Arfaptin2 alone are able to inhibit proteasome activity and subsequently induce polyQ-huntingtin aggregation in neuronal cells. On the other hand, expression of the C-terminus of Arfaptin2 (HC-AIP2) showed extensively decreased aggregate formation. This aggregate formation inhibition was found to be through the proteasome pathway, as inhibition of proteasome pathway by lactacystin reversed the inhibitory effect of HC-AIP2 [18].

Consistent with the discussion in the earlier section, phosphorylation pattern of Arfaptin2 is another factor which may be a key determinant in protein aggregation process. It has been reported that phosphorylated Arfaptin2 at serine residue 260 (Ser260) can reduce huntingtin aggregation [19]. Insulin-like growth factor 1 decreases the PolyQ-huntingtin neurotoxic effect through phosphorylating Akt. The phosphorylated Akt in turn phosphorylates the polyQ-huntingtin. However, Akt has been shown to have another pathway for inhibiting the polyQ-huntingtin neurotoxic effect that is huntingtin phosphorylation-independent. Neuronal cells transfected with *huntingtin* that contain the pathologic poly-glutamine expansion but lacks the phosphorylation site showed significantly induced survival and decreased intracellular inclusion formation after treatment with Akt. It has been shown that Akt phosphorylates the full-length Arfaptin2 at Ser260. The dephosphorylation of Arfaptin2 by mutating Ser260 causes its redistribution from the perinuclear region to form a network structure throughout the cytoplasm in a microtubule-dependent manner. In addition, primary striatal neuron cultures from HD embryonic rats were double transfected with Arfaptin2 and an active form of Akt showed that Arfaptin2 was phosphorylated by Akt leading to significant increase in survival and decreased protein inclusion formation. This survival was decreased when cells were transfected with a mutant dephosphorylated form of Arfaptin2 [19].

Also, Arfaptin2 expression was found to be increased in brain of HD mouse [18] and patients [19]. Arfaptin2 has been found to disrupt the proteasome function in HD cell models [18,19].

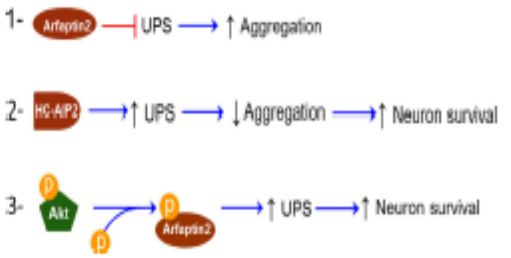

Fig. 2. Schematic presentation of suggested pathways of Arfaptin2 involvement in neuronal survival in Huntington's disease.

Therefore, two hypotheses were raised. Firstly, Arfaptin2 is involved in the pathogenesis of HD by inhibiting the proteasome degradation pathway, whereas its truncated HC-AIP2 works as a negative modulator for Arfaptin2 [18]. Secondly, Arfaptin2 is a defence protein that, when phosphorylated, retains the proteasome function and inhibits protein aggregation [19] (Fig. 2).

7. Future perspectives for Arfaptin2 as a therapeutic target

Whether a similar Arfaptin2-induced pathogenesis in degenerating neurons applies to other disorders such as ALS and AD is still to be investigated. Though the exact function of Arfaptin2 is not fully understood, knowing its binding partners gave some insight of its function. Arfaptin2 involvement in Akt pathway, which inhibits apoptosis, suggests its importance in cell survival. In addition, it binds to proteins involved in endosomal trafficking and protein degradation [6,7,13]. Evidences also showed that modulation of Arfaptin2 decreases motor neuron death in Huntington's disease by rescuing the proteasome activity [18,19]. As proteasome activities are impaired in neurodegenerative disorders and dephosphorylated Arfaptin2 was shown to inhibit proteasome activities, Arfaptin2 protein can provide a novel target for therapeutic interventions against neurodegenerative diseases.

Executive summary

- One of the cellular pathological hallmarks of neurodegenerative diseases such as Alzheimer's, Parkinson's, Huntington's and motor neuron disease, is accumulation of proteins into aggregates.
- It is thought that interference with key cellular pathways such as ubiquitin proteasome degradation and endosomal trafficking contributes significantly to the formation of protein aggregates (aggresomes), in which some of the proteins become sequestered and hence lose its normal functions.
- Research into one of the neurodegenerative diseases, Huntington's disease, has led to a discovery of a ribosylation factor-interacting protein Afraptin2 association with these protein inclusions.

- Given the commonalities between the cellular neuronal degeneration pathways in other neurodegenerative conditions, it is proposed that Arfaptin2 may also be involved in protein aggregate formation in motor neuron disease.
- Structural insights into Arfaptin2 protein sequence suggest its involvement in multiple pathways, including DNA binding, proteasome and Akt pathways, as well as association with trans-Golgi network.
- Further analyses into the mechanisms leading to Arfaptin2 directly or indirectly triggering aggregate formation are necessary; however, currently there are significant clues suggesting its inhibition may lead to rescuing the protein aggregation formation. This will further enhance the research into Arfaptin2 being a potential target against neurodegenerative conditions.

References

[1] W.E. Balch, R.A. Kahn, R. Schwaninger, ADP-ribosylation factor is required for vesicular trafficking between the endoplasmic reticulum and the cis-Golgi compartment, J. Biol. Chem. 267 (1992) 13053–13061.

[2] R.H. Baloh, TDP-43: the relationship between protein aggregation and neurodegeneration in amyotrophic lateral sclerosis and frontotemporal lobar degeneration, FEBS J. 278 (2011) 3539–3549.

[3] L.C. Bilsland, E. Sahai, G. Kelly, M. Golding, L. Greensmith, G. Schiavo, Deficits in axonal transport precede ALS symptoms in vivo, Proc. Natl. Acad. Sci. USA 107 (2010) 20523–20528.

[4] C.G. Burd, T.I. Strochlic, S.R.G. Setty, Arf-like GTPases: not so Arf-like after all, Trends Cell. Biol. 14 (2004) 687–694.

[5] C. Cheroni, M. Peviani, P. Cascio, S. Debiasi, C. Monti, C. Bendotti, Accumulation of human SOD1 and ubiquitinated deposits in the spinal cord of SOD1G93A mice during motor neuron disease progression correlates with a decrease of proteasome, Neurobiol. Dis. 18 (2005) 509–522.

[6] D. Cruz-Garcia, M. Ortega-Bellido, M. Scarpa, J. Villeneuve, M. Jovic, M. Porzner, T. Balla, T. Seufferlein, V. Malhotra, Recruitment of arfaptins to the trans-Golgi network by PI(4)P and their involvement in cargo export, EMBO J. 32 (2013) 1717–1729.

[7] C. D'Souza-Schorey, R.L. Boshans, M. McDonough, P.D. Stahl, L. Van Aelst, A role for POR1, a Rac1-interacting protein, in ARF6-mediated cytoskeletal rearrangements, EMBO J. 16 (1997) 5445–5454.

[8] M.A. De Matteis, C. Wilson, G. D'Angelo, Phosphatidylinositol-4-phosphate: the Golgi and beyond, Bioessays 35 (2013) 612–622.

[9] L. Fetralluolo, J. Kirby, A.J. Gfierson, M. Sendtner, P.J. Shaw, Molecular pathways of motor neuron injury in amyotrophic lateral sclerosis, Nat. Rev. Neurol. 7 (2011) 616–630.

[10] A.K. Gillingham, S. Munro, The small G proteins of the arf family and their regulators, Annu. Rev. Cell Dev. Biol. 23 (2007) 579–611.

[11] N.R. Jana, E.A. Zemskov, G. Wang, N. Nukina, Altered proteasomal function due to the expression of polyglutamine-expanded truncated N-terminal huntingtin induces apoptosis by caspase activation through mitochondrial cytochrome c release, Hum. Mol. Genet. 10 (2001) 1049–1059.

[12] J.A. Johnston, C.L. Ward, R.R. Kopito, Aggresomes: a cellular response to misfolded proteins, J. Cell Biol. 143 (1998) 1883–1898.

[13] H. Kanoh, B.T. Williger, J.H. Exton, Arfaptin 1, a putative cytosolic target protein of ADP-ribosylation factor, is recruited to Golgi membranes, J. Biol. Chem. 272 (1997) 5421–5429.

[14] H.Y. Li, P.A. Yeh, H.C. Chiu, C.Y. Tang, B.P. Tu, Hyperphosphorylation as a defense mechanism to reduce TDP-43 aggregation, PLoS One 6 (2011) e23075.

[15] Z. Man, Y. Kondo, H. Koga, H. Umino, K. Nakayama, H.W. Shin, Arfaptins are localized to the trans-Golgi by interaction with Arl1, but not Arfs, J. Biol. Chem. 286 (2011) 11568–11578.

[16] R.A. Nixon, D.S. Yang, Autophagy failure in Alzheimer's disease-locating the primary defect, Neurobiol. Dis. 43 (2011) 38–45.

[17] B.J. Peter, H.M. Kent, I.G. Mills, Y. Vallis, P.J. Butler, P.R. Evans, H.T. McMahon, BAR domains as sensors of membrane curvature: the amphiphysin BAR structure, Science 303 (2004) 495–499.

[18] P.J. Peters, K. Ning, F. Palacios, R.L. Boshans, A. Kazantsev, L.M. Thompson, B. Woodman, G.P. Bates, C. D'Souza-Schorey, Arfaptin 2 regulates the aggregation of mutant huntingtin protein, Nat. Cell Biol. 4 (2002) 240–245.

[19] H. Rangone, R. Pardo, E. Colin, J.A. Girault, F. Saudou, S. Humbert, Phosphorylation of arfaptin 2 at Ser260 by Akt Inhibits PolyQ-huntingtin-induced toxicity by rescuing proteasome impairment, J. Biol. Chem. 280 (2005) 22021–22028.

[20] A.J. Ridley, H.F. Paterson, C.L. Johnston, D. Diekmann, A. Hall, The small GTP-binding protein rac regulates growth factor-induced membrane ruffling, Cell 70 (1992) 401–410.

[21] A. Salminen, K. Kaarniranta, A. Kauppinen, J. Ojala, A. Haapasalo, H. Soininen, M. Hiltunen, Impaired autophagy and APP processing in Alzheimer's disease: the potential role of Beclin 1 interactome, Prog. Neurobiol. 106–107 (2013) 33–54.

[22] K.O. Schink, C. Raiborg, H. Stenmark, Phosphatidylinositol 3-phosphate, a lipid that regulates membrane dynamics, protein sorting and cell signalling, Bioessays 35 (2013) 900–912.

[23] T. Serafini, L. Orci, M. Amherdt, M. Brunner, R.A. Kahn, J.E. Rothman, ADP-ribosylation factor is a subunit of the coat of Golgi-derived COP-coated vesicles: a novel role for a GTP-binding protein, Cell 67 (1991) 239–253.

[24] A. Shisheva, PtdIns5P: news and views of its appearance, disappearance and deeds, Arch. Biochem. Biophys. 538 (2013) 171–180.

[25] M. Takalo, A. Salminen, H. Soininen, M. Hiltunen, A. Haapasalo, Protein aggregation and degradation mechanisms in neurodegenerative diseases, Am. J. Neurodegener. Dis. 2 (2013) 1–14.

[26] K.D. van Dijk, E. Persichetti, D. Chiasserini, P. Eusebi, T. Beccari, P. Calabresi, H. W. Berendse, L. Parnetti, W.D. van de Berg, Changes in endolysosomal enzyme activities in cerebrospinal fluid of patients with Parkinson's disease, Mov. Disord. Off. J. Mov. Disord. Soc. 28 (2013) 747–754.

[27] J. van Eersel, Y.D. Ke, A. Gladbach, M. Bi, J. Götz, J.J. Kril, L.M. Ittner, Cytoplasmic accumulation and aggregation of TDP-43 upon proteasome inhibition in cultured neurons, PLoS One 6 (2011) e22850.

[28] T.L. Williamson, D.W. Cleveland, Slowing of axonal transport is a very early event in the toxicity of ALS-linked SOD1 mutants to motor neurons, Nat. Neurosci. 2 (1999) 50–56.

[29] J.D. Wood, T.P. Beaujeux, P.J. Shaw, Protein aggregation in motor neurone disorders, Neuropathol. Appl. Neurobiol. 29 (2003) 529–545.

[30] M. Xie, R. Shi, Y. Pan, T. Zeng, Q. Chen, S. Wang, X. Liao, Proteasome inhibition-induced downregulation of Akt/GSK-3beta pathway contributes to abnormality of Tau in hippocampal slice, Mol. Neurobiol. (2014).

[31] Y. Yang, A. Hentati, H.X. Deng, O. Dabbagh, T. Sasaki, M. Hirano, W.Y. Hung, K. Ouahchi, J. Yan, A.C. Azim, N. Cole, G. Gascon, A. Yagmour, M. Ben-Hamida, M. Pericak-Vance, F. Hentati, T. Siddique, The gene encoding alsin, a protein with three guanine-nucleotide exchange factor domains, is mutated in a form of recessive amyotrophic lateral sclerosis, Nat. Genet. 29 (2001) 160–165.